EFFECTS OF PHYSICAL AND CHEMICAL PRETREATMENTS ON THE CRYSTALLINITY OF BAGASSE

A Dissertation

by

MAXINE JANETTE JONES

Submitted to the Office of Graduate Studies of
Texas A&M University
in partial fulfillment of the requirements for the degree of

DOCTOR OF PHILOSOPHY

August 2007

Major Subject: Chemical Engineering

EFFECTS OF PHYSICAL AND CHEMICAL PRETREATMENTS ON THE CRYSTALLINITY OF BAGASSE

A Dissertation

by

MAXINE JANETTE JONES

Submitted to the Office of Graduate Studies of
Texas A&M University
in partial fulfillment of the requirements for the degree of

DOCTOR OF PHILOSOPHY

Approved by:

Chair of Committee, Mark T. Holtzapple
Committee Members, Richard R. Davison
Charles Glover
Cady Engler
Head of Department, N.K. Anand

August 2007

Major Subject: Chemical Engineering

ABSTRACT

Effects of Physical and Chemical Pretreatments on the Crystallinity of Bagasse.

(August 2007)

Maxine Janette Jones, B.S., Mississippi State University

Chair of Advisory Committee: Dr. Mark T. Holtzapple

Biomass conversion technologies are receiving increasing attention due to global climate change and most recently plans from the President of the United States to reduce fossil fuel consumption. The MixAlco process converts a variety of feedstocks, such as agricultural residues, municipal solid waste, and sewage sludge, into mixed alcohols via microbial fermentation, which can then be used as fuel additives or independently as an alternative fuel. Optimizing the pretreatment step of this process is critical to improving product yields. The process uses lime pretreatment, which can be enhanced using new decrystallization pretreatment methods, namely hydrodynamic cavitation and shock tube pretreatment.

Previous studies on biomass decrystallization showed an increase in biomass digestibility when hydrodynamic cavitation was utilized as a pretreatment step. This previous work was expanded by studying both acoustic and hydrodynamic cavitation. Computational fluid dynamics (CFD) was used to model the cavitator to improve its efficiency. The crystallinity before and after pretreatment was analyzed. A new laboratory-scale MixAlco lime-pretreatment system was developed to produce greater quantities of lime-pretreated biomass that could be subjected to decrystallization experiments.

The length of pretreatment, water loading, and bagasse loadings were varied for the shock tube experiments. After each pretreatment, enzymatic hydrolysis was performed, and the equivalent glucose yield was measured by the DNS (dinitrosalicylic acid) assay. Additionally, mixed-acid fermentation was performed to show the benefits of reduced crystallinity on the MixAlco fermentation.

The acoustic and hydrodynamic cavitation pretreatments had a modest effect on crystallinity. In contrast, the shock tube pretreatment shows greater promise as an effective decrystallization pretreatment, even for lime-treated bagasse. Repeated shocks had little effect on digestibility and the crystallinity; however, the water temperature used in shock tube pretreatment played an important role in bagasse digestibility and crystallinity.

DEDICATION

To God for giving me the ability to succeed

To my parents for inspiring me to dream big

and motivating me to never give up

ACKNOWLEDGEMENTS

Firstly, I want to thank God for allowing me to achieve this significant goal. Without Him it would have been impossible to even begin this journey. I want to sincerely thank my advisor, Dr. Mark Holtzapple, for his tremendous help in guiding me throughout my graduate years. His wealth of knowledge has been invaluable to me. I want to thank each of my committee members, Dr. Richard Davison, Dr. Charles Glover, and Dr. Cady Engler, for giving me fresh perspectives on my work and for challenging me to improve it.

I must thank my lab mates for their constructive comments and helpful suggestions as we worked together in the lab. I am indebted to Rocio Sierra for the insightful discussions on my work and for helping me to submit my dissertation on time! Without your help, my struggles would have been almost unbearable. I want to give special thanks to Dr. Cesar Granda who has been a excellent mentor to me. Thank you also for your help in building the laboratory-scale lime pretreatment apparatus. Thanks to Dr. Frank Agbogbo, Dr. Jonathon O'Dwyer, Dr. Li Zhu and Dr. Zhihong Fu for keeping me inspired to finish this task.

Additionally, I must thank Aaron Smith for helping me to construct the hydrodynamic cavitation set-up. I truly appreciate your assistance while running my experiments at the pilot plant. I thank Stanley Coleman for making my work in the lab more enjoyable and for challenging me to finish this summer. I also give my deepest thanks to my student workers Angela Kuhr and Hilliard Rotzler for all of their hard work in helping me to analyze my samples and in washing my bagasse samples. Furthermore, I thank Andrea Forrest for her assistance and suggestions in running my fermentation experiments.

Thanks to Randy Merck for his help in constructing the cavitators and providing tools and supplies for all of my other projects. I thank Manuel Gonzalez at Gooseneck Trailer for his help and expertise in running the shock tube experiments. Thank you also for your words of wisdom.

Finally, I thank my parents, Mr. Walter C. Jones and Mrs. Thelma L. Jones, for their endless support and encouragement throughout the years. I thank my sisters, Abby, Carolyn, Cindy, and Shnae for their advice and encouragement, especially when I was stressed. Lastly, my heartfelt thanks goes to David Madison for his continuous love and support. Thank you for always believing in me.

TABLE OF CONTENTS

LIST OF TABLES

LIST OF FIGURES

Page

Page

CHAPTER I
INTRODUCTION

For the following reasons, there has been an increasing interest in alternative energy sources:

- There is concern over the dependence on foreign sources of petroleum to meet our energy requirements.
- Oil prices are rising because increasing demand is putting pressure on limited supplies.
- The public has grown more interested in proper waste disposal and efforts to preserve the environment.
- The EPA has cited new and stronger evidence for the buildup of greenhouse gases – primarily carbon dioxide – that contribute to global warming. (United States EPA, 2006).

Biological conversion of waste and other lignocellulosic material can address each of the concerns above. Processes that convert lignocellulose into usable products have been studied for many years (Wyman, 2001; Malherbe and Cloete; 2002; Lonsane et al., 1985; Fan et al., 1980, Fan and Lee, 1982). The MixAlco process converts biomass into mixed alcohols such as 2-propanol, 2-butanol, and higher alcohols. Via mixed-acid microbial fermentation, this process is especially attractive because it converts a variety of feedstocks (e.g., crop wastes, municipal solid waste, sewage sludge) into mixed alcohols, which can then be used as fuel additives or independently as an alternative fuel. Additionally, the combustion of MixAlco fuels will not contribute to global warming because there is no net addition of carbon dioxide into the atmosphere.

This dissertation follows the style and format of Bioresource Technology.

BIOMASS STRUCTURE

Lignocellulosic biomass is the world's most abundant biological material and is composed primarily of cellulose, hemicellulose, and lignin. Cellulose is a linear, unbranched polymer of β-glucose, which provides structure to plants due to its crystalline configuration (Holtzapple, 1993; Puri, 1984). Its structure is shown in Figure 1.1. There are two sections of cellulose: crystalline and amorphous. Amorphous sections are more disordered and allow water to penetrate, thereby increasing susceptibility to enzymatic hydrolysis, whereas crystalline sections are more resistant to enzymatic hydrolysis (Weimer et al., 1995; Fan and Lee, 1983). These sections are depicted in Figure 1.2.

Hemicellulose is more readily hydrolyzed than cellulose due to its amorphous structure. It is primarily composed of three hexoses and two pentoses. Some of the monomers of hemicellulose are glucose, galactose, mannose, xylose, arabinose, and glucuronic acid (Figure 1.3). Hemicellulose polymers are shorter than those of cellulose. Hemicellulose has a degree of polymerization (DP) in the range of 50 – 200, whereas cellulose has a DP of 500 – 15000.

Lignin is a phenyl-propane polymer that acts as a glue to hold the hemicellulose and cellulose together. Its monomers p-coumaryl alcohol, coniferyl alcohol, and sinapyl alcohol are shown in Figure 1.4. Lignin has a DP of about 54. In plant cell walls, cellulose provides the cell structure and strength and is enclosed in a hemicellulose matrix surrounded by lignin, which holds the entire framework together (Holtzapple, 1993). A model of the plant cell wall (without lignin) is displayed in Figure 1.5.

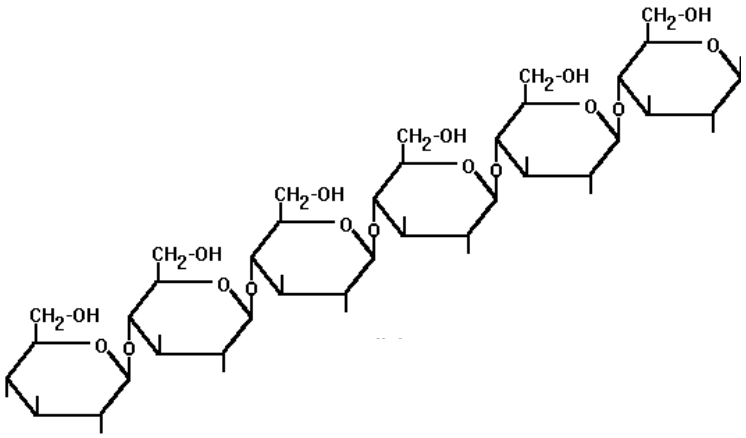

Figure 1.1. Cellulose polymer.

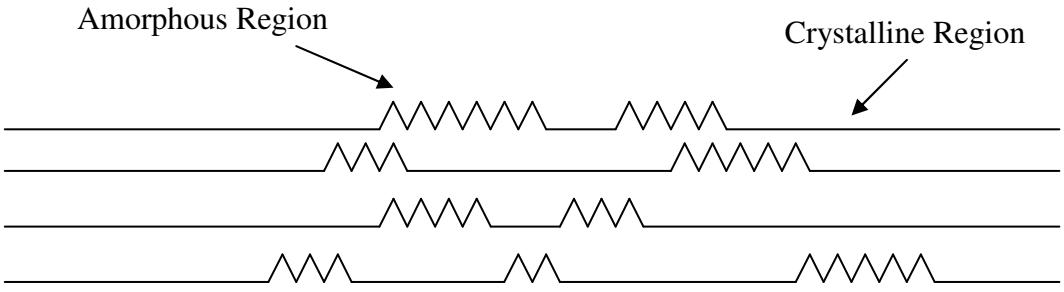

Figure 1.2. Cellulose regions.

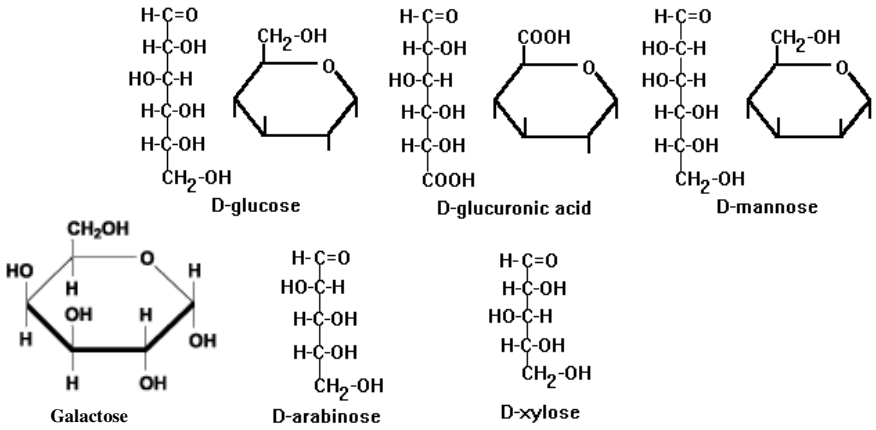

Figure 1.3. Monomers of hemicellulose.

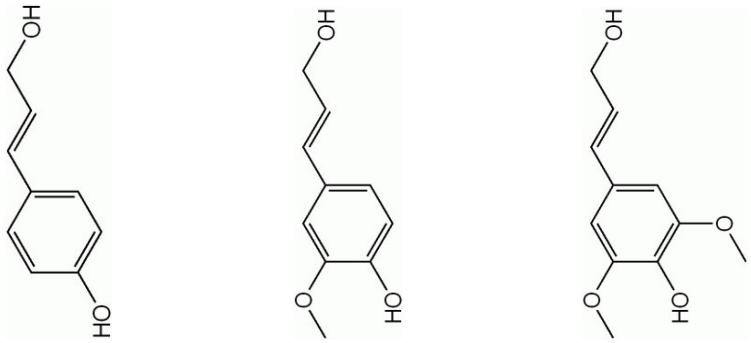

Figure 1.4. Monomers of lignin: p-coumaryl alcohol, coniferyl alcohol, and sinapyl alcohol.

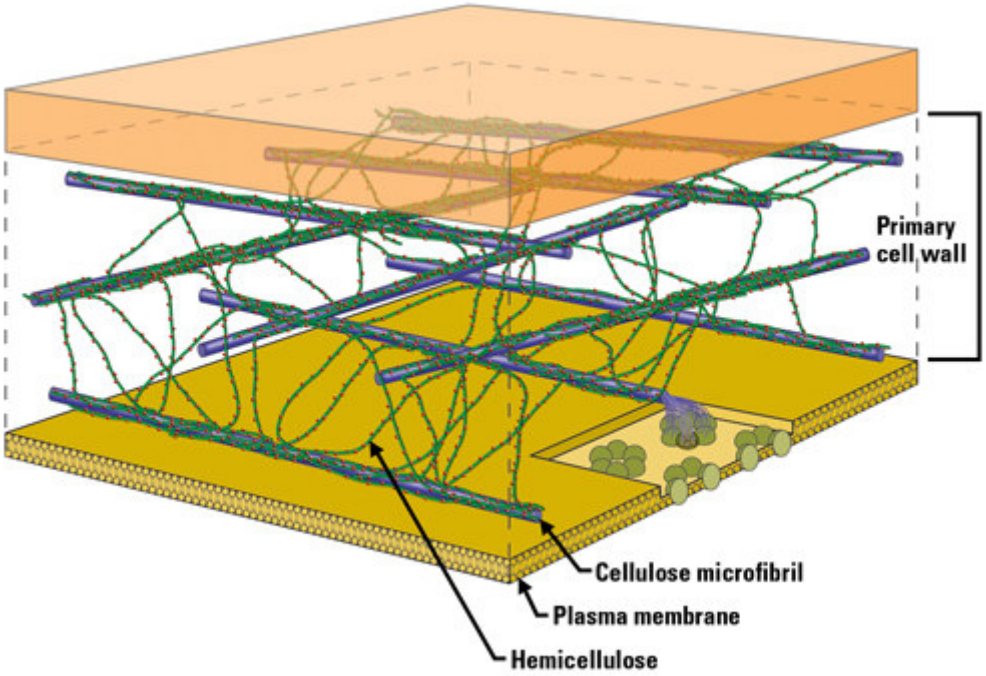

Figure 1.5. Simplified model of a plant cell wall (lignin not shown). (Genomics GTL, 2007)

MIXALCO PROCESS

The MixAlco process has been studied for over 16 years by Holtzapple et al (1997). A schematic of the process is displayed in Figure 1.6. The pretreatment step is very important because it increases biomass digestibility. Currently, lime pretreatment is used in the MixAlco process because it is relatively inexpensive and safe. Lime pretreatment involves mixing the biomass and calcium hydroxide into a large pile. Air is then purged through the pile, and the pile is flooded with water for about one month. This pretreatment effectively removes lignin from the biomass thereby enhancing digestion during fermentation.

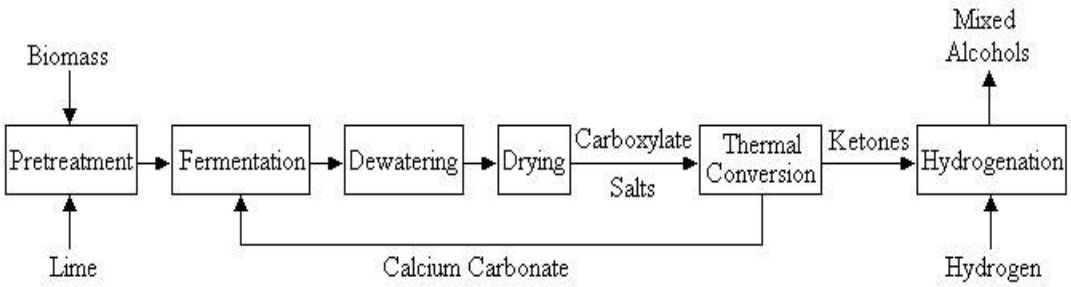

Figure 1.6. MixAlco process (Holtzapple et al., 1997)

Fermentation is the next step of the process and is currently the most costly. Anaerobic microorganisms are added to the pretreated material that produce carboxylic acids from the biomass. Methane inhibitors, such as iodoform, are added to the fermentation to prevent the production of methane gas. As a result, higher carboxylic acids are produced such as propionate and butyrate (Bauchop, 1967; Russell and Martin, 1984).

The carboxylic acids produced in the fermentation react with the calcium carbonate buffer to give carboxylate salts (e.g., calcium acetate, propionate, and butyrate). Next, the salts are dried using a vapor-compression evaporator and then are thermally converted to ketones (e.g., acetone, methyl ethyl ketone, etc.). Finally, the ketones are hydrogenated to their corresponding alcohols (e.g., isopropanol, butanol, and pentanol) (Holtzapple et al., 1997). A recent variation of the process uses ammonium bicarbonate as a buffer.

CRYSTALLINITY

Crystallinity is a measure of the relative amounts of the amorphous and crystalline regions of cellulose found in biomass (Fan et al., 1980). It is often described

by the crystallinity index (CrI); a higher CrI denotes a more crystalline material. Segal et al. (1959) developed the following expression for calculating crystallinity:

$$CrI = \frac{I_{002} - I_{am}}{I_{002}} \times 100 \qquad (1.1)$$

where,

I_{002}, intensity at 2θ = 22.5°
I_{am}, intensity at 2θ =~ 18.7°

The crystallinity is measured using an X-ray diffractometer (XRD). Figure 1.7 shows the typical diffraction pattern of 10-mesh bagasse obtained from the XRD.

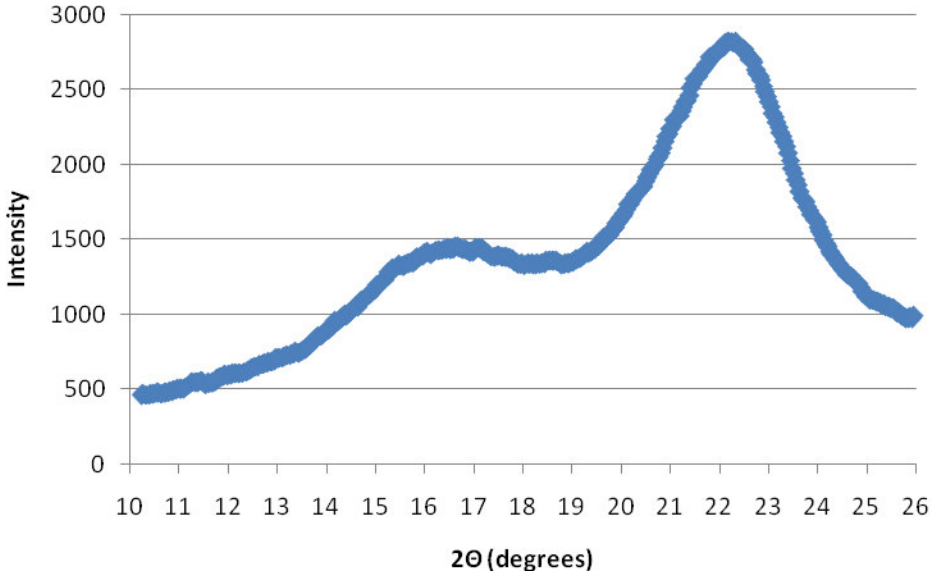

Figure 1.7. Typical X-ray diffraction pattern of raw knife-milled 10-mesh bagasse. CrI = 53.

DECRYSTALLIZATION AND DELIGNIFICATION METHODS

The crystalline structure of cellulose hinders enzymatic hydrolysis by limiting the number of enzyme adsorption sites (Fan et al., 1980; Abraham and Kurup, 1997; Mosier et al., 2005). To increase the extent of biomass digestion during the MixAlco process, Chang and Holtzapple (2000) found the two main variables to consider are the lignin content and the degree of crystallinity. The lignin content and the CrI are inversely related to digestibility (Chang and Holtzapple, 2000; Fan et al., 1981); therefore, the most effective pretreatment is one that both delignifies and decrystallizes the biomass.

PHYSICAL PRETREATMENTS

Physical pretreatments are classified as mechanical (e.g., milling or grinding) or non-mechanical (e.g., radiation). Both milling and radiation pretreatments reduce crystallinity, but require high capital costs and lack energy efficiency. Thermal pretreatments include autohydrolysis, steam explosion, and hydrothermolysis. Autohydrolysis and steam explosion subject biomass to high-pressure steam for an allotted time, followed by a sudden release in pressure. Hydrothermolysis involves subjecting biomass to high-pressure liquid water at high temperatures. Thermal pretreatments result in biomass degradation (Ghosh and Singh, 1993). There are many physical pretreatments that can disrupt the crystalline structure of the cellulose. Three methods are studied in this project: ball-milling, cavitation, and shock tube pretreatment.

Ball-milling is an energy-intensive means of reducing crystallinity (Krycer and Hersey, 1980). It entails grinding a substance into a fine powder using a rotating cylinder partially filled with grinding media such as balls or pebbles. The milling process is extremely inefficient (Parrot, 1990) and, due to the high energy input, the milled powder may contain disordered regions (Krycer and Hersey, 1980) presumed to be concentrated on the surface of particles which have amorphous characteristics (Ward and Schultz, 1995). Zhao et al. (2006) confirmed that ball-milling produced small levels

of disorder on amorphous material found in crystalline α-cellulose and found that ball-milling significantly increased the non-crystalline regions of crystalline α-cellulose as well as the hydrolysis rate. Ball-milled bagasse was utilized as a control for the physical pretreatments studied in this work.

Cavitation is the phenomena of the formation, growth, and rapid collapse of gas or vapor-filled bubbles. There are two main types of cavitation: acoustic and hydrodynamic.

Acoustic cavitation is caused by pressure variations from ultrasonic waves passing through a fluid. Acoustic waves create microcavities where gas bubbles grow and then collapse. The collapse generates "shock waves" that cause mechanical effects such as particle erosion in a substance (Shah et al., 1999). Applications of acoustic cavitation are seen in power ultrasound, which is used for cleaning and welding (Mason, 2003). For this study, a sonicator was used to decrystallize the biomass via acoustic cavitation.

Hydrodynamic cavitation occurs when a moving fluid encounters a sudden change in velocity that results in a localized pressure drop. This can be accomplished in a pipe by throttling a valve downstream of a pump. Cavities form when the pressure just downstream of the valve falls below the vapor pressure of the fluid. The bubbles collapse downstream of the valve when pressure is recovered. The scheme of hydrodynamic cavitation is shown in Figure 1.8.

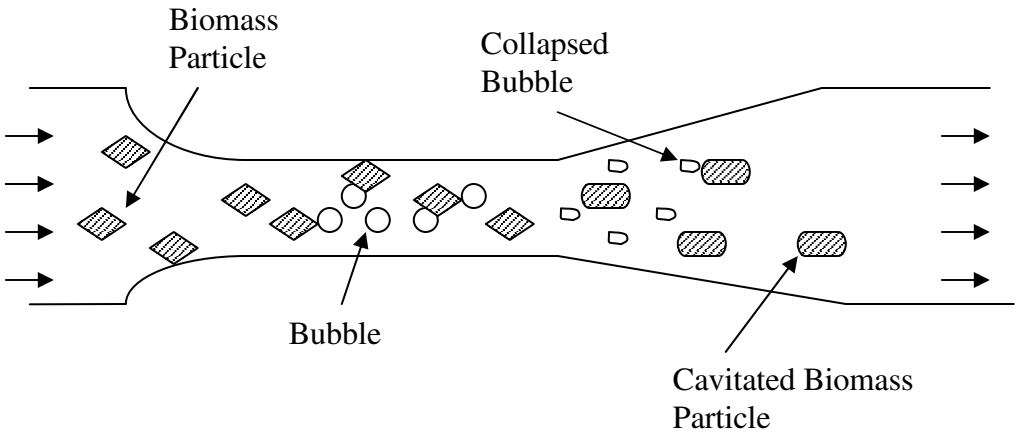

Figure 1.8. Schematic of cavitation in a venturi cavitator.

When biomass is pretreated by hydrodynamic cavitation, the implosion of the bubbles created during cavitation seems to alter the cellulose structure (Coward-Kelly, 2002). Essentially, biomass is fragmented due to the mechanical impact of the collapsing bubbles, which in turn increases available surface area and improves enzyme effectiveness during enzyme hydrolysis (Mason, 2003).

There are two main features of bubble dynamics related to cavitation: the maximum size of the bubble and the distance traveled by the bubble before collapse, which is referred to as the life of the bubble. The maximum bubble size in cavitation defines the cavitation intensity. Bubbles grow when the pressure is reduced or the temperature is increased (Shah et al., 1999). Larger bubbles implode with a higher intensity and can cause greater effects on a substance than smaller bubbles. This is depicted for acoustic cavitation in Figure 1.9. From its definition, the bubble life is a measure of the active volume of the reactor at which actual cavitation effects are observed. Generally, bubble life decreases as the region of active cavitation decreases and vice versa.

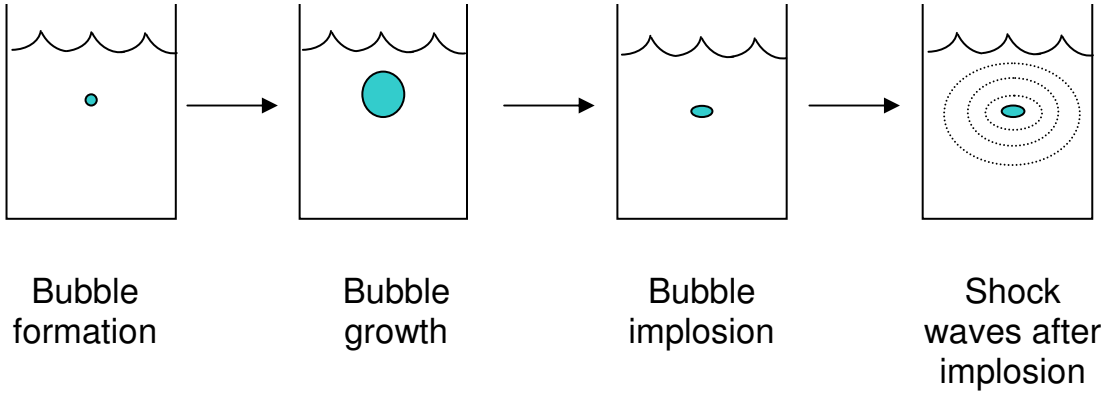

Figure 1.9. Schematic of acoustic cavitation.

A simple *shock tube* is usually a steel pipe in which a low-pressure gas and a high-pressure gas are separated by a diaphragm. The diaphragm bursts open under predetermined conditions and produces a shock wave. The shock tube as a wave reactor has been widely used in kinetic studies to examine the molecular decomposition of gases, oxidation reactions, and reactions involving aerosols, to name a few (Bhaskaran and Roth, 2002). Shock tubes have not previously been used to pretreat biomass. A diagram of the shock tube that was constructed to decrystallize biomass is given in Figure 1.10. It will be described more fully later in the dissertation.

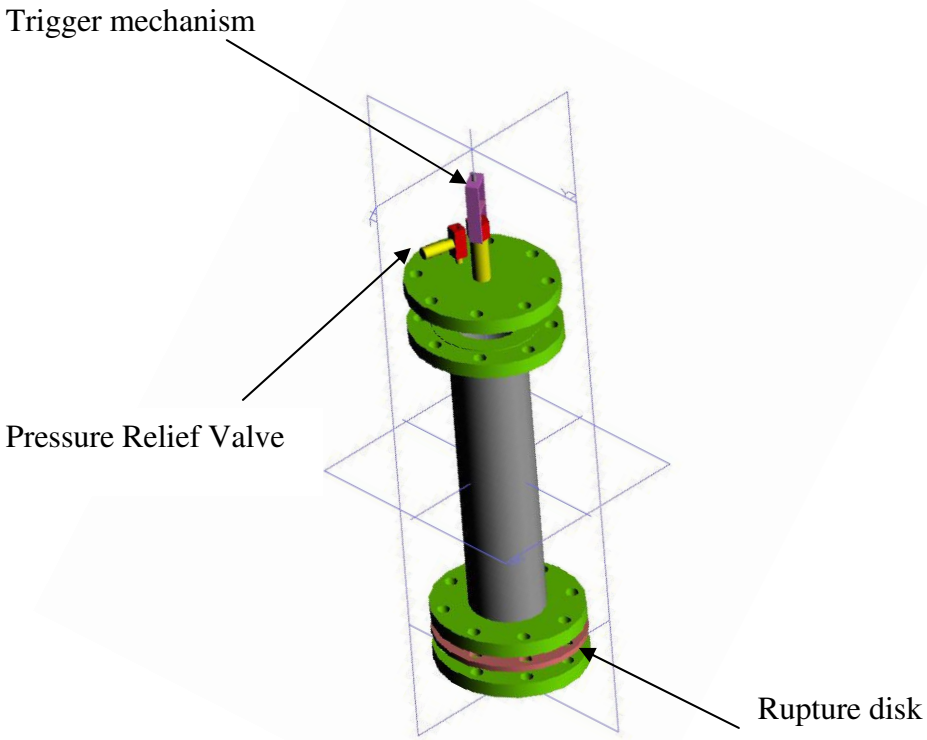

Figure 1.10. Shock tube diagram.

CHEMICAL PRETREATMENTS

Chemical pretreatments are effective, but may produce waste chemicals that cannot be easily disposed of. These pretreatments include dilute-acid pretreatments using sulfuric, hydrochloric, nitric, and phosphoric acids; solvent delignification with aqueous ethanol and butanol; and alkali pretreatments with agents such as sodium hydroxide, lime, or ammonia (Ghosh and Singh, 1993). Alkali pretreatments successfully remove lignin and are performed at lower temperatures and pressures compared to other pretreatments; however, the biomass must usually be pretreated for hours or days (Mosier et al., 2005). Some advantages for using ammonia as a

pretreatment reagent are its effectiveness as a swelling reagent of lignocellulosic biomass, its high selectivity for reactions with lignin over carbohydrates, and its high volatility rendering it easy to recycle and reuse (Kim et al., 2003).

Lime pretreatment is used in the MixAlco process as mentioned above. The recommended lime loading of 0.1 g $Ca(OH)_2$ / g dry biomass and water loading of 10 mL/g of biomass was determined by Chang et al. (1998). The major structural features that affect digestibility are the extent of acetylation, lignification, and crystallization (Fan et al., 1980; Abraham and Kurup., 1997). Long-term lime pretreatment is very effective at deacetylation and delignification; it removes all acetyl groups and half of the lignin present in biomass (Kim and Holtzapple, 2006). The degree of lignocellulose crystallinity is a key factor in resisting enzymatic hydrolysis (Chang and Holtzapple, 2000; Puri, 1984) and thus it is expected to limit the digestibility of biomass during fermentation.

BATCH FERMENTATION

Crystallinity and lignin removal (e.g., ball-milling and lime pretreatment) were studied to show their role in anaerobic fermentation. Batch fermentation (Appendix H) was performed to analyze the effects of decrystallization and delignification.

CHAPTER II
MATERIALS AND METHODS

BAGASSE

Sugarcane bagasse was obtained from the W. R. Cowley Sugar House, a sugar mill in Santa Rosa TX. To preserve freshness, it was stored in the freezer until ready for use. Before use, the bagasse was thawed under a hood for 1 – 2 days. Then the moisture content was determined using NREL standard procedure No. 001.

Three types of bagasse were used in this work: unmilled, raw knife-milled, and ball-milled bagasse. Unmilled bagasse denotes bagasse in the form it was received from the sugar mill before any size reduction. Raw knife-milled bagasse was milled in a Thomas-Wiley laboratory knife mill (Arthur H. Thomas Company, Philadelphia, PA) located in the Food Protein Department in the Cater-Mattil building at Texas A&M. It was then sieved to pass through a 10-mesh or 80-mesh screen.

The ball-milling apparatus is shown in Figures 2.1 and 2.2. A rotary ball mill, built with two 1/6-hp 156-rpm AC gear motors (Dayton Electric Mfg. Co., Niles, IL), was used to ball mill bagasse. The ball mill consisted of four 1-in diameter × 25-in long steel shafts enclosed with 1.5-in O.D. Buna-N rubber tubing (McMaster-Carr, Atlanta, GA). The ball-milling procedure involved loading 10 g of biomass into a 300-mL porcelain jar, adding 0.375-in zirconia grinding medium (U.S. Stoneware, East Palestine, OH), and allowing the jar to rotate between the rollers at 68 rpm for a defined length of time. The zirconium grinding media was added in a ratio of 43 g balls:1 g of biomass. This filled each jar to 50 to 75% of its total volume. In this project, samples were ball-milled for 3 days. The pounding action of the beads against the biomass was effective at lowering the crystallinity.

Figure 2.1. Zirconia grinding media inside porcelain jar.

Figure 2.2. Ball mill with porcelain jars loaded between the rollers.

CRYSTALLINITY

The crystallinity of the samples was measured before and after pretreatment to determine the effect of each pretreatment. A Brukar D8 Powder X-ray Diffractometer Long Arm located in the Chemistry Building, Room 2407, at Texas A&M University was used to measure the crystallinity of each sample. The XRD equipment is displayed in Figures 2.3 to 2.5. The samples were filled flush to the top of an aluminum sample holder and were scanned at 1^{o}/min from $2\theta = 10^{o}$ to 26^{o} with a step size of 0.04^{o}.

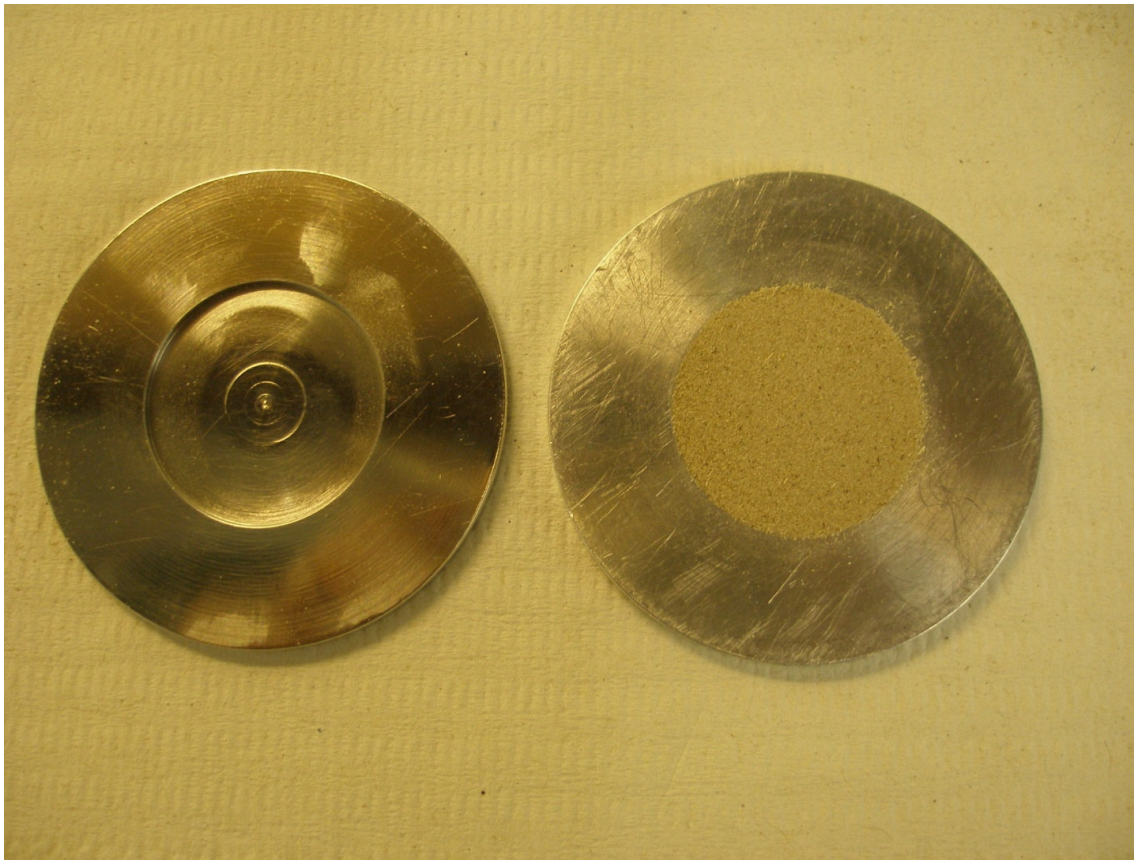

Figure 2.3. Empty aluminum sample tray and raw knife-milled 80-mesh bagasse loaded in a sample tray.

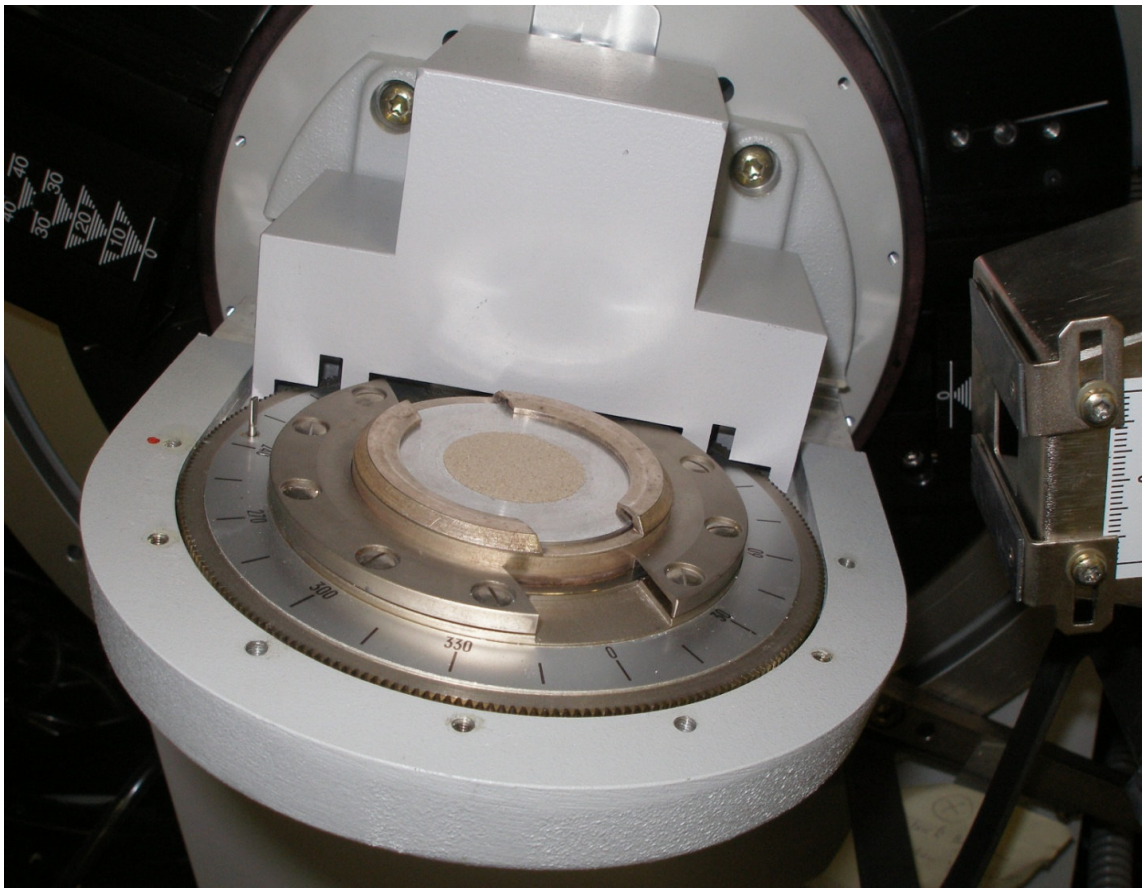

Figure 2.4. Sample loaded in XRD sample holder.

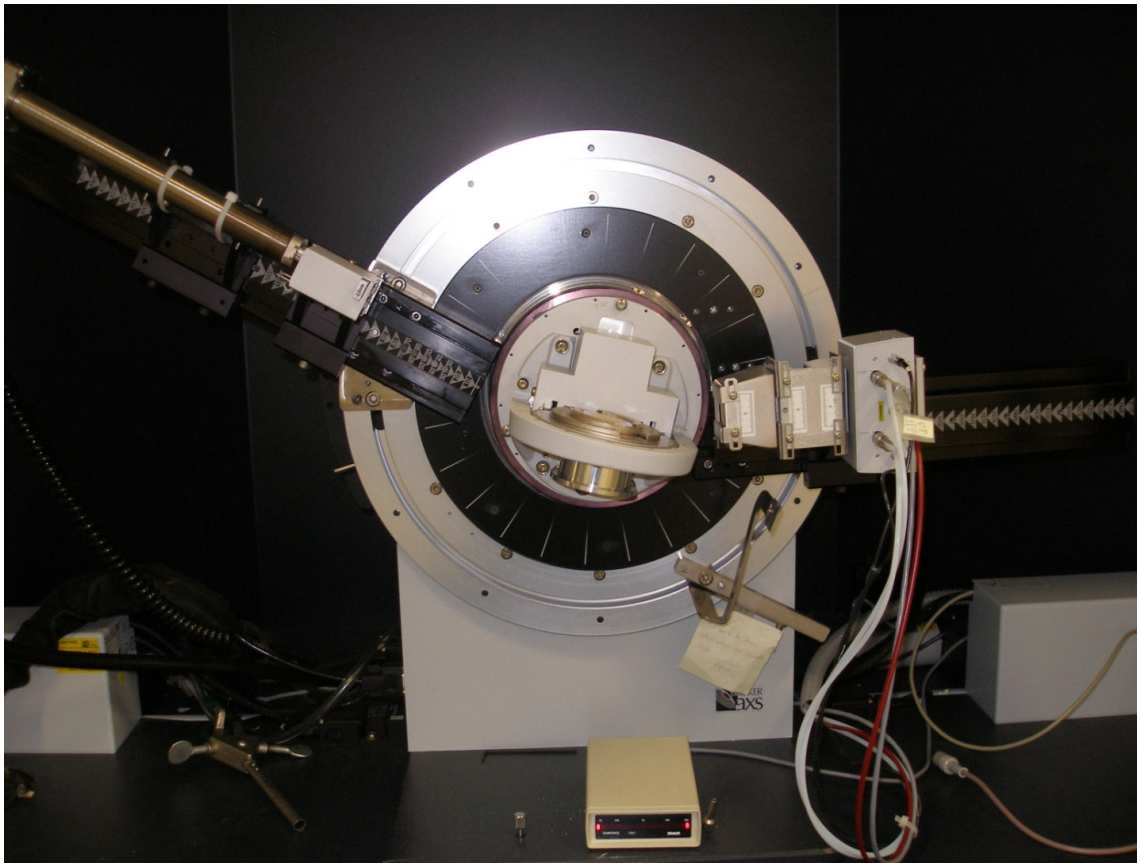

Figure 2.5. Brukar D8 Powder X-ray Diffractometer Long Arm.

After each pretreatment, the samples were dried according to Appendix K. Then the samples were ground in a coffee grinder for approximately 1 minute to obtain a more uniform and homogenous sample before performing crystallinity analysis. This was essential for obtaining accurate, repeatable results from the XRD due to the size of the sample trays. The bagasse crystallinity was unchanged upon grinding in the coffee grinder (see Chapter III).

LIME PRETREATMENT

Two long-term aerated lime pretreatments were used in this study. The first method was a small-scale method that involved placing 45 g of bagasse along with 4.5 g of lime ($Ca(OH)_2$) and 450 mL of distilled water into a centrifuge bottle. The samples were then incubated at 55°C for one month. Air was scrubbed by a lime slurry to prohibit the carbon dioxide in the air from reacting with the lime in the reactors, and then was bubbled through the reactors. The pretreatment was run in duplicate so that the total pretreated amount was 90 g.

After one month, the samples were neutralized to a pH of 7 by bubbling carbon dioxide through the reactors. This also converted any unreacted calcium hydroxide to calcium carbonate. Afterwards, the samples were continuously washed until the filtrate was clear.

The second lime pretreatment method was performed at a larger scale and allowed approximately 5 kg of bagasse to be pretreated instead of only 90 g in the small-scale pretreatment discussed above. In a large plastic storage bin (L × W × H = 3 ft × 2 ft × 2 ft), approximately 5 kg of bagasse was mixed with lime and then added on top of a rock bed. A water sprayer above the pile kept the biomass wet, and the water was recycled through a water heater and a heat exchanger to maintain a constant temperature of 50°C. Additionally, air was bubbled through the biomass with air diffusers. Figures 2.6 to 2.8 depict this pretreatment set-up.

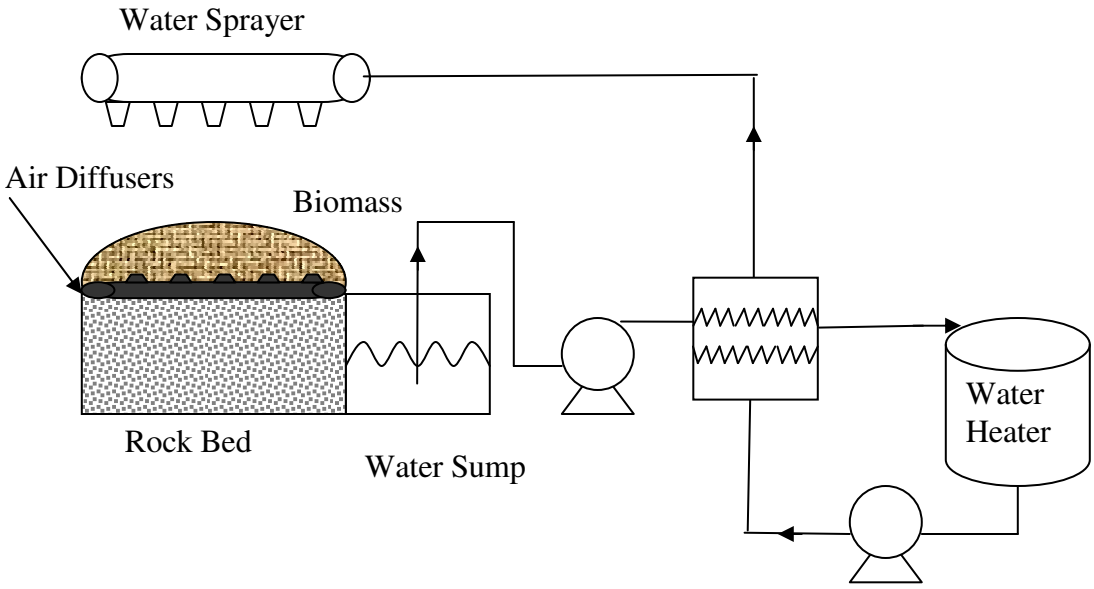

Figure 2.6. Laboratory-scale lime pretreatment diagram.

Figure 2.7. Laboratory-scale lime pretreatment apparatus.

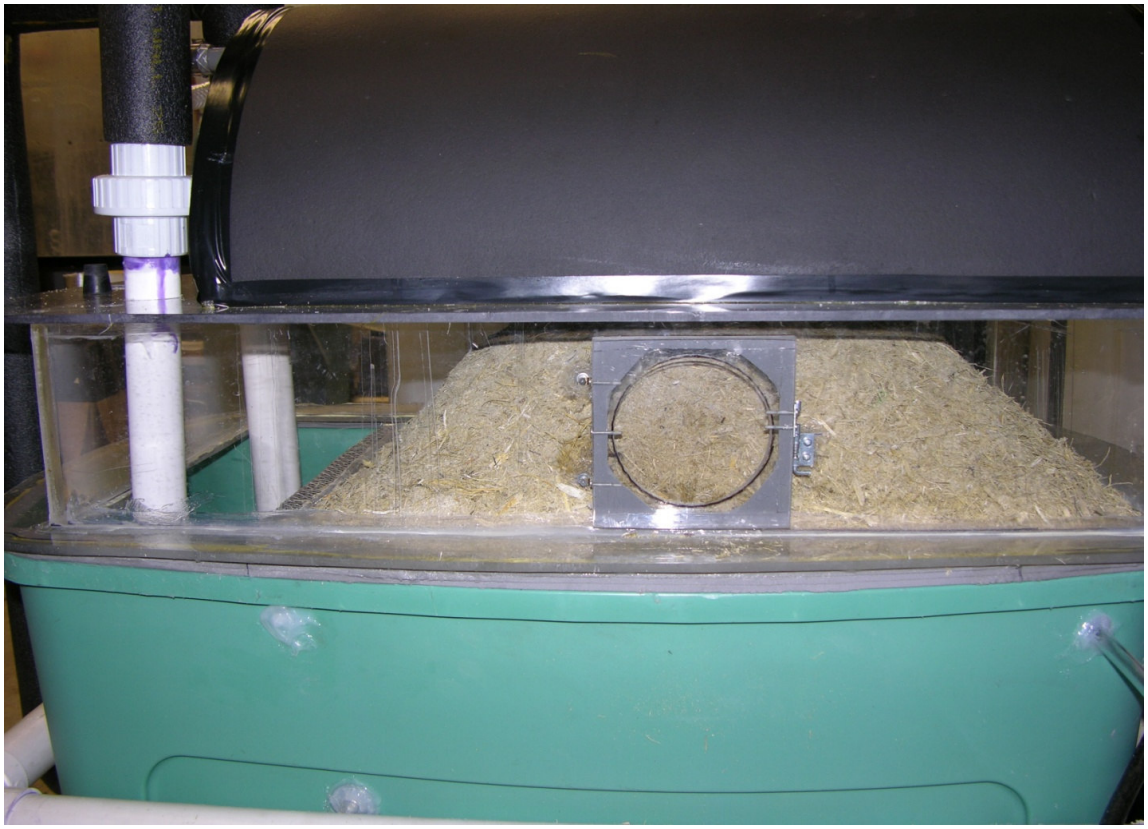

Figure 2.8. Close-up of the unmilled bagasse pile inside the laboratory lime pretreatment system before pretreatment began.

ENZYMATIC HYDROLYSIS

To determine the amount of reducing sugars released after each pretreatment (digestibility), enzymatic hydrolysis (Appendix E) was performed on the samples by directly adding cellulase enzymes, cellobiase, citrate buffer, and inhibitor. Then the samples were incubated for 3 days at 50^{o}C inside a shaking incubator to maintain the optimal reaction temperature and to ensure the samples were thoroughly mixed. Samples were taken at time zero, 1 h, and 72 h to determine the concentration of glucose in the sample, the initial digestion rate, and the extent of digestion, respectively.

The enzymatic procedure was modified for the cavitation pretreatment samples and shock tube pretreatment samples. Zhu et al. (2007) recently discovered that crystallinity greatly affects the initial hydrolysis rate, whereas lignin content plays a

more important role in the extent of digestion. So, instead of taking the initial hydrolysis rate samples at 1-h, samples were taken at 6-h because the 1-h sample released too little sugar to obtain accurate, reliable measurements.

After the incubation period, the samples were boiled to denature the enzymes and stop the hydrolysis. Then the dinitrosalicylic (DNS) assay detailed in Appendix F was performed to determine the equivalent glucose yield. The equivalent glucose sugars were measured with a spectrophotometer.

ACOUSTIC CAVITATION

Acoustic cavitation (sonication) was performed using a Fisher Ultrasonic Dismembrator, Model 300 shown in Figures 2.9 and 2.10. The 60% power setting was used based on previous results from Coward-Kelly (2002). Pure microcrystalline cellulose (Avicel PH-101), raw knife-milled 10-mesh, and knife-milled lime-treated 10-mesh bagasse were analyzed. The sonication procedure consisted of adding 2.5 dry g of bagasse or Avicel microcrystalline cellulose to 30 mL of water in a 50-mL centrifuge tube. The sample was then placed in an ice bath for 10 minutes. Finally, the sample was sonicated in the ice bath from 0 to 150 minutes in 15-minute increments as detailed in Appendix B.

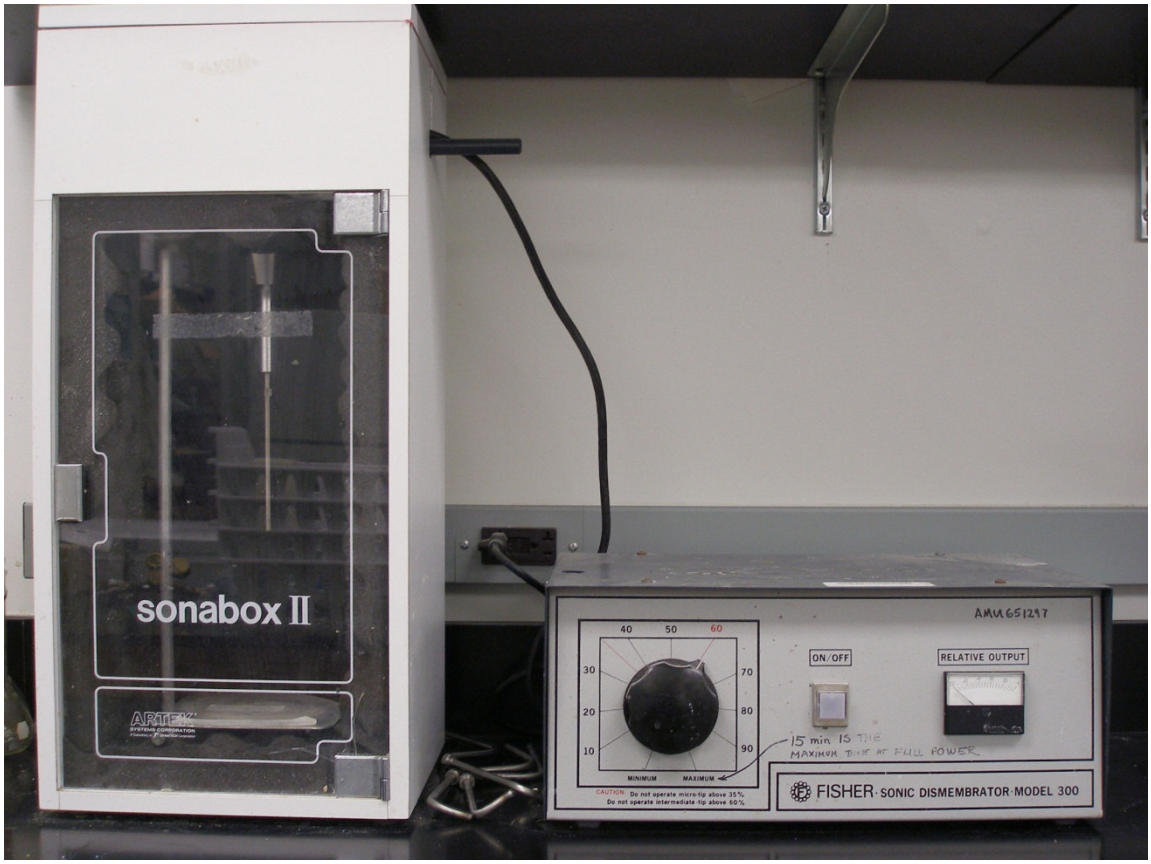

Figure 2.9. Fisher Ultrasonic Dismembrator, Model 300.

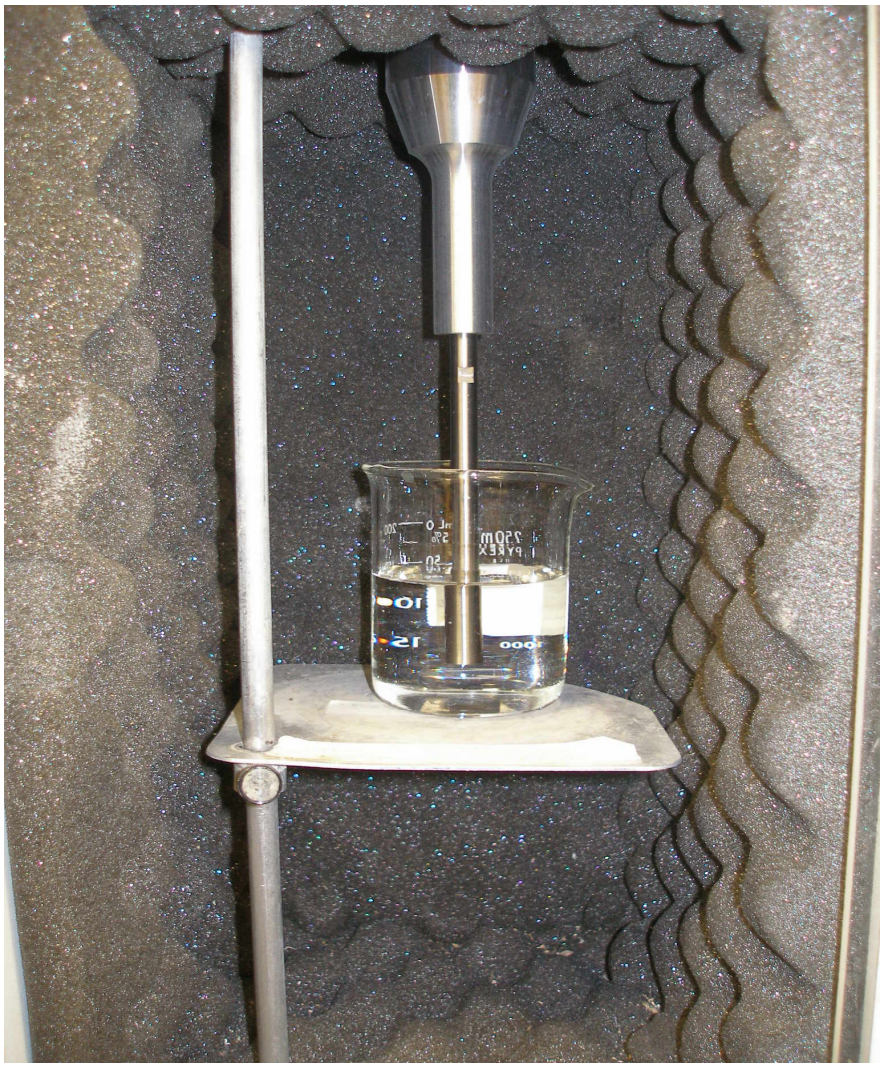

Figure 2.10. Sonication chamber showing the sonication probe inside a beaker filled with water.

HYDRODYNAMIC CAVITATION

A modified venturi meter (cavitator) was used to decrystallize the biomass via hydrodynamic cavitation (Figure 2.11). Hydrodynamic cavitation experiment samples were mixed in an open 200-L jacketed tank with a mixer powered by a variable-speed motor (Figure 2.12). A low mixing rate of approximately 30 rpm was required to keep the biomass suspended in the water. A centrifugal pump was used to force the biomass slurry through the system.

Experiments were conducted with 55 L of water and 550 grams of bagasse (1%). Tests were run using raw knife-milled 10-mesh bagasse for up to 2 hours at a time. The temperature was controlled to 22°C by adding ice to the water. This temperature was chosen because previous results showed higher digestibilites at 22°C (Coward-Kelley, 2002). Approximately 40 lbs of ice were required to maintain the temperature at 22°C for the duration of the 120 minute treatment. Samples were taken at 0, 20, 40, 60, and 120 minutes. The solids were then separated from the liquid and allowed to air dry. Afterwards, enzymatic hydrolysis was performed on the samples, and XRD analysis was performed as well.

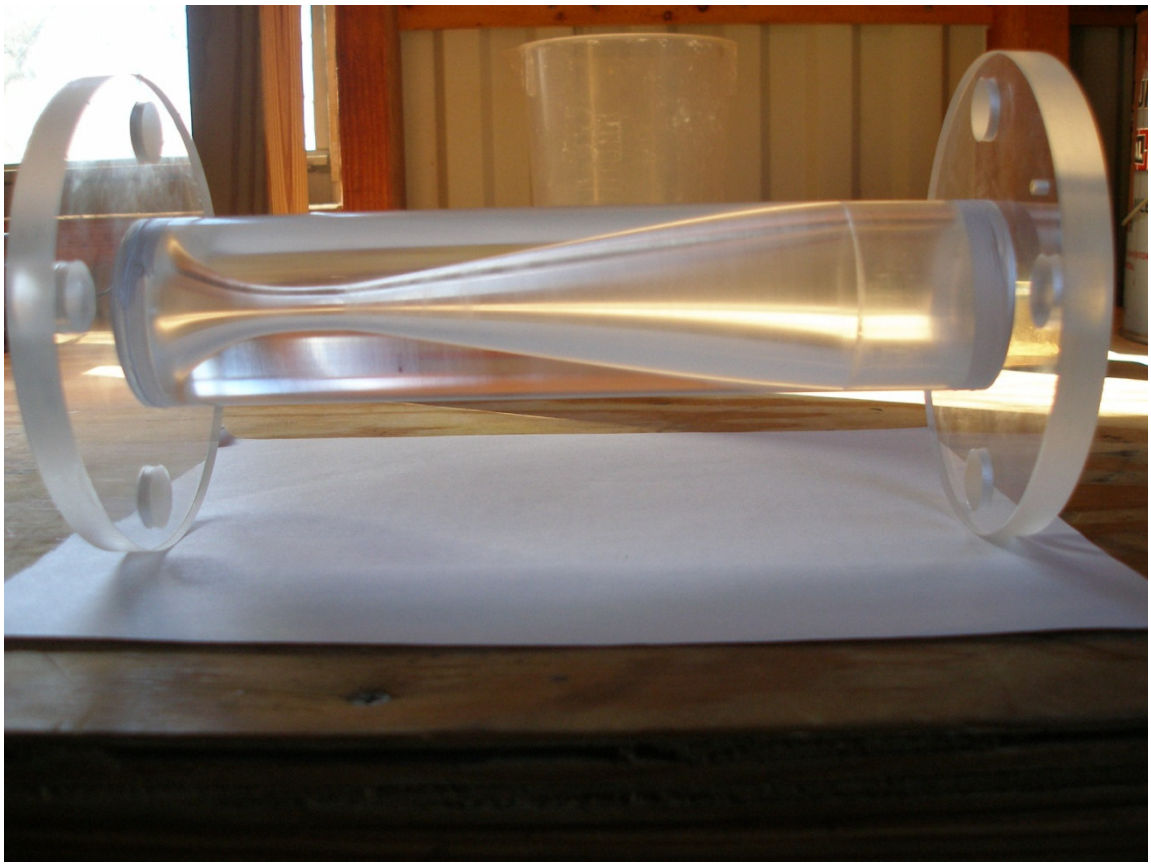

Figure 2.11. Cavitator constructed of plexiglass.

Figure 2.12. Hydrodynamic cavitation system containing an open 200-L jacketed reactor with a mixer powered by a variable-speed motor, a centrifugal pump, and the cavitator.

SHOCK TUBE

Until now, shock tube pretreatment has never been imposed on biomass. This pretreatment was performed using a shock tube constructed of a 4-in Schedule 80 steel pipe with flanged ends shown in Figure 2.13. The shock tube was 22 inches long.

Initially, the shock tube was located inside a 55-gallon metal drum filled with sand to provide a safety barrier to the user. A metal cylinder was inserted into the metal drum to surround the shock tube so it could be easily removed without disturbing the sand (Figure 2.14). A rupture disk was located between the bottom flanges as a safety measure in the event of overpressure within the tube. The pressure was recorded by a glycerin-filled pressure gauge located at the top of the tube.

To perform the shock tube pretreatment, unmilled bagasse and water were added to the shock tube. The cover was then bolted shut, and a shotgun shell was loaded into the trigger mechanism and released by pulling the cord connected to it from 10 feet away. Initially, Remington Express 12-gauge, 2.75-in shells were used. Upon release of the trigger, the exploding shotgun shell provided the shock needed to decrystallize the biomass. Figure 2.15 shows the loading of the shotgun shell.

Due to the cumbersome task of lifting the heavy shock tube into the metal drum for each test, the experimental set-up was modified as shown in Figures 2.16 and 2.17. Steel plates were mounted onto a steel frame to provide protection between the shock tube and the user. The cord that was tied to the trigger mechanism was released from behind the plates.

Eventually, the shotgun shells were changed to Remington Express Buckshot 12-gauge, 3.5- in Magnum. These more powerful shells were selected to test if a more powerful shock would result in a further decrease of crystallinity.

Figure 2.13. Shock tube.

Figure 2.14. Metal drum filled with sand and protective metal liner for shock tube.

Figure 2.15. Loading shotgun shell into shock tube inside metal drum.

Figure 2.16. Modified experimental set-up with metal plates as a protective barrier.

Figure 2.17. Shock tube behind steel plates.

FERMENTATION

Substrates

Both physically and chemically pretreated bagasse were used in the batch fermentation including the following: unmilled, ball-milled, knife-milled lime pretreated 80-mesh, and ball-milled lime pretreated bagasse. 80-mesh bagasse was used to minimize any differences from the ball-milled bagasse fermentation that could be attributed to the different particle sizes. The 80-mesh bagasse is a similar particle size to ball-milled bagasse.

Neutralization

After lime pretreatment, the bagasse was neutralized to a pH of 7 by adding glacial acetic acid. Afterwards, the bagasse was washed several times until the effluent was clear to avoid any false measurements of acetic acid production during the batch fermentation experiments.

Fermentor

Each fermentor (Figure 2.18) was made using a Nalgene 1 L polypropylene centrifuge bottle (98 x 169 mm). The bottles were capped with a size-11 rubber stopper which had a hole drilled in the middle of it. A glass tube was placed in the hole, and the tube was closed with a rubber septum. This septum was used to measure and release the gas produced during fermentation. If the gases were not released regularly, the pressure would build inside the fermentor (above the bottle rating of 2 atm) and possibly cause it to explode.

Each rubber stopper also had two small holes drilled on each side and two 0.25-in stainless steel tubes with welded ends were inserted in the holes. These tubes were used as stirrers to keep the fermentation components well-mixed. A large hole was drilled in the centrifuge cap so that it could be placed around the rubber stopper to hold the stopper in place.

The fermentors were incubated at 40^{o}C inside a Wheaton Modular Cell Production Roller Apparatus (Model III). The fermentors were rotated horizontally at 1 rpm.

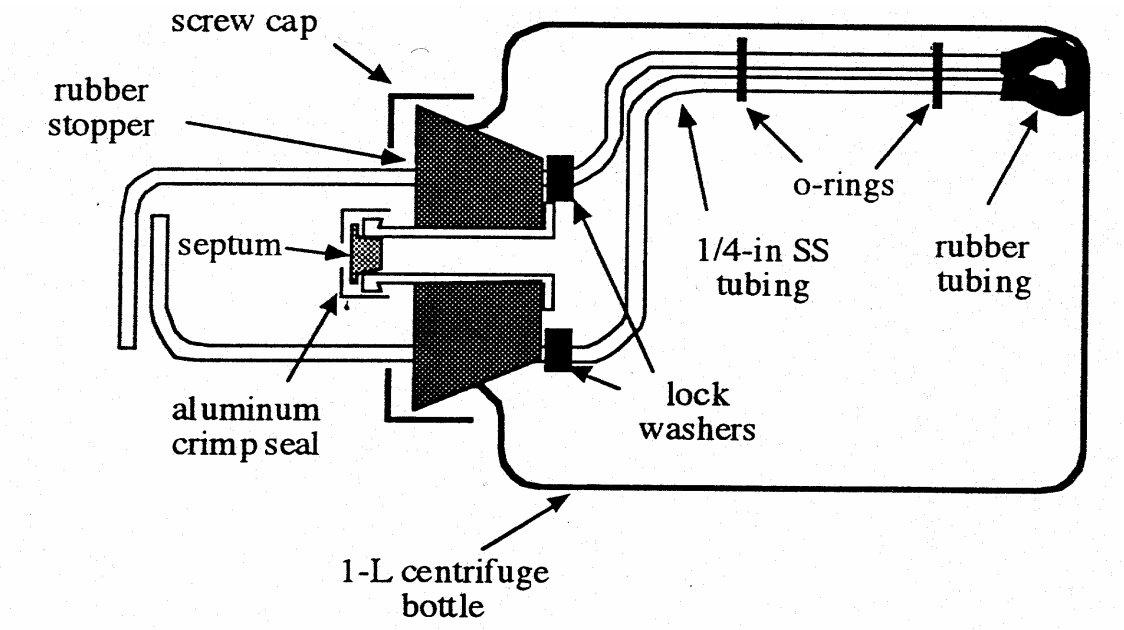

Figure 2.18. Centrifuge bottle fermentor (Ross and Holtzapple, 2001).

Media and Nutrients

The fermentation medium consisted of deoxygenated water, sodium sulfide, and cysteine hydrochloride (Appendix I). Dry nutrients were added to each fermentor to enhance the growth of the microorganisms. The dry nutrient mixture corresponds to the modified Caldwell and Bryant medium (Caldwell and Bryant, 1966). Dried chicken manure was also added a nutrient source.

Inocula

Marine inoculum was used from a previous fermentation of sugarcane bagasse/chicken manure (Fu, 2007). The original inoculum was gathered from the sediments of three coastal swamps in Galveston, Texas: East Beach, Harborside, and Sportman's Road. The sediment was collected from 0.5-m-deep holes into bottles filled with deoxygenated medium.

Inhibitor

Iodoform (CHI_3) was used as a methane inhibitor in these fermentations. A solution was prepared containing 20 g inhibitor/L ethanol. The inhibitor was kept in a tinted bottle due to its light sensitivity and was stored in the refrigerator until needed.

pH control

Ammonium bicarbonate was added during these batch fermentations to control the pH to 7. The ammonium salts produced during fermentation are beneficial because they inhibit methanogenesis. Additionally, the ammonium bicarbonate buffer provides a supplemental nitrogen source for microorganisms (Agbogbo, 2005).

Analytical Methods

Gas production was measured daily using an inverted graduated glass cylinder apparatus (water displacement apparatus) filled with a solution of 30% $CaCl_2$. $CaCl_2$ was added to minimize microbial growth in the water tank, reduce water evaporation, and prevent CO_2 adsorption.

A needle was inserted in the rubber septum of the fermentor to release the gas. The released gases displaced liquid inside the glass cylinder, and the amount displaced was measured by recording the difference in the initial water level of the cylinder (using the incremental measuring lines on the cylinder) and the final water level of the cylinder.

Methane and carbon dioxide production was measured by using a needle to take a 3-mL sample of gas through the rubber septum. The sample was analyzed using an Agilent 6890 series gas chromatograph equipped with a thermal conductivity detector (TCD). Samples were injected manually. Helium was used as the carrier gas, and the total run time per sample was 10 minutes.

The fermentation broth is a mixture of carboxylate salts and carboxylic acids. The carboxylic acid analysis procedure (Appendix J) converts the salts to their corresponding acids which allows the product concentrations to be measured as g carboxylic acid/L. To measure the acid production, a 2-mL sample was taken from the

fermentor every two days. Each sample was centrifuged and then mixed with equal parts (1 mL each) of an internal standard (4-methyl-*n*-valeric acid) and 3-M phosphoric acid. The samples were analyzed for carboxylic acid production using the Agilent 6890 series gas chromatograph equipped with a flame ionization detector (FID) and a 7683 series injector. Helium was used as the carrier gas, and the total run time per sample was 17 minutes.

CHAPTER III
ACOUSTIC CAVITATION

INTRODUCTION

Effective pretreatments should open the biomass structure to make it more accessible to enzymes (Ghosh and Singh, 1993). Smaller biomass particle sizes and larger biomass surface areas resulting from cavitation generate higher cellulose digestibilities. Acoustic cavitation reduces particle sizes likely resulting from erosion caused by collapsing gas bubbles. Additionally, acoustic cavitation appears to lower crystallinity. Preliminary studies have shown an increase in biomass digestibility when cavitation is used as a pretreatment step (Coward-Kelly, 2002).

Microcrystalline cellulose was sonicated from 0 to 150 minutes in 15-minute increments whereas raw knife-milled 10-mesh bagasse and knife-milled lime pretreated 10-mesh bagasse were sonicated for time lengths from 0 to 120 minutes as explained below. The effect of the acoustic cavitation pretreatment was assessed by enzymatic hydrolysis. The DNS assay was used to measure the resulting sugars. Each sample was run in triplicate.

RESULTS AND DISCUSSION

Sample Preparation

The sugarcane bagasse used throughout this work was kept in the freezer to maintain its freshness. On average, bagasse was stored in the freezer for six months before it was used for any experiments. Crystallinity samples were run in duplicate to determine the effect of storing the bagasse in the freezer. Figure 3.1 shows that there was no significant increase in crystallinity from storing the ball-milled bagasse in the freezer, within an error band of ± 2 standard deviations (approximately the 95% confidence interval). However, there was a slight increase in crystallinity from storing the raw knife-milled 80-mesh bagasse in the freezer. Therefore, the results obtained in

this work are considered conservative because fresh bagasse (not previously frozen) will be used industrially for the MixAlco process.

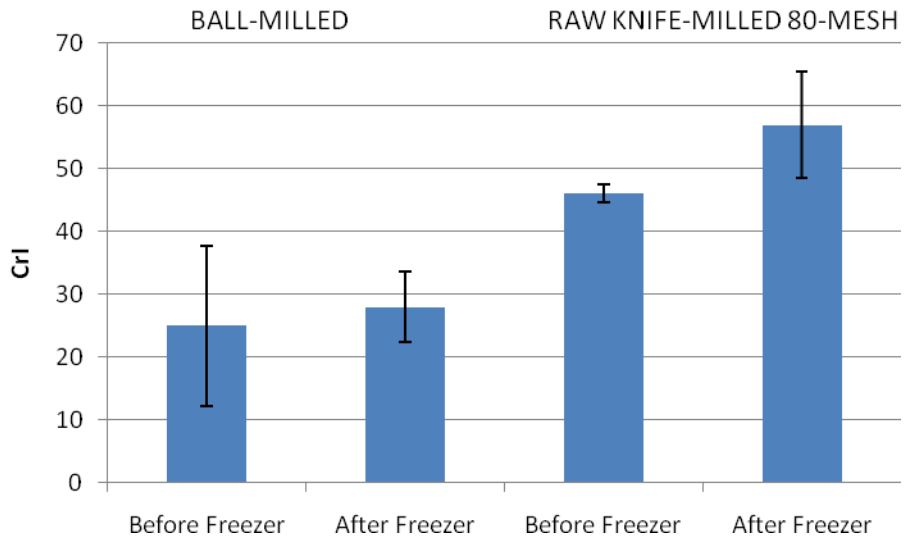

Figure 3.1. Effect of freezing on bagasse crystallinity (error bars = ± 2 standard deviations, n = 2).

After each pretreatment, samples were air-dried and ground before testing the crystallinity. Samples were ground using a 12-cup coffee grinder (Mr. Coffee Precision Coffee Grinder with Chamber Maid Cleaning System, Model #IDS77) on the fine setting for approximately 1 minute to achieve a homogenous sample. Grinding the samples improved the accuracy and repeatability of the crystallinity analysis, and there was no significant effect of the grinding on crystallinity as shown in Figure 3.2.

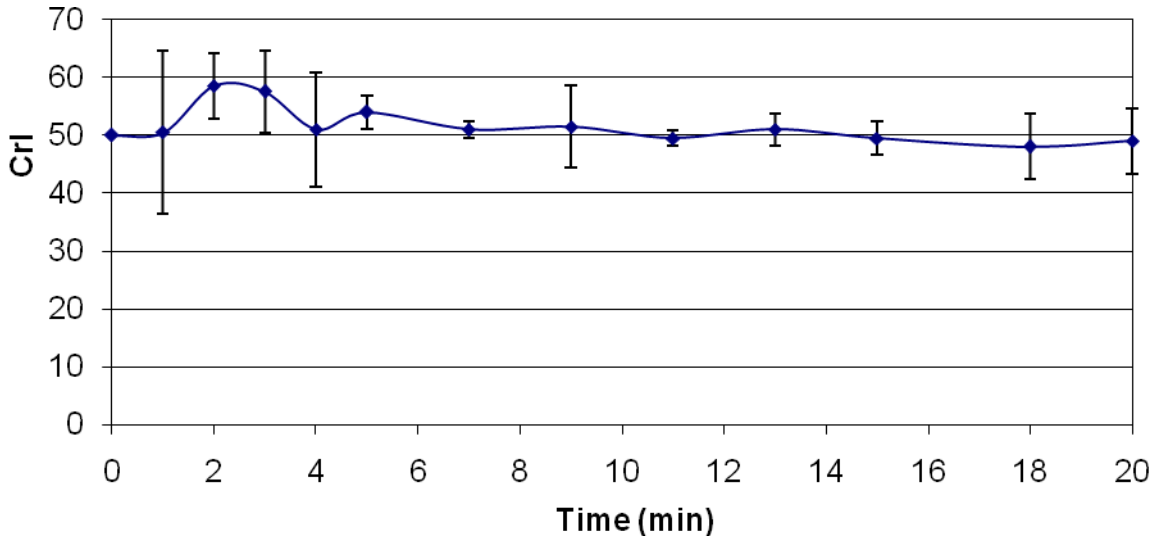

Figure 3.2. Effect of grinding samples after pretreatment on crystallinity (error = ± 2 standard deviations, n = 2).

The composition of the bagasse used in this work is shown in Table 3.1. Fresh bagasse was obtained from the W. R. Cowley Sugar House, a sugar mill in Santa Rosa TX. Its quality is designated as fresh because it was used fairly quickly after it was obtained. The 2-month laboratory lime pretreatment began approximately one month after obtaining the bagasse from the sugar house. It was stored in the freezer for one month before its use. The 1-month laboratory lime pretreatment was stored in the freezer for six months before its use. The bagasse designated as "old" was also obtained from the W. R. Cowley Sugar House; however, the "old" bagasse had been stored in the freezer for well over a year before it was used for the small-scale lime pretreatment.

Table 3.1. Composition of bagasse samples studied in this work.

Bagasse	Bagasse Quality[a]	Lignin %	Glucan %	Xylan %	Total[b] %
Raw knife-milled 10-mesh	Fresh	25	55	28	83
1 month unmilled lime-treated, laboratory scale, 50°C	Fresh	16	58	27	85
2 month unmilled lime-treated, laboratory scale, 50°C	Fresh	13	47	36	83
1 month knife-milled lime-treated 10-mesh, small scale, 55°C	Old	16	39	16	55

[a] Fresh bagasse was used within 6 months of receiving it. Old bagasse had been stored in the freezer for over a year.

[b] Total is equal to the summation of the glucan and xylan components.

Acoustic Cavitation Results

The microcrystalline cellulose results (Figures 3.3 and 3.4) indicate an increase in the 1-h and 3-d digestibilities after acoustic cavitation pretreatment. Compared to untreated microcrystalline cellulose, the 1-h and 3-day hydrolysis showed a 39% and 37% increase in digestibility, respectively. The 135-minute and 150-minute results dropped to that of the untreated microcrystalline cellulose. This is most likely due to a sonicator malfunction above treatment times of 120 minutes. After this time length, the sonicator casing became very hot to the touch and a loud screeching sound was emitted from the machine. Thus, for the subsequent bagasse runs, the maximum bagasse treatment time was limited to 120 minutes.

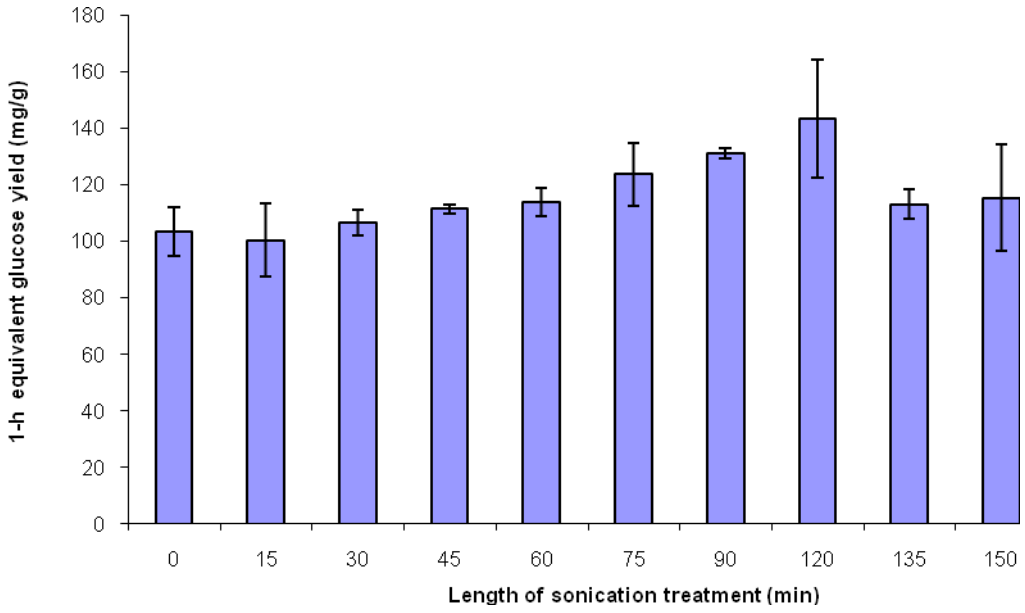

Figure 3.3. Effect of sonication treatment time on microcrystalline cellulose for 1-h enzymatic digestibility (error bars = ± 2 standard deviations, n = 3).

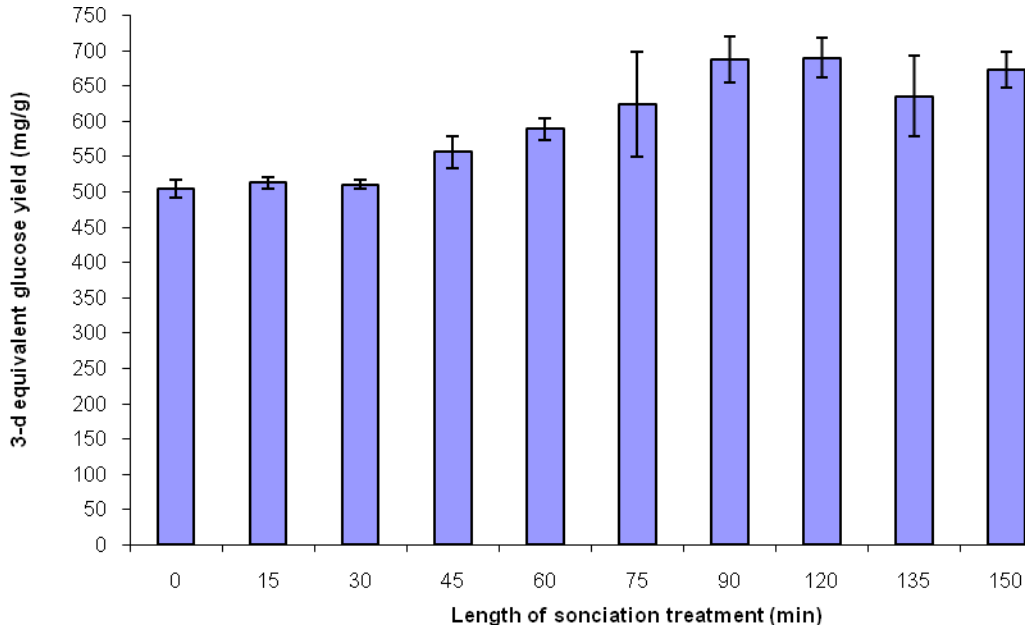

Figure 3.4. Effect of sonication treatment time on microcrystalline cellulose for 3-d enzymatic digestibility (error bars = ±2 standard deviations, n= 3).

Small-scale aerated lime pretreatment was performed on bagasse samples as described previously in Chapter II for 1 month at 55°C. Figures 3.5 and 3.6 show the results of sonication pretreatment on lime-treated bagasse. There is an increase in digestibility in lime-treated bagasse with no sonication treatment (t = 0 min) versus that of raw knife-milled 10-mesh bagasse. This results because lignin is removed during lime pretreatment giving the enzymes greater accessibility to the cellulose. However, based on a 95% confidence interval (2 standard deviations), sonicating lime-treated bagasse does not improve the 1-h and 3-d digestibility.

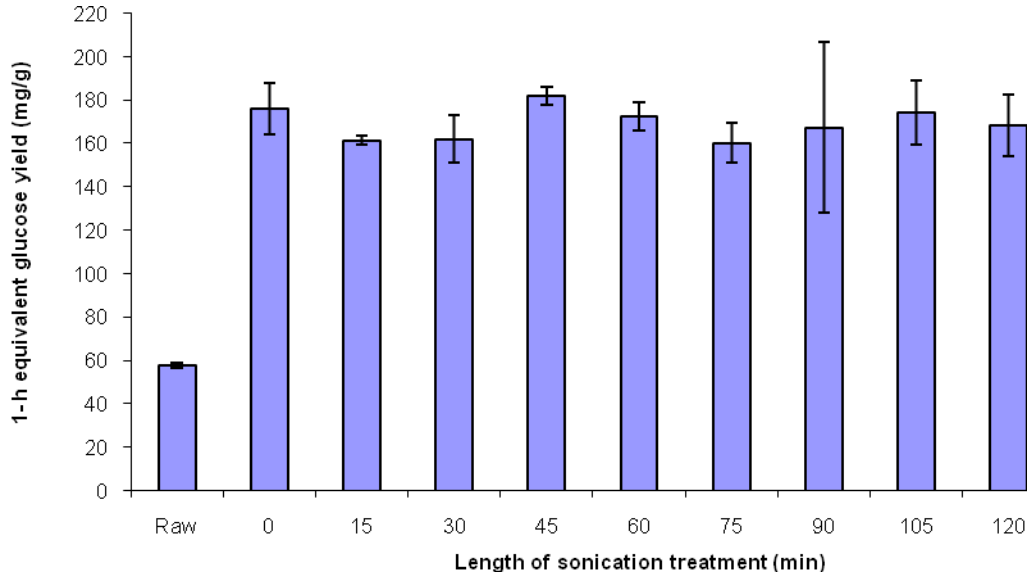

Figure 3.5. Effect of sonication treatment time on lime-treated bagasse for 1-h enzymatic digestibility (error bars = ±2 standard deviations, n = 3).

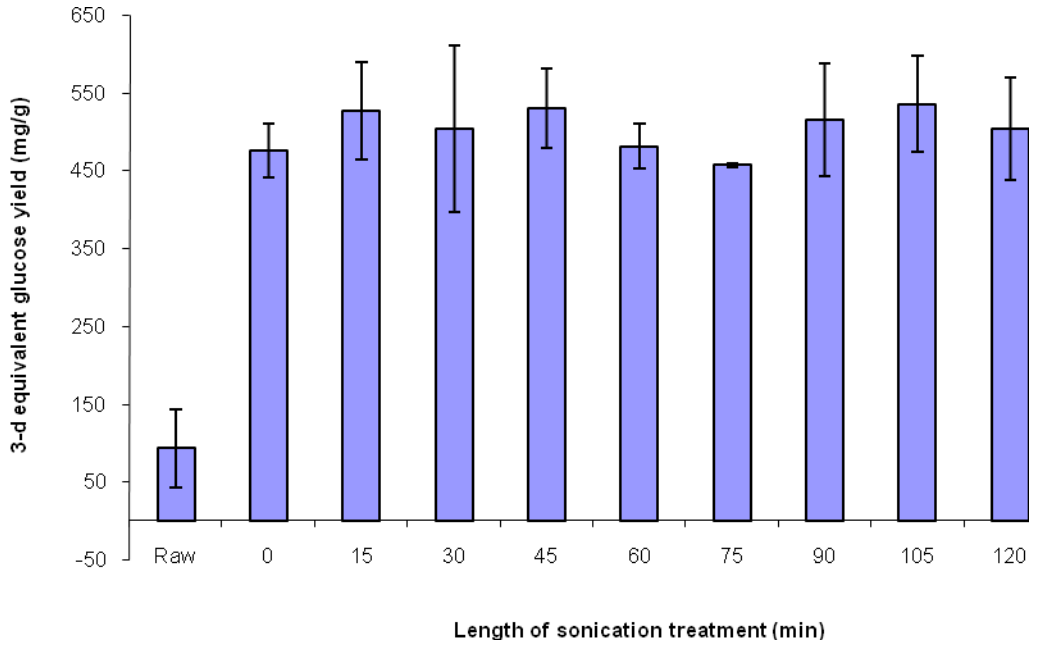

Figure 3.6. Effect of sonication treatment time on lime-treated bagasse for 3-d enzymatic digestibility (error bars = ±2 standard deviations, n = 3).

CONCLUSIONS

In this study, sonication successfully increased microcrystalline cellulose digestibility, yet there was no significant effect on lime-treated bagasse**.** Sonication may not be effective with lime-treated bagasse because it contains hemicellulose and lignin. (Note: Lime pretreatment removes ~50% of the lignin content.) The amorphous components may absorb the shock waves and protect the crystalline regions of cellulose.

CHAPTER IV
HYDRODYNAMIC CAVITATION

INTRODUCTION

Cavitation involves the formation, growth, and rapid collapse of gas or vapor-filled bubbles. There are two types of cavitation: acoustic and hydrodynamic. Hydrodynamic cavitation results when a moving fluid encounters a sudden change in velocity that results in a localized pressure drop. This can be accomplished in a pipe by throttling a valve downstream of a pump. Cavities form when the pressure near the valve falls below the vapor pressure of the fluid. The bubbles collapse downstream of the valve when the pressure is recovered. Current hydrodynamic cavitation applications include water treatment (Jyoti and Pandit, 2001), cell disruption for the recovery of enzymes (Balasundaram and Pandit, 2001), refining of wood pulp, and creating agitation in chemical reactors (Pandit et al., 1999). Acoustic cavitation is caused by pressure variations from ultrasonic waves passing through a fluid. This high-power, low-frequency ultrasound is usually used to create a permanent chemical or physical change in a substance (Shah et al., 1999).

Bubble size and bubble life play an important role in bubble dynamics. The maximum bubble size in cavitation defines the cavitation intensity. Larger bubbles collapse with a higher intensity which can cause greater effects on a substance than smaller bubbles. Because of the large number of exploding bubbles acting on the biomass during hydrodynamic cavitation, its molecular structure is altered so that the available surface area increases, which improves enzymatic digestibility. The scheme of hydrodynamic cavitation is shown in Figure 4.1.

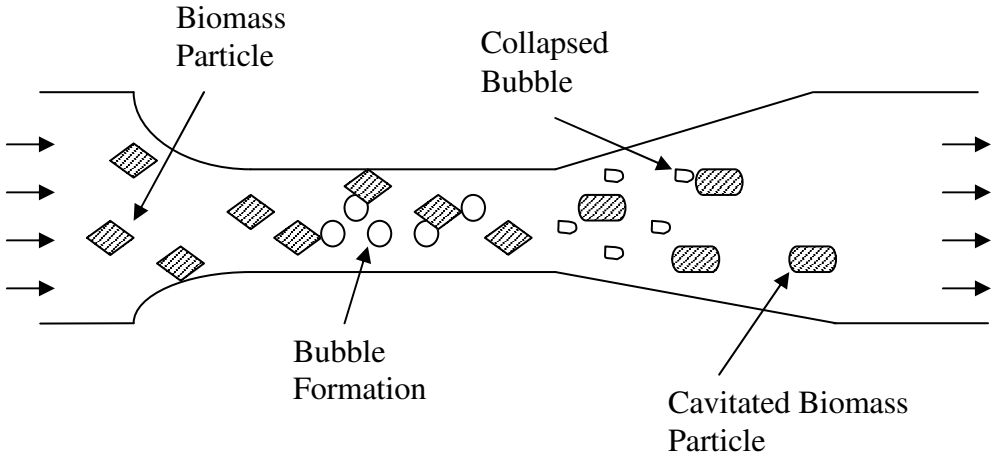

Figure 4.1. Scheme of cavitation in a venturi cavitator.

Hydrodynamic cavitation is easier and more economical to scale-up than acoustic cavitation (Gogate and Pandit, 2005). In addition, the numerous local low-intensity temperature and pressure pulses produced in hydrodynamic cavitation make it ideal for reactions that require moderately mild temperature and pressure conditions (Pandit and Gogate, 2000).

There are many factors that affect cavitation, including the viscosity and vapor pressure of the fluid, size and geometry of the chemical reactor, and the cavitation number or acoustic power and frequency. The more viscous the fluid used in cavitation, the higher the energy input needed to create cavitation. Vapor pressure also correlates inversely with energy input; a fluid with a low vapor pressure requires more energy to generate cavitation. The size and geometry of the chemical reactor will affect the efficiency of cavitation (Shah et. al., 1999).

The cavitation number, C_v, measures the resistance of the flow to cavitation. It is a dimensionless parameter and is given by the following equation:

$$C_v = \frac{P_f - P_v}{1/2\rho U^2} \tag{4.1}$$

where P_f is the downstream pressure, P_v is vapor pressure of the fluid, ρ is the density of the fluid, and U is the average velocity near the orifice. A high cavitation number indicates cavitation will not likely occur and vice versa. If cavitation is already occurring, lowering the cavitation number by decreasing the pressure or by increasing the flow rate will increase the cavitation intensity. Raising the cavitation number may stop cavitation altogether (Shah et. al., 1999). At low cavitation numbers, bubbles may combine to form larger bubbles or bubble clusters, which are carried away with the liquid thereby reducing cavitation effectiveness (Kumar et al, 2000).

Smaller biomass particle sizes and larger biomass surface areas as a result of cavitation generate higher cellulose digestibilities. Hydrodynamic cavitation pretreatment swells the biomass and creates a larger accessible area for enzymatic hydrolysis, which is important for successful pretreatment (Ghosh and Singh, 1993). Preliminary studies have shown an increase in biomass digestibility when cavitation is used as a pretreatment step (Coward-Kelly, 2002).

COMPUTATIONAL FLUID DYNAMICS

Before constructing the venturi cavitator, it was simulated using computation fluid dynamics (CFD). Computational fluid dynamics is advantageous over experimental fluid dynamics for four main reasons:

1. Significantly reduce lead time in design and development
2. Simulate flow conditions not reproducible in experimental model tests
3. More detailed and comprehensive information
4. Lower energy consumption

Ultimately, CFD is a quick and inexpensive method of solving complex problems. It is an established tool for flow-based physical simulation (Watanawanavet, 2005).

The geometry of the cavitator was modeled in GAMBIT, and the process parameters were modeled using Fluent 2d. GAMBIT is a state-of-the-art preprocessor for engineering analysis and is Fluent's geometry and mesh generation software (Fluent, 2007). The simulation process is summarized below in Figure 4.2.

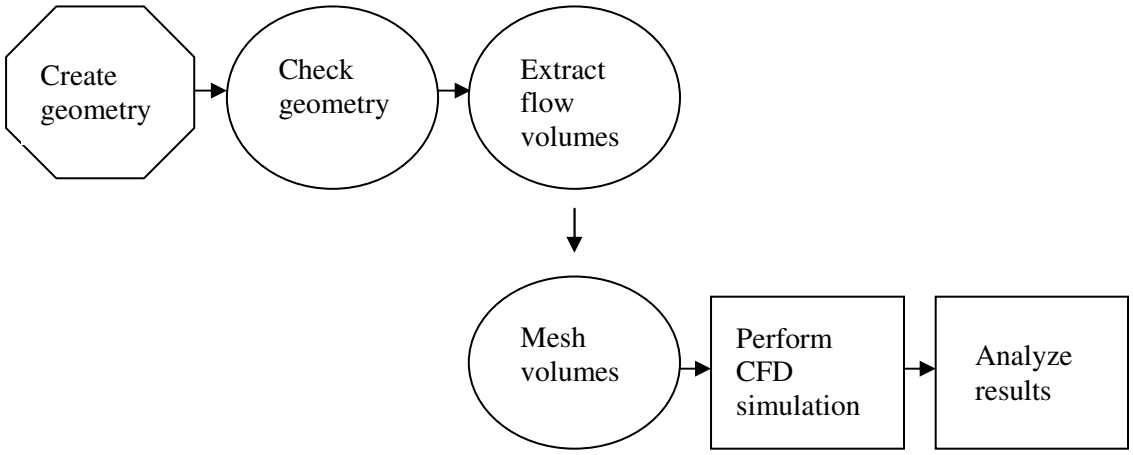

Figure 4.2. CFD simulation flowchart (adapted from Fluent, 2007).

The process begins with the geometric design or the geometric shape of the desired object to be modeled. It is important that there are no breaks in the geometric lines of the object so that the simulator will function properly. This is why the geometry check is important. CFD deals with flow through or around solid objects and this step is represented by "Extract flow volumes." All of the aspects associated with the flow around the object being modeled including fluid type and fluid boundaries fall within this step. Afterwards, the object is meshed to specification, exported into the solver for simulation, and finally the results are analyzed (Fluent, 2007).

As recommended by Somsak Watanawanavet, a Texas A&M doctoral student with four years experience in CFD modeling, the simulation was specified using steady-state 2-D compressible flow and the κ-ε turbulence model. The geometry in GAMBIT was drawn using the axi-symmetric mode around a symmetric axis. Figure 4.3 shows the boundary conditions specified in GAMBIT, and Table 4.1 details the selections made to model the cavitator.

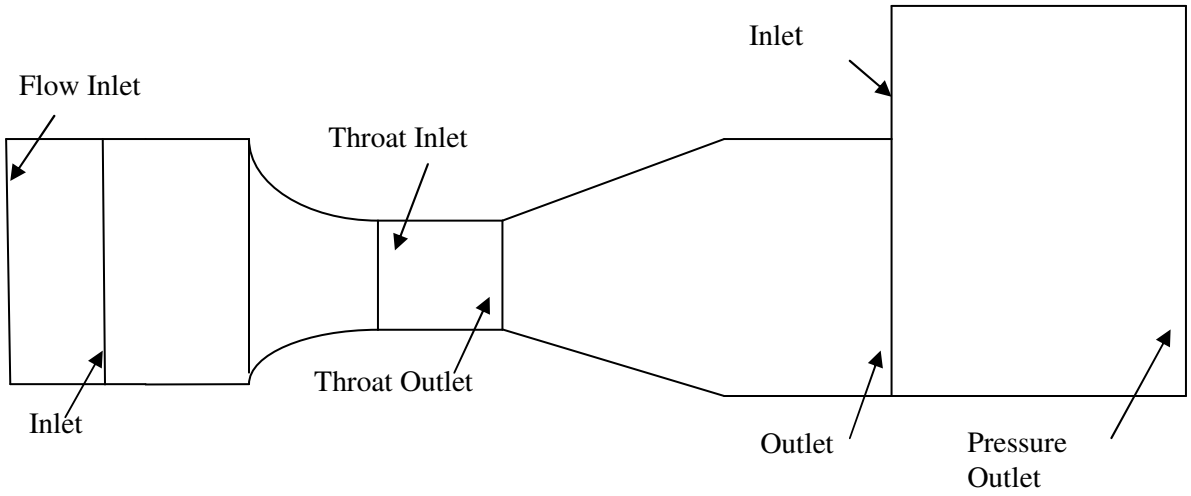

Figure 4.3. Schematic of the cavitator showing boundary conditions.

Table 4.1. Parameters specified in CFD cavitator model.

Parameter	**Selection**
Numerical Solver	Segregated
Turbulence Model	Standard κ-ε model
Boundary Conditions	
Flow inlet	Mass flow inlet
Inlet	Interior
Throat Inlet	Pressure Inlet
Throat Outlet	Interior
Outlet	Interior
Pressure Inlet	Pressure Inlet
Pressure Outlet	Pressure Outlet

Both the throat length and throat diameter of the cavitator were optimized using CFD to determine which gave the greatest pressure drop across the throat while maximizing the overall pressure recovery from the inlet of the cavitator to the outlet of the cavitator. Based on the results of the aforementioned criterion in numerous simulations performed in GAMBIT and Fluent 2d, two final designs were chosen: one used a throat diameter of 20% of the overall diameter, or 0.762 cm, and the second design used a throat diameter of 15% of the overall pipe diameter, or 0.572 cm. The schematic generated from GAMBIT for the 20% throat diameter is shown in Figure 4.4. Both designs used a throat length of 1 cm which is explained in the following section.

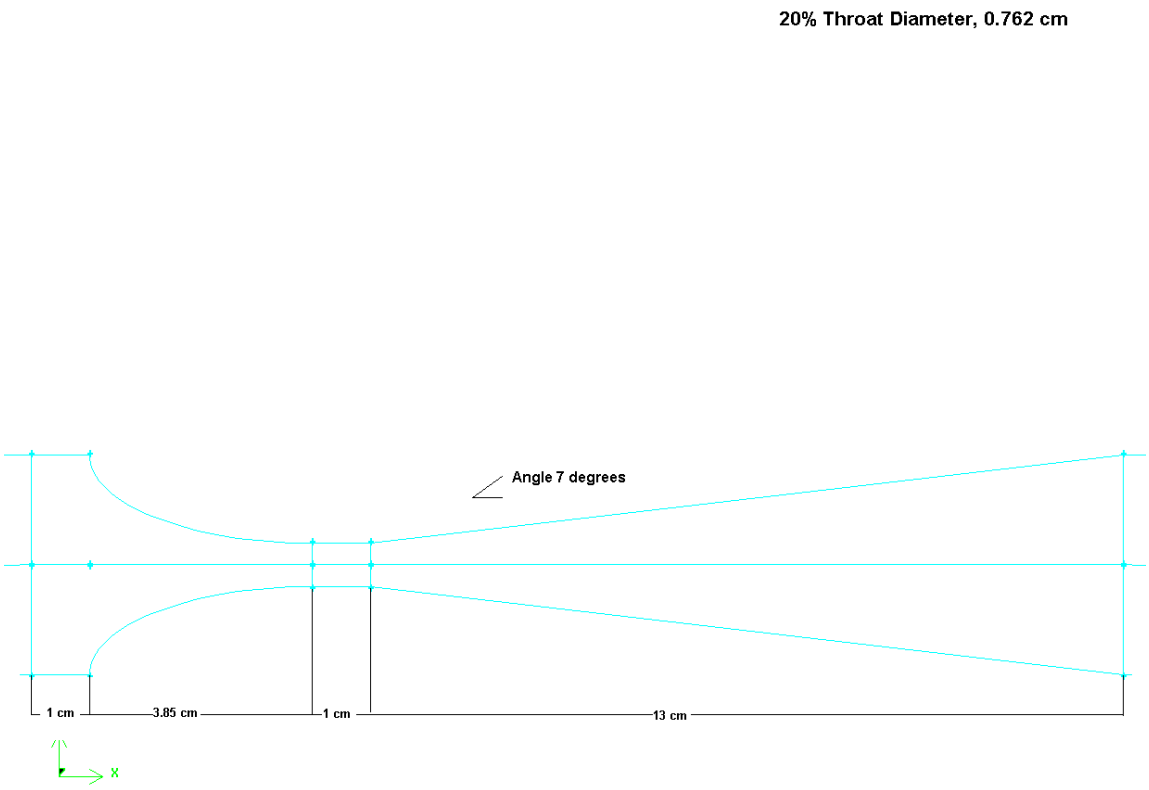

Figure 4.4. GAMBIT schematic of venturi cavitator with 0.762 cm throat diameter. The inlet and outlet diameters are 3.81 cm.

Previous results obtained by Coward-Kelly (2002) showed that a pressure drop of approximately 4 atm from the cavitator inlet to the throat was sufficient to produce cavitation capable of increasing bagasse digestibility. Therefore the best cavitator design was chosen as the one that gave a pressure drop of approximately 4 atm. Based on the CFD results, the optimum throat diameter was chosen as 20% of the pipe diameter or 0.762 cm. Figure 4.5 displays the pressure drop along the length of the cavitator for the 20% throat diameter cavitator.

For each of the pressures that were input (specified by the user) into the simulation ranging from 1 to 3 atm, the graph shows the subsequent calculated pressures from Fluent 2d. Each input pressure has four calculated data points. The first point represents the cavitator inlet. The second and third points represent the throat inlet and

throat outlet, respectively, and the fourth data point represents the cavitator outlet. The CFD software allows for negative pressures, which are physically unrealistic. The CFD software does not model the cavitation process, so any pressure calculated to be below the vapor pressure of water is also unrealistic. If a pressure is calculated to be below the water vapor pressure, cavitation will occur.

Figure 4.5 shows that for the 20% diameter at each input pressure, the calculated pressure drop from the cavitator inlet to the throat inlet is approximately 4.5 atm. Thus, it corresponded closely with previous experimental results mentioned above and was chosen as one of the designs to be constructed. An additional design of 15% of the cavitator diameter or 0.572 cm was also constructed for comparison purposes. (For clarity throughout the rest of this thesis, the 15% throat diameter cavitator will be referred to as Cavitator A and the 20% throat diameter cavitator as Cavitator B.)

The vapor pressure of water is shown in Figure 4.5 for 25^{o}C as 0.032 atm. It was important that the throat pressure fall below the vapor pressure of water to allow cavitation to occur. The throat length was chosen based on which one produced the smallest pressure drop across the throat. As an example, Figure 4.6 shows that the 1-cm throat length gives the smallest pressure difference across the throat for Cavitator B when the inlet pressure was kept constant (as specified by the user). Accordingly, the throat length of 1 cm was selected for both Cavitators A and B.

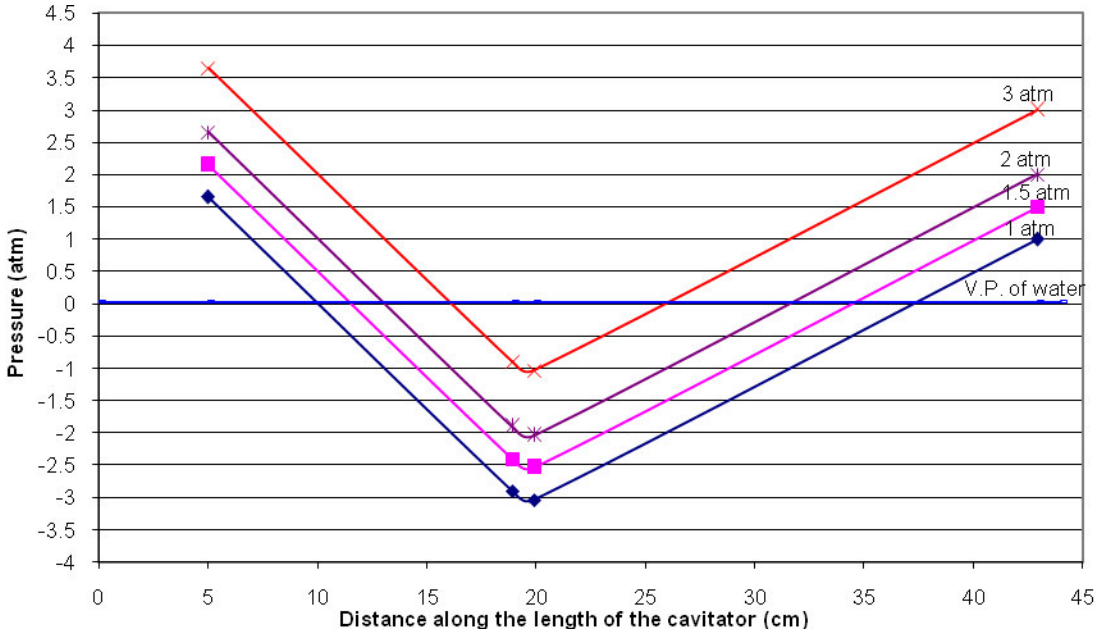

Figure 4.5. CFD calculated pressures along the length of Cavitator B.

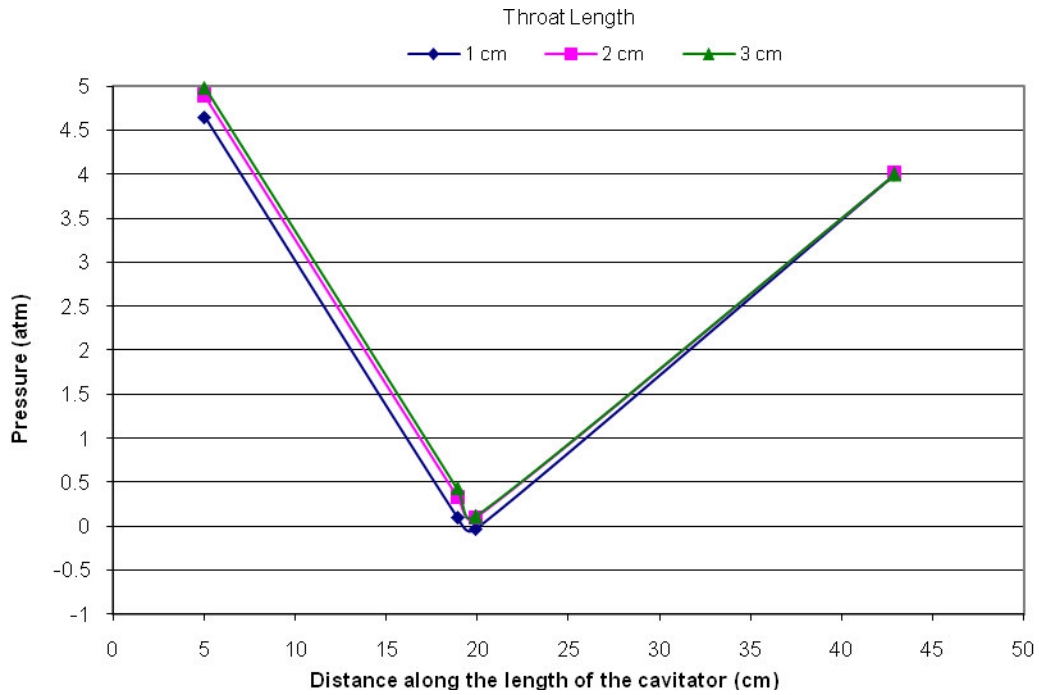

Figure 4.6. CFD calculated pressure as the throat length varies for Cavitator B.

After the design specifications were produced using CFD, the cavitators were constructed of Plexiglass in the chemical engineering workshop. After construction, each cavitator was incorporated into the hydrodynamic cavitation experimental apparatus at the pilot plant. Figures 4.7 to 4.11 show the cavitator before being installed at the pilot plant, after installation, and during an experimental test of raw knife-milled 10-mesh bagasse at the pilot plant.

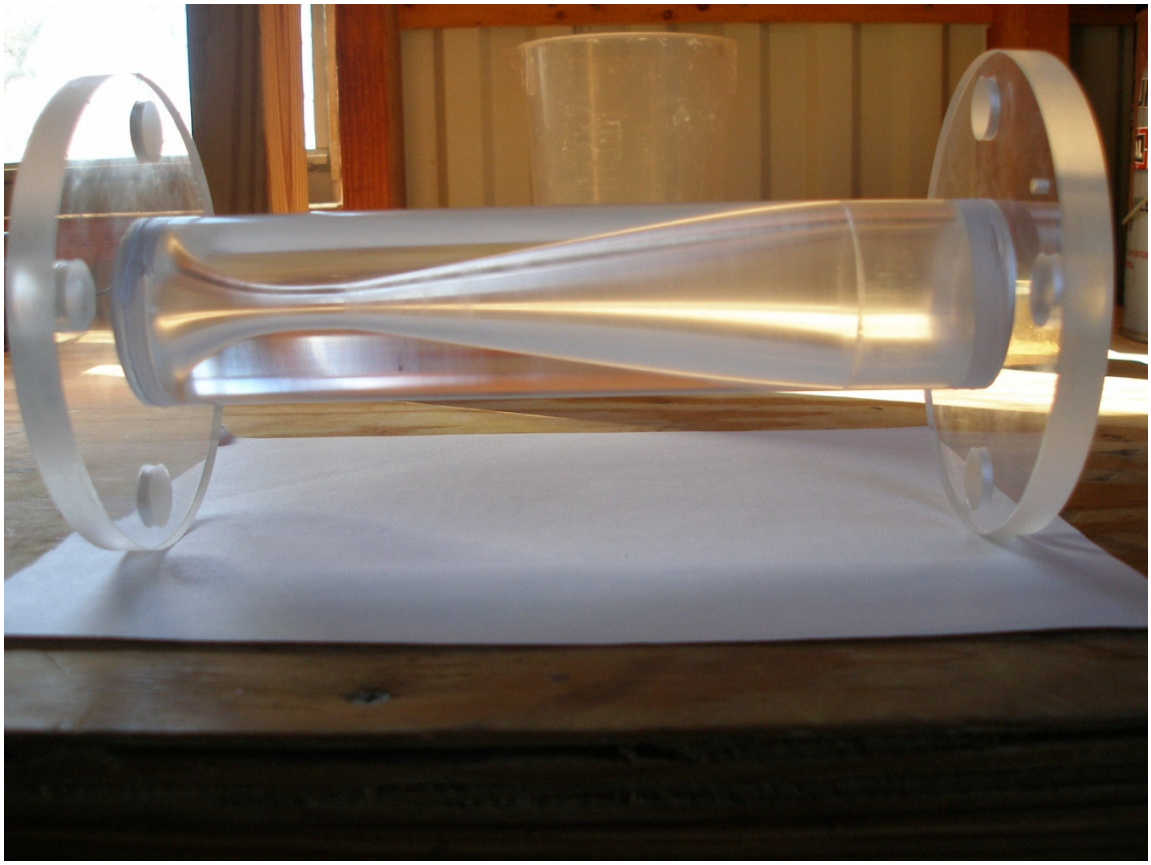

Figure 4.7. Cavitator B before installation into the hydrodynamic cavitation apparatus.

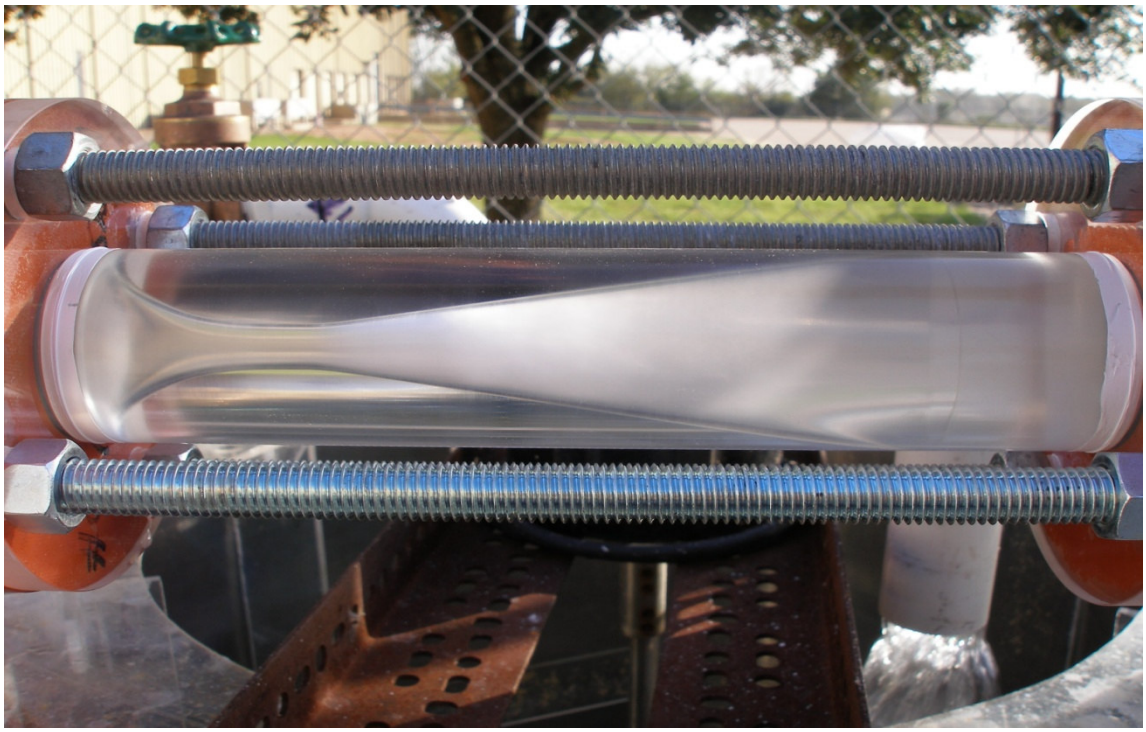

Figure 4.8. Cavitation bubbles forming in water across the throat of the cavitator and collapsing in the expansion section of the cavitator.

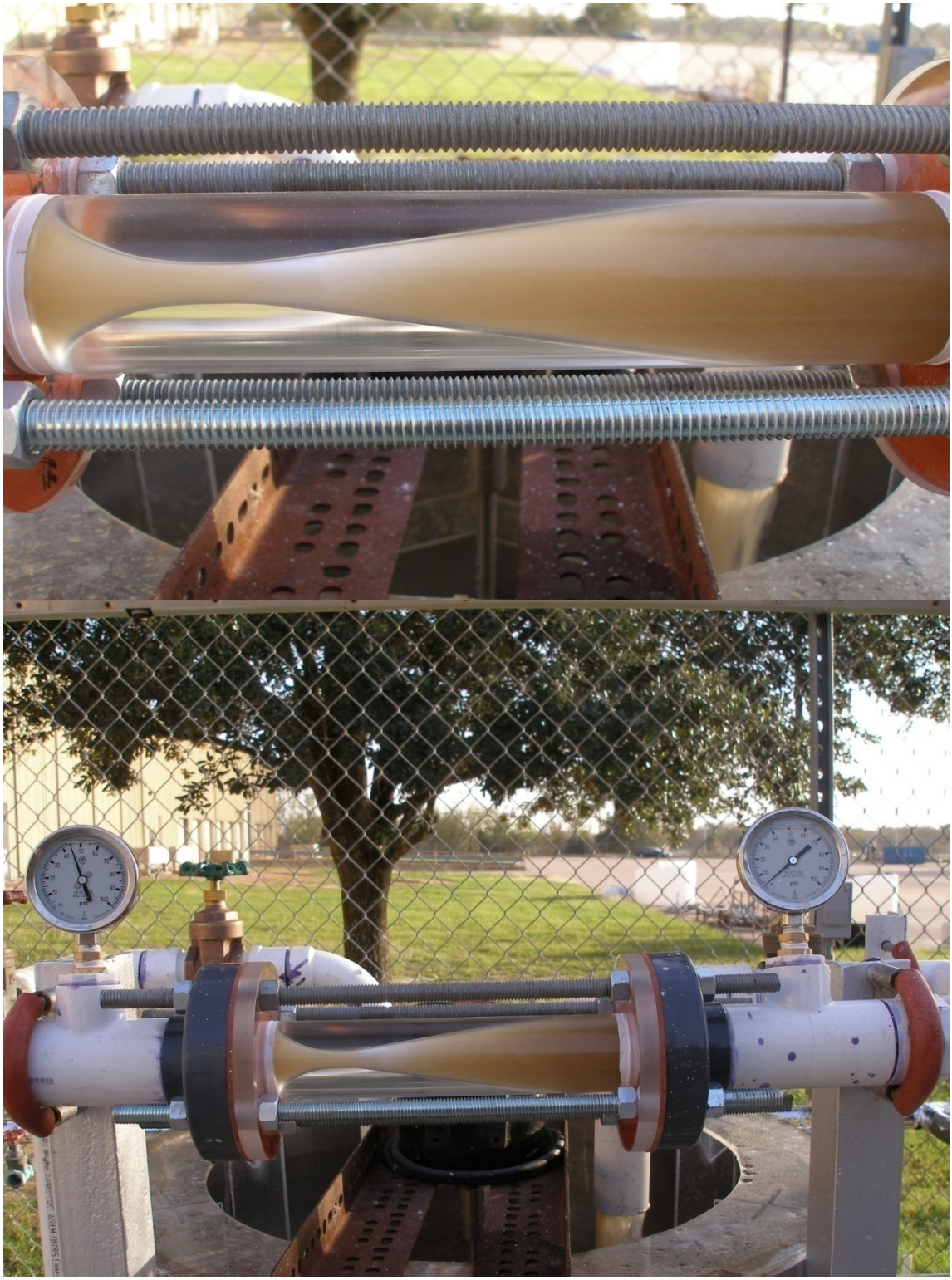

Figure 4.9. Testing raw knife-milled 10-mesh bagasse in the cavitator.

Figure 4.10. The pilot plant experimental apparatus includes a 200-L jacketed mixing tank, pump, cavitator, and valves.

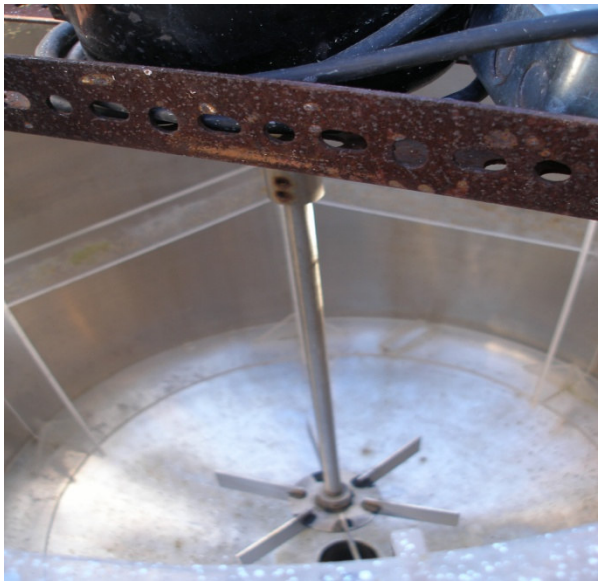

Figure 4.11. Close-up of mixer inside mixing tank.

RESULTS AND DISCUSSION

Tests were performed without the cavitator using raw knife-milled 10-mesh bagasse to determine if the centrifugal pump alone was able to decrystallize the bagasse. Therefore, a portion of straight 1.5-in Plexiglass pipe (the same length as the cavitator) was installed in the experimental set-up instead of the cavitator for this test. The experimental conditions are given in Table 4.2 for all of the hydrodynamic cavitation tests. (Note: The 100% diameter pipe is represented as Cavitator C.) In preliminary studies, Coward-Kelly (2002) produced his best results using an inlet pressure of 50 psig and an outlet pressure of 10 psig because he found that higher outlet pressures caused bubbles to collapse with greater intensity. An outlet pressure of 14 psig was chosen because it was the maximum pressure that could be obtained by closing the valve downstream of the cavitator while keeping cavitation from occurring in the downstream piping (as could be observed by the returning liquid into the tank). Likewise, the maximum inlet pressures that could be obtained for Cavitators A and B were 39 and 41 psig, respectively. All tests were run in duplicate.

The enzymatic procedure was modified for the cavitation pretreatment samples and shock tube pretreatment samples. Zhu et al. (2007) recently discovered that crystallinity greatly affects the initial hydrolysis rate, whereas lignin content plays a more important role in the extent of digestion. Instead of taking the initial hydrolysis rate samples at 1 h, samples were taken at 6 h because the 1-h sample released too little sugar to obtain accurate, reliable measurements.

Table 4.2. Hydrodynamic cavitation experimental conditions.

Cavitator	**Cavitator Throat Diameter (cm)**	**Inlet Pressure (psig)**	**Outlet Pressure (psig)**	**Average Flow (L/s)**	**Average Temperature (^{o}C)**
A	15% (0.572)	39	14	1.13	22
B	20% (0.762)	41	14	1.25	22
C	100% (3.81)	0	0	0.97	22

The CFD model predicted an inlet pressure of 68 psi and an outlet pressure of 59 psi, which gives a pressure drop of 9 psi for Cavitator B. Due to the constraints of the system, those exact inlet and outlet pressures could not be tested. Based on the maximum inlet and outlet pressures achieved, the experimental results for Cavitators A and B give pressure drops of 25 and 27 psi, respectively, which were approximately three times higher than the predicted value. The Fluent 2d software used in this study did not have the capability of modeling the cavitation process; therefore, CFD did not produce an accurate model of the hydrodynamic cavitation system.

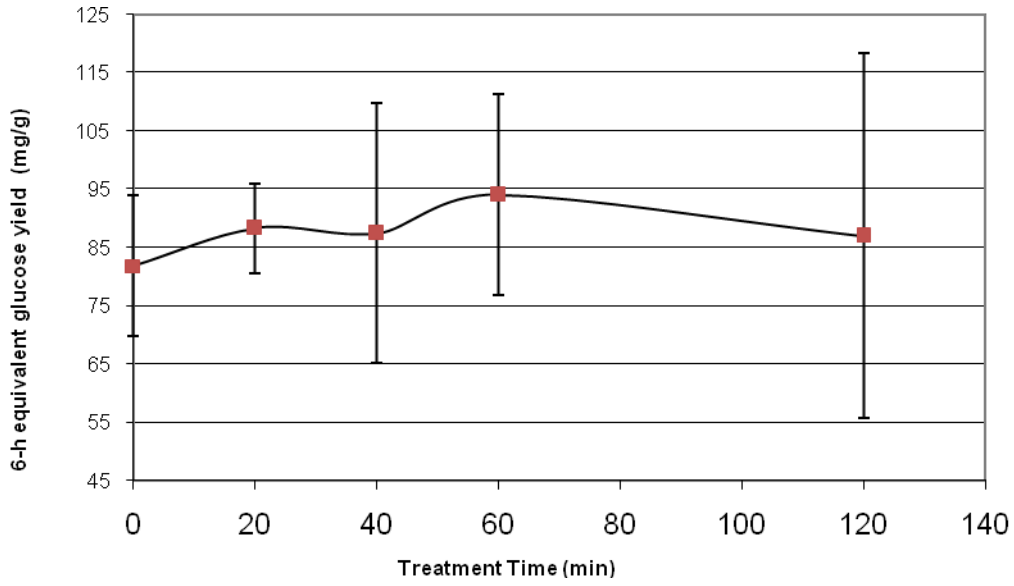

Figure 4.12. Cavitator C 6-h enzymatic hydrolysis results (error bars = ± 2 standard deviations).

Figures 4.12 and 4.13 show the enzymatic hydrolysis results for Cavitator C. Statistically, there is no effect from Cavitator C. This experiment showed no statistically significant change in crystallinity or enzymatic hydrolysis (Figures 4.14 to 4.20) for Cavitator A, B or C.

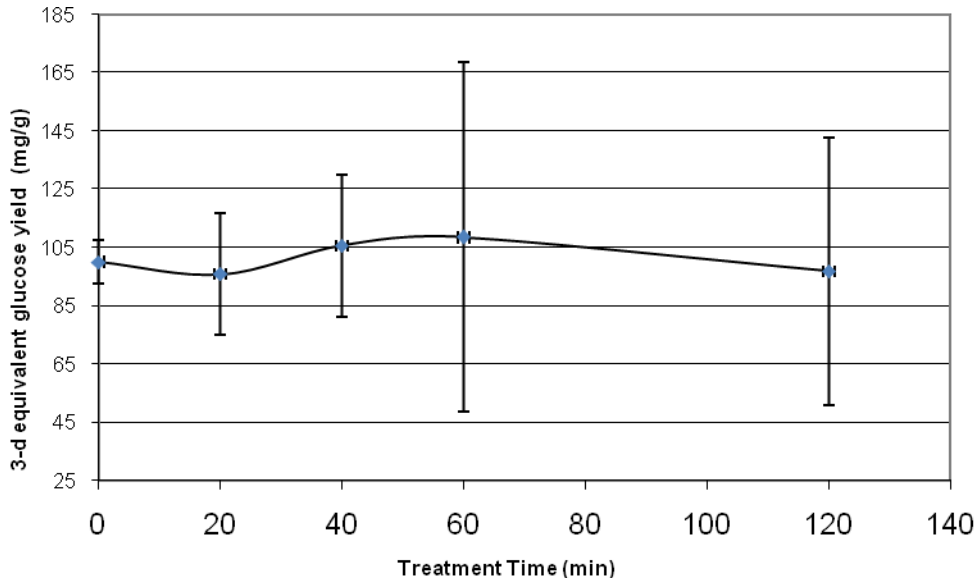

Figure 4.13. Cavitator C 3-d enzymatic hydrolysis results (error bars= ± 2 standard deviations).

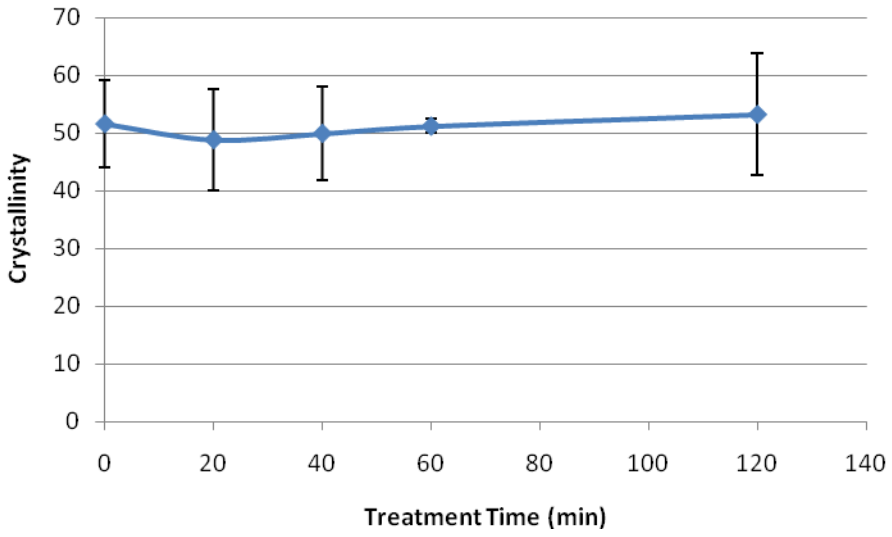

Figure 4.14. Cavitator C crystallinity results (error bars = ±2 standard deviations).

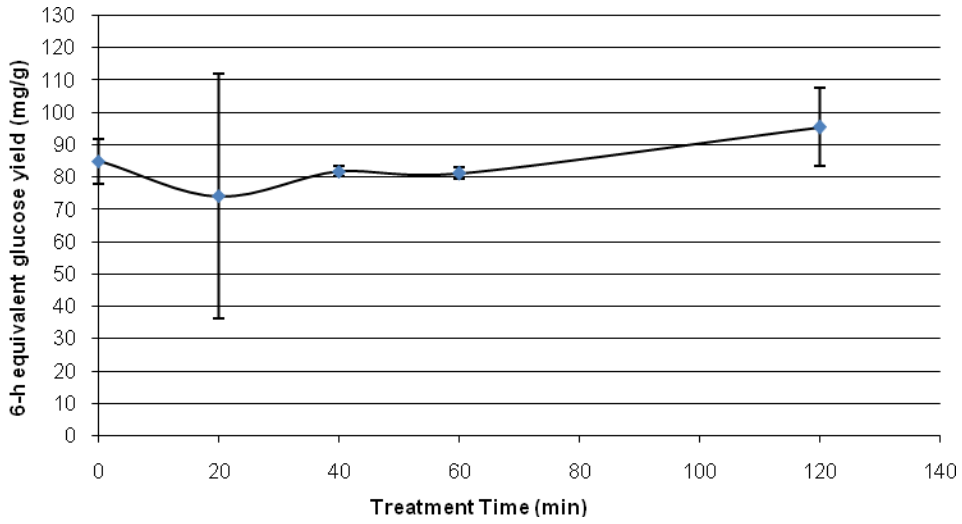

Figure 4.15. Cavitator A 6-h enzymatic hydrolysis results (error bars = ±2 standard deviations).

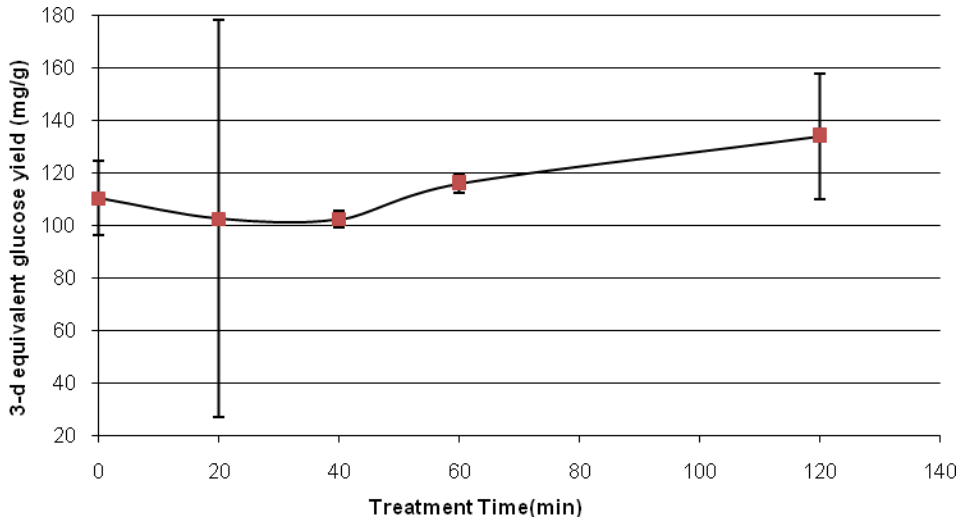

Figure 4.16. Cavitator A 3-d enzymatic hydrolysis results (error bars = ±2 standard deviations).

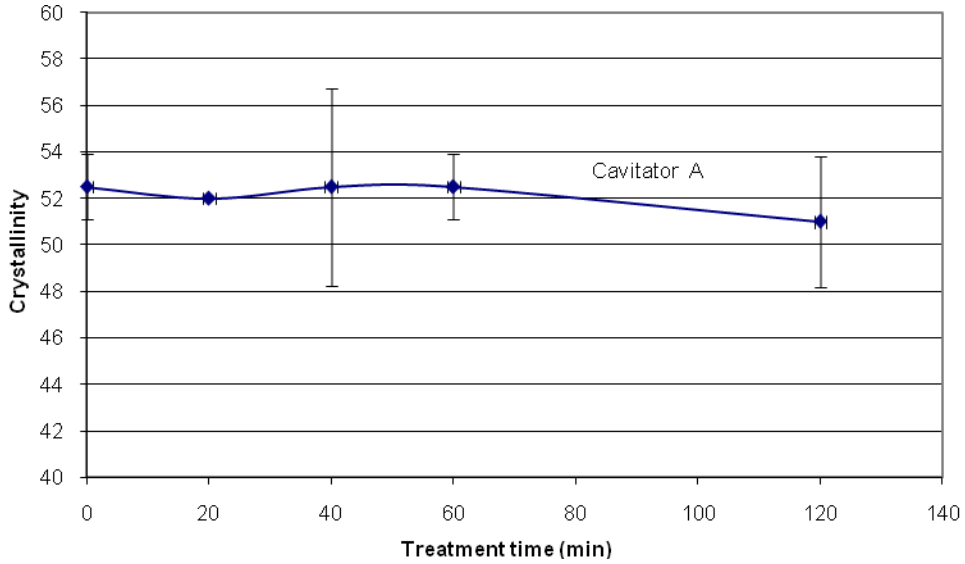

Figure 4.17. Cavitator A crystallinity (error bars = ±2 standard deviations).

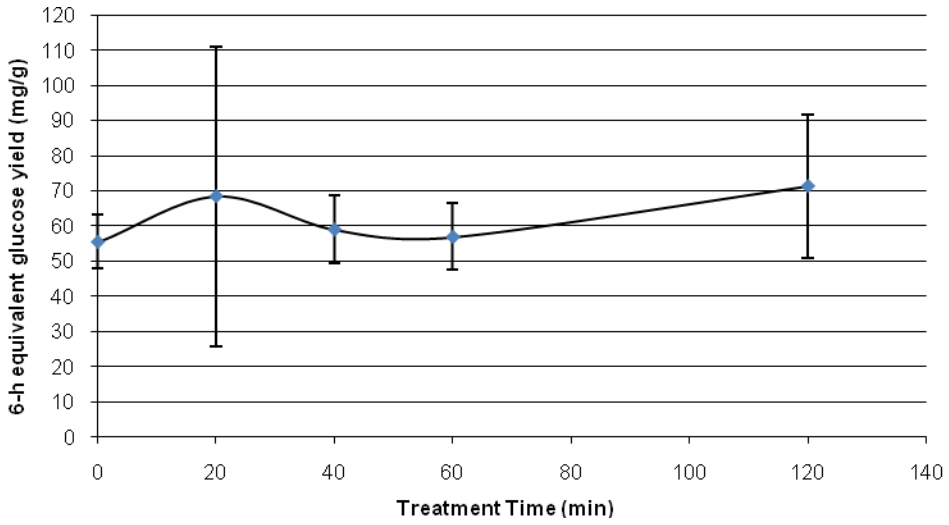

Figure 4.18. Cavitator B 6-h enzymatic hydrolysis results (error bars = ±2 standard deviations).

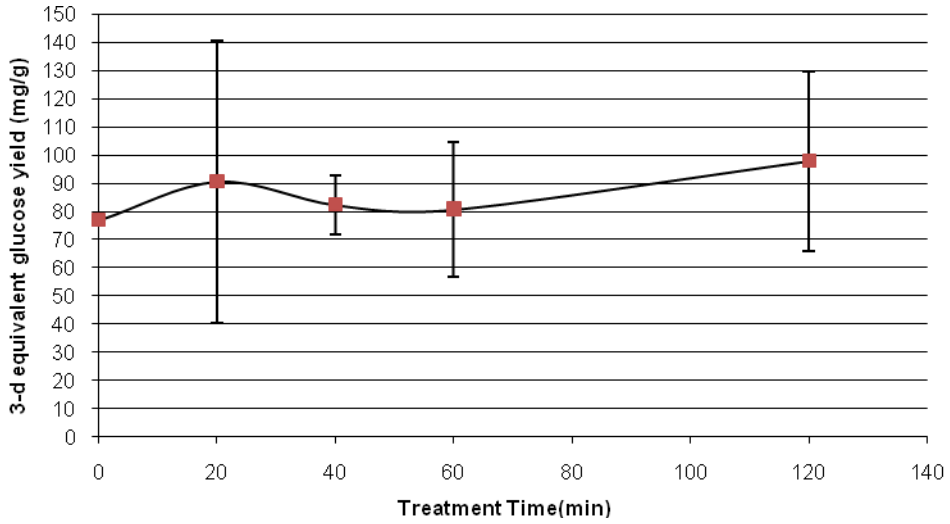

Figure 4.19. Cavitator B 6-h enzymatic hydrolysis results (error bars = ±2 standard deviations).

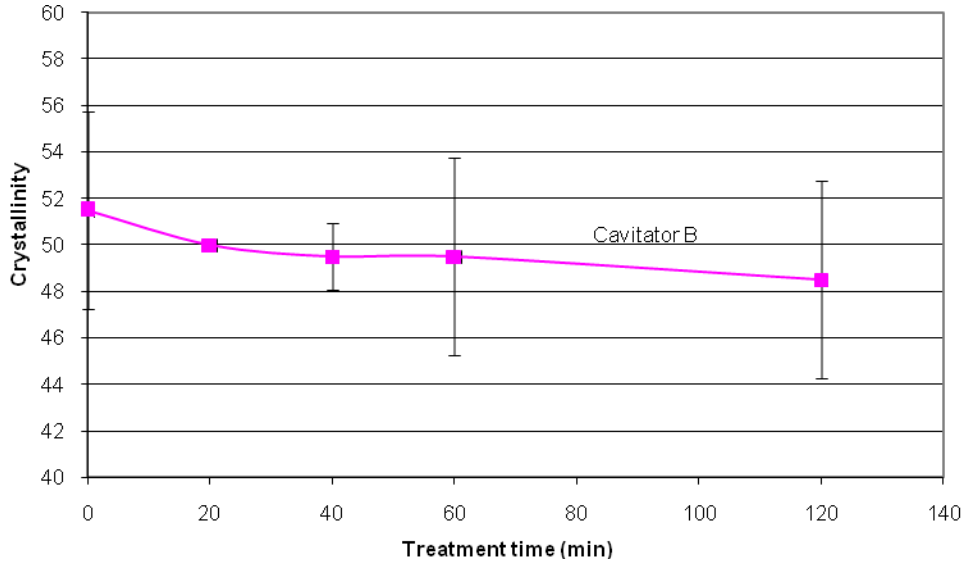

Figure 4.20. Cavitator B crystallinity (error bars = ±2 standard deviations).

A short-term aerated lime pretreatment was performed on bagasse samples as described previously by Chang et al., (1998) for 2 h at 100°C. The recommended lime loading of 0.1 g $Ca(OH)_2$/g dry biomass and water loading of 10 mL/g of biomass was used. The effect of hydrodynamic cavitation on lime-treated knife-milled 10-mesh bagasse is given in Figures 4.21 and 4.22. Hydrodynamic cavitation was not able to reduce the crystallinity of the lime-treated knife-milled 10-mesh bagasse. (Enzymatic hydrolysis was not performed on lime-treated samples.)

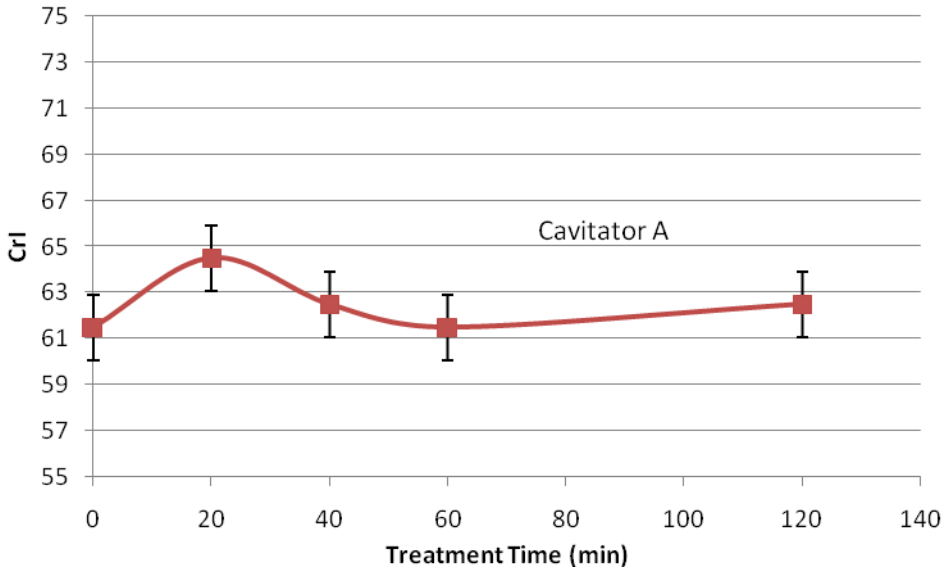

Figure 4.21. Effect of cavitation on crystallinity for lime-treated knife-milled 10-mesh bagasse for Cavitator A (error bars = ± 2 standard deviations).

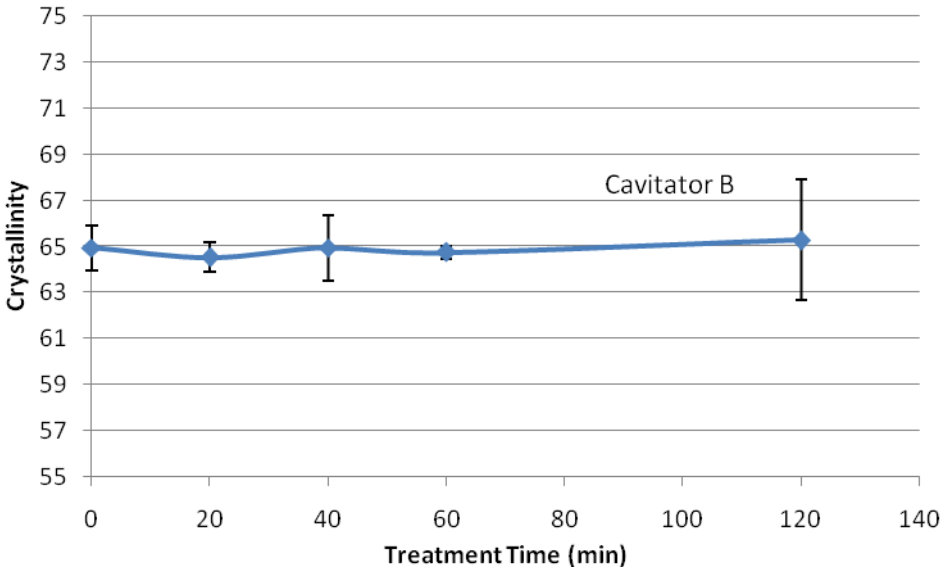

Figure 4.22. Effect of cavitation on crystallinity for lime-treated knife-milled 10-mesh bagasse for Cavitator B (error bars = ± 2 standard deviations).

The power required for each of the cavitators can be calculated from the following equation:

$$\text{Power} = Q\,\Delta P \tag{4.2}$$

where Q is the volumetric flow rate of the liquid, and ΔP is the difference in the pressure between the inlet and outlet of the cavitator. Energy consumption can be calculated from the following equation:

$$\text{Energy} = \frac{\text{Power (kW)} \times \text{Treatment time (h)}}{\text{Quantity of biomass treated (kg)}} \tag{4.3}$$

Table 4.3 summarizes the power required for each cavitator based on the operating conditions given in Figure 4.13. It also shows the energy required to treat 0.55 kg of bagasse for 2 hours. Assuming an electricity costs of $0.08/kWh, the energy cost is $96/tonne.

Table 4.3. Summary of power required for each cavitator.

Cavitator	**Average Q (m^3/s)**	**ΔP (Pa)**	**Power (W)**	**Energy needed for a 2-h treatment (kWh/kg biomass)**
A	0.0011	287511	309	1.12
B	0.0013	273722	359	1.31

CONCLUSIONS

In preliminary studies performed by Coward-Kelly (2002), it was determined that the highest increase in digestibility could be obtained by using cavitation treatment first and following that with lime pretreatment. Due to time constraints, this condition was not tested; instead, raw knife-milled 10-mesh bagasse was tested alone. Results from Coward-Kelly showed a 22% increase in 3-d digestibility for raw knife-milled 10-mesh bagasse. This study gives a 22% increase in 3-d digestibility for Cavitator A and a 27% increase for Cavitator B; however, at a 95% confidence interval, these results are not significant.

The amount of error produced in this study was too large to determine any effect of cavitation pretreatment on raw knife-milled 10-mesh bagasse or lime-treated knife-milled 10-mesh bagasse. Some of the error could possibly be inherent to the cavitation process. Ultimately, the energy cost of hydrodynamic cavitation is about $96/tonne, which is too expensive to be economical.

CHAPTER V
SHOCK TUBE PRETREATMENT

INTRODUCTION

A simple shock tube is usually a steel pipe in which a low-pressure gas and a high-pressure gas are separated by a diaphragm. The diaphragm bursts open under predetermined conditions and produces a shock wave. The shock tube as a wave reactor has been widely used in kinetic studies to examine the molecular decomposition of gases, oxidation reactions, and reactions involving aerosols, to name a few (Bhaskaran and Roth, 2002). However, studies have not been done using shock tubes as a means to decrystallize biomass.

MATERIALS AND METHODS

The shock tube shown in Figure 5.1 was 22 inches long and was constructed of 4-in Schedule 80 steel pipe with flanged ends. The maximum allowable pressure was 2000 psi. Originally, the shock tube was located inside a 55-gallon metal drum filled with sand to provide a safety barrier to the user. A metal cylinder was inserted into the metal drum to surround the shock tube so it could be easily removed without disturbing the sand. Later, the shock tube tests were performed behind steel plates to eliminate the need to lift the heavy shock tube. A rupture disk was located between the bottom flanges as an additional safety measure in the event of overpressure within the tube.

Figure 5.1. Shock tube photograph.

Appendix D details the procedure for loading and unloading the shock tube. First, tests were run to find the optimal water content. Then, the water content was controlled while varying the bagasse loading to find the optimal bagasse loading. Finally, samples were run using various water temperatures to see if temperature played a role in the effectiveness of the shock tube tests. Tests were performed with one, two, and three shells (one, two, and three shocks) to see if repeated shocks resulted in further reduction of crystallinity.

The temperatures chosen were 0, 20, 30, 40, 60, and 80^{o}C to give a range from cold water temperatures to hot water temperatures. Unmilled bagasse, raw knife-milled 10-mesh bagasse, and unmilled lime-treated bagasse were all used for initial studies of the shock tube; however, for the temperature-controlled tests, only unmilled bagasse was used. Figures 5.2 and 5.3 show the shock tube after shock pretreatment on raw knife-milled 10-mesh bagasse and unmilled bagasse, respectively.

It was hypothesized that reducing the available volume of the shock tube would result in more effective pretreatment because the shock would impact the bagasse with more force within a smaller area versus a larger one. To test whether reducing the volume of the shock tube would result in a lower crystallinity, two 5-in-long spacers were constructed of 3.5-in-diameter steel pipe. One spacer is shown in Figure 5.4.

Figure 5.2. Shock tube after shock treatment on raw knife-milled 10-mesh bagasse**.** The sample filled half of the shock tube.

Figure 5.3. In some of the unmilled bagasse tests, the pressure from the shotgun shell release caused a thin layer of bagasse to rise to the top of the shock tube as shown, leaving an empty space about 5 inches between the layer and the rest of the sample.

The spacer fit snugly inside the shock tube so that there was essentially no gap between the spacer wall and the shock tube wall. Tests were performed using only one spacer as well as with both spacers. Then the samples were loaded the same way as in previous tests, and the shock tube tests were performed.

Figure 5.4. Spacer: 5 inches long and 3.5 inches wide.

RESULTS AND DISCUSSION

The first tests that were performed using the shock tube determined the water content that would be used (Figures 5.5 and 5.6). The shock tube held approximately 4 liters of water; therefore, the water loading was varied from 0 L (no water) to 3 L to account for the bagasse volume. The bagasse loading was kept constant at 200 g. This bagasse loading was chosen because it half-filled the shock tube, which seemed like a good starting point. Unmilled, raw knife-milled 10-mesh, and unmilled lime-treated bagasse were tested. The laboratory-scale MixAlco lime pretreatment apparatus detailed in Chapter II was used for all of the lime-treated bagasse in the shock tube tests. Bagasse was lime-treated at 50^{o}C for two months. The moisture content of the bagasse used in all of the shock tube tests was 10%. The tests for the water loading and bagasse

loading used the Remington Express 12-gauge, 2.75-in shotgun shells. All of the tests were run in duplicate. Cold tap water was used for the water loading, bagasse loading, and multiple shock tests (Figures 5.5 to 5.13). The water temperature was not controlled. As shown in Figures 5.5 to 5.7 the water loading had no effect on crystallinity.

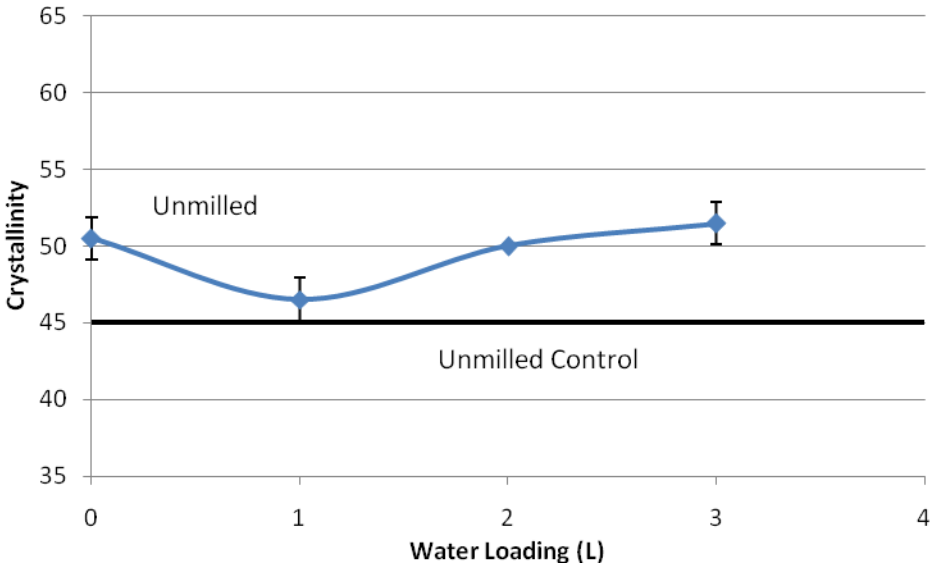

Figure 5.5. Effect of water loading on unmilled bagasse crystallinity (error bars = ± 2 standard deviations).

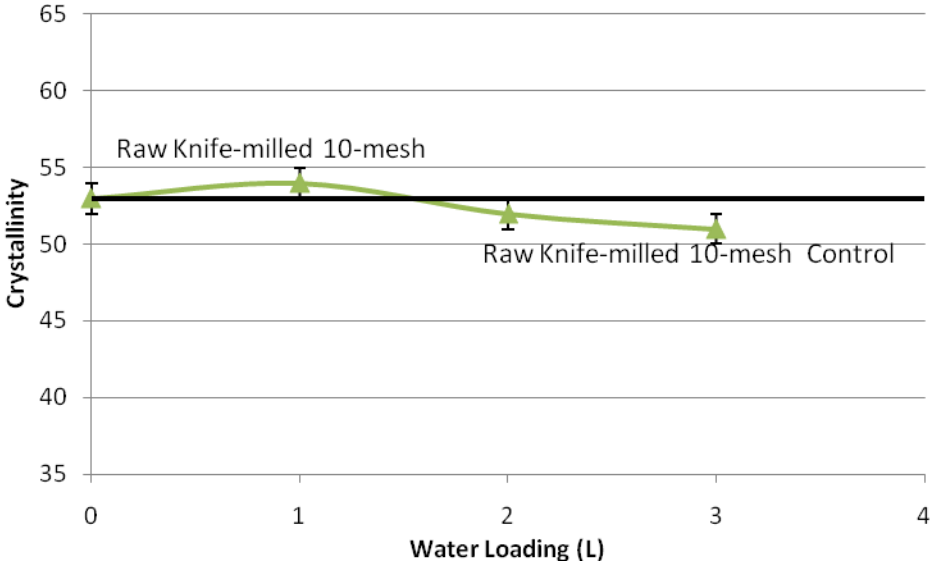

Figure 5.6. Effect of water loading on raw knife-milled 10-mesh bagasse crystallinity (duplicate measurements produced the same values).

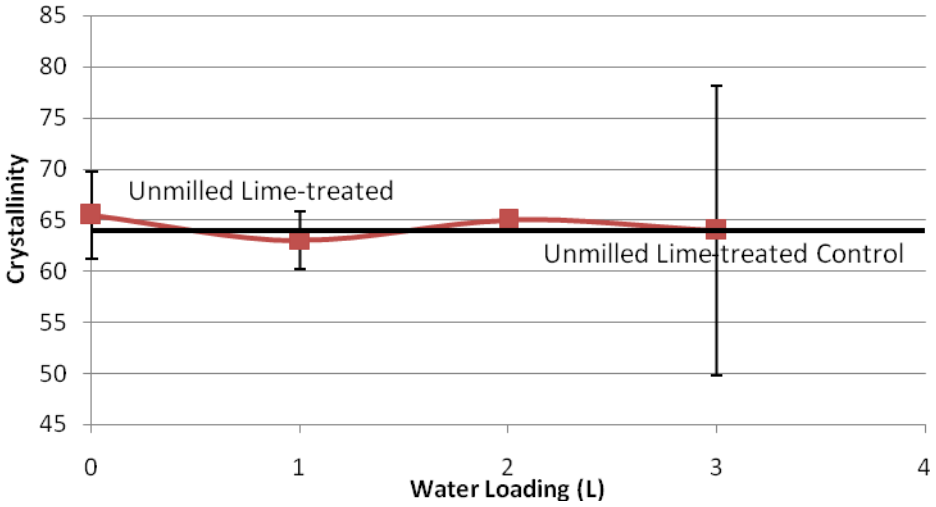

Figure 5.7. Effect of water loading on unmilled lime-treated bagasse crystallinity (error bars = ± 2 standard deviations).

Figures 5.8 to 5.10 show the effect of varying the bagasse loading while keeping the water loading constant (1 L, unmilled bagasse and unmilled lime-treated bagasse; 3 L, raw knife-milled 10-mesh bagasse). In the case of the unmilled lime-treated bagasse, there was no statistical effect of bagasse loading on crystallinity. However, the raw knife-milled 10-mesh and the unmilled bagasse showed a statistically significant reduction in crystallinity with higher bagasse loadings.

Based on the mean crystallinity, the selected bagasse and water loadings shown in Table 5.1 were used to run tests using multiple shocks (Figures 5.11 to 5.13). The multiple shock tests also used Remington Express 12-gauge, 2.75-in Magnum shotgun shells. There was no statistically significant effect of multiple shocks on bagasse crystallinity.

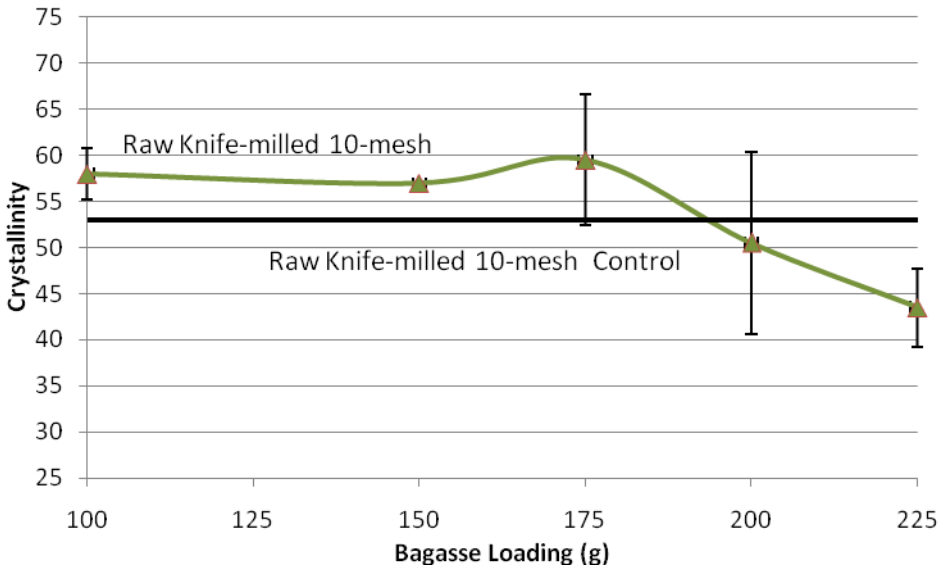

Figure 5.8. Effect of raw knife-milled 10-mesh bagasse loading on crystallinity (error bars = ± 2 standard deviations).

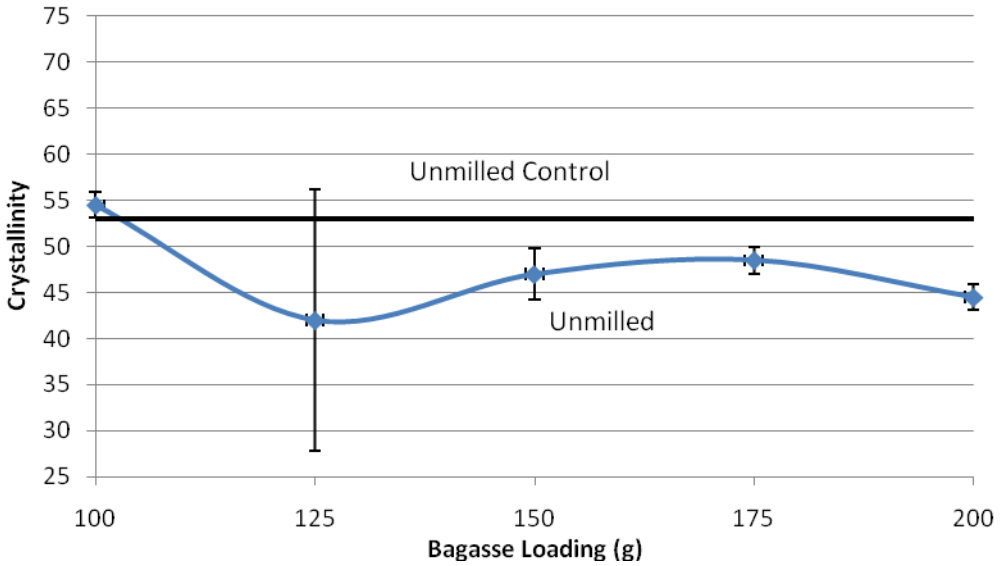

Figure 5.9. Effect of unmilled bagasse loading on crystallinity (error bars = ± 2 standard deviations).

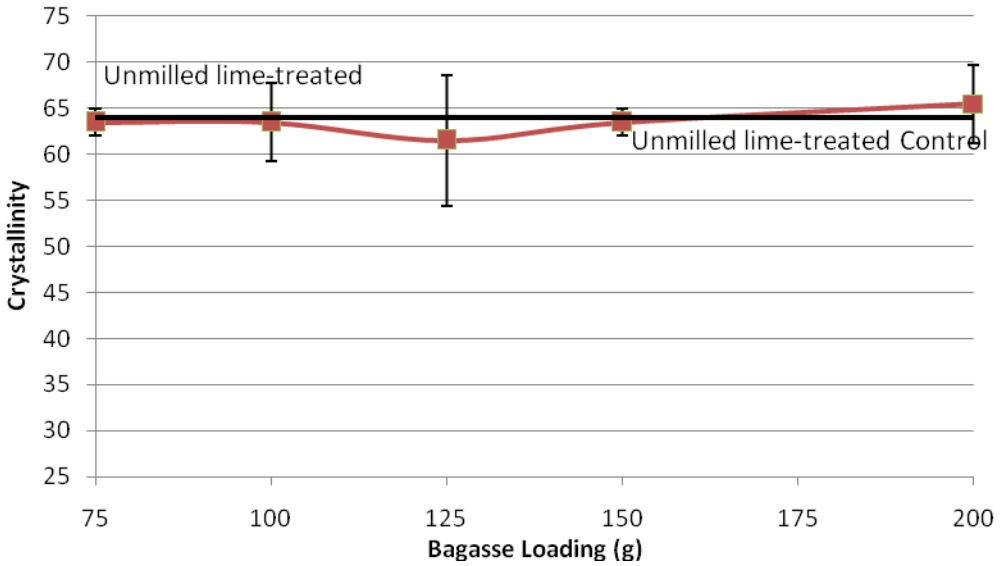

Figure 5.10. Effect of unmilled lime-treated bagasse loading on crystallinity (error bars = ± 2 standard deviations).

Table 5.1. Water loading and bagasse loading results using Remington Express 12-gauge, 2.75-in shells.

Bagasse Type	**Water Loading (L)**	**Bagasse Loading (g)**
Unmilled	1	125
Raw knife-milled 10-mesh	3	225
Unmilled lime-treated	1	125

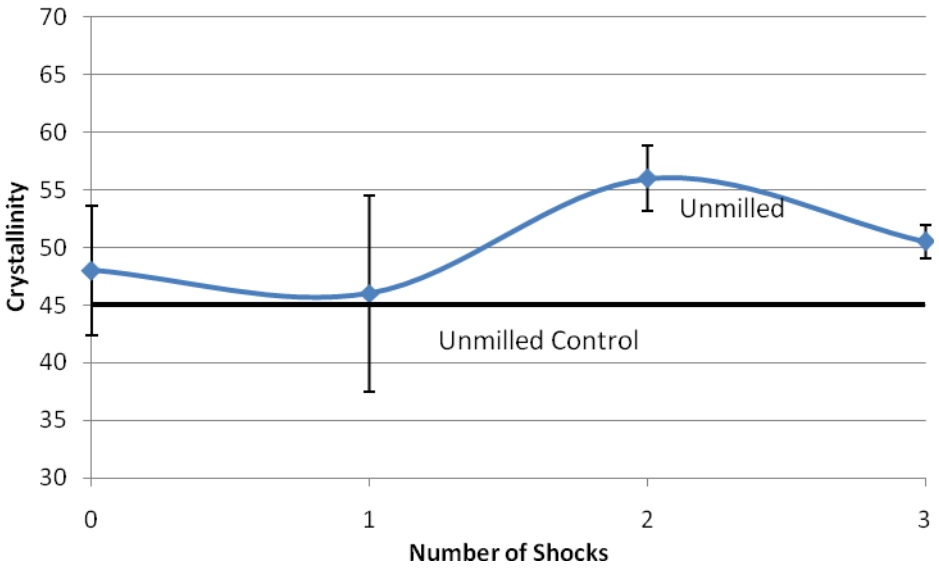

Figure 5.11. Effect of multiple shocks on unmilled bagasse crystallinity (error bars = ± 2 standard deviations).

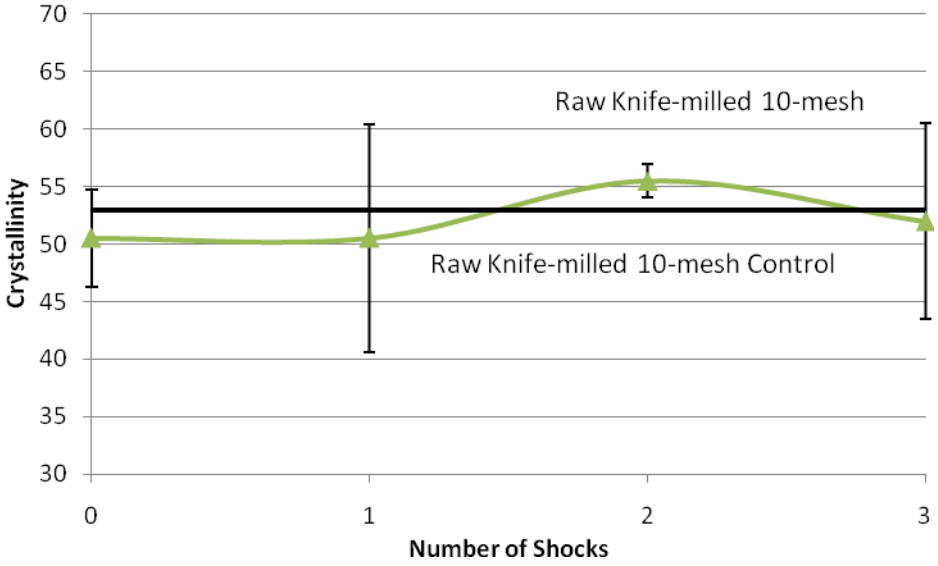

Figure 5.12. Effect of multiple shocks on raw knife-milled 10-mesh bagasse crystallinity (error bars = ± 2 standard deviations).

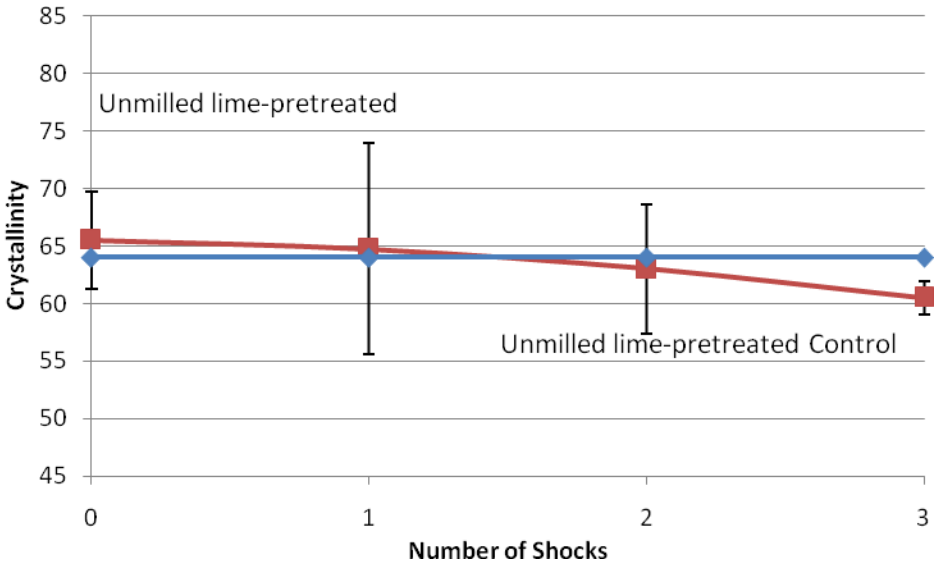

Figure 5.13. Effect of multiple shocks on unmilled lime-treated bagasse crystallinity (error bars = ± 2 standard deviations).

In the initial testing of the shock tube, the water loading, bagasse loading, and multiple shock tests were performed using Remington Express 12-gauge, 2.75-in shotgun shells. In later tests, it was hypothesized that a larger shotgun shell would produce a greater decrystallization effect and further improve digestibility. Therefore, Remington Express Buckshot 12-guage 3.5-in Magnum shotgun shells were selected for the subsequent shock tube tests.

Some typical pressures produced during shock tube pretreatment are displayed in Table 5.2. The highest pressure, 1100 psi, was recorded from the shock tube test of 100 g of raw knife-milled 10-mesh bagasse in 3 L of water using the Remington Express Buckshot 12-gauge, 3.5-in Magnum shotgun shells.

Table 5.2. Typical pressures produced from shock tube pretreatment.

Water (L)	**Bagasse (g)**	**Bagasse Sample**	**Pressure (psi)**			
			2.75-in Shells		**3.5-in Shells**	
1	125	Unmilled	100	100	100	100
1	125	Unmilled	200	100	100	100
1	125	Unmilled	100	100	100	100
3	200	Raw knife-milled 10-mesh	700	550	800	750
3	200	Raw knife-milled 10-mesh	400	600	1000	500
3	200	Raw knife-milled 10-mesh	900	600	1100	950
1	125	Unmilled Lime-treated	500	700	200	200
1	125	Unmilled Lime-treated	400	400	200	200
1	125	Unmilled Lime-treated	400	400	200	200

Figures 5.14 to 5.16 shows the role temperature played on the shock tube pretreatment for unmilled bagasse without using the spacers. Unless otherwise noted, all

of the following tests were performed using the Remington Express Buckshot 12-gauge, 3.5-in Magnum shotgun shells. Each unmilled sample was run using 175 g bagasse with and 1 L of water. (The lowest crystallinity was produced with 175 g bagasse using the Remington Express Buckshot 12-gauge, 3.5-in Magnum shells.) All tests were run in duplicate.

Based on the data shown in Figures 5.14 to 5.16, the following conclusions may be reached:

- At 0, 60, and 80°C, a single shock is sufficient to significantly reduce the crystallinity.
- At 20, 30, and 40°C, two shocks are required to significantly reduce crystallinity, but the third is unnecessary.

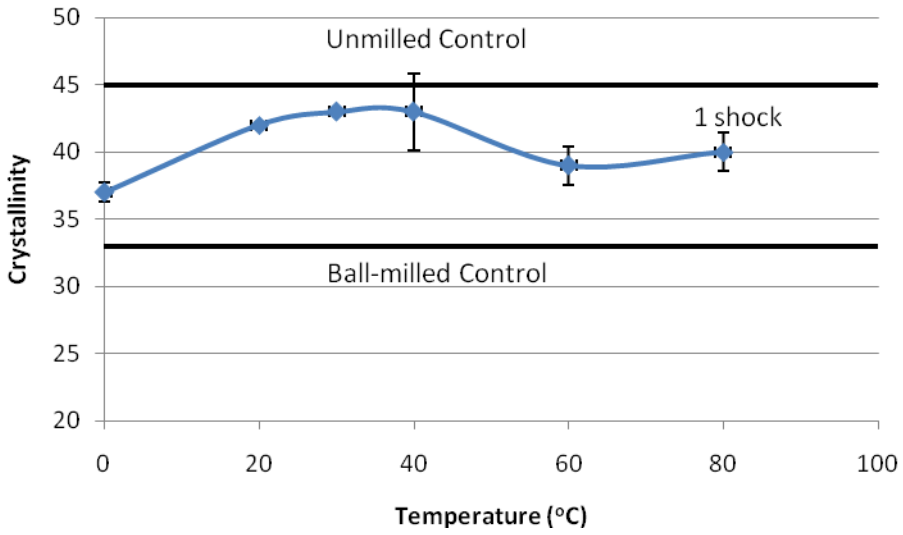

Figure 5.14. Effect of temperature on crystallinity with one shock (error bars = ± 2 standard deviations).

.

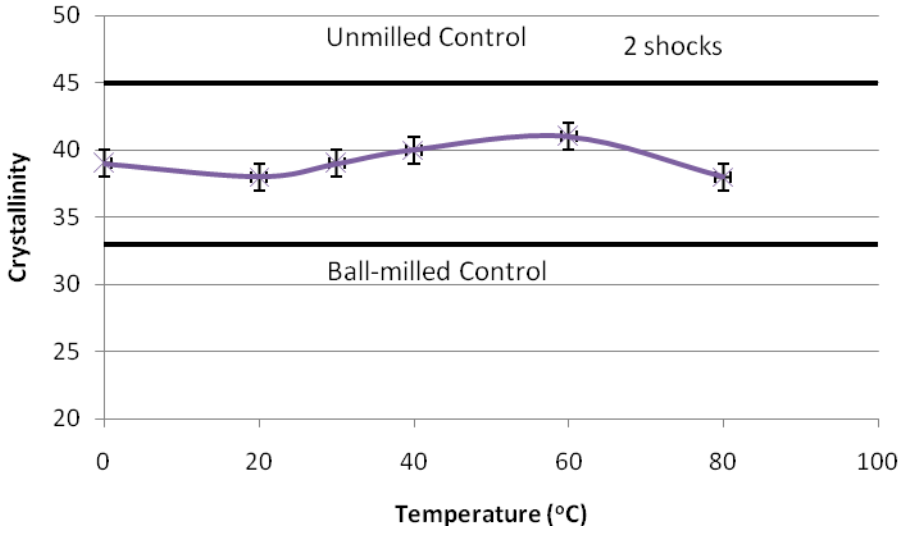

Figure 5.15. Effect of temperature on crystallinity with two shocks (error bars = ± 2 standard deviations).

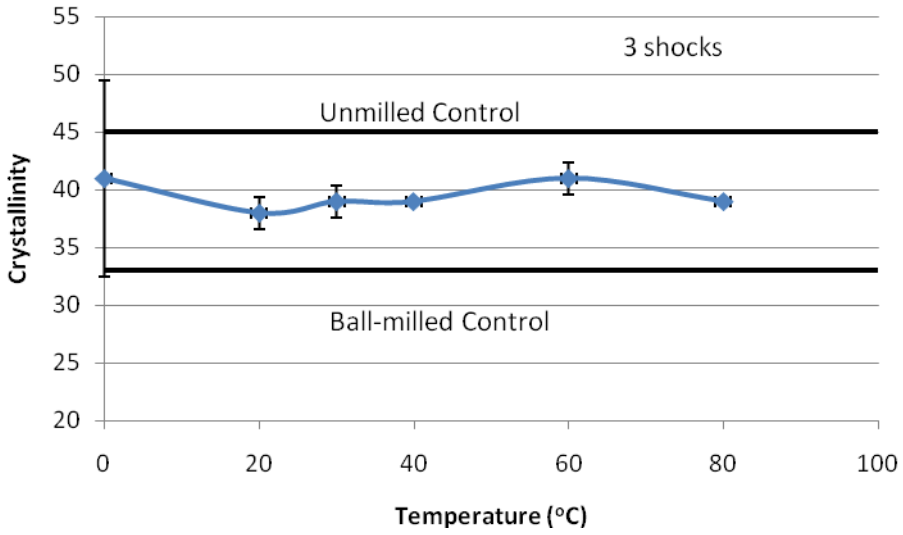

Figure 5.16. Effect of temperature on crystallinity with three shocks (error bars = ± 2 standard deviations).

Figures 5.17 to 5.22 illustrate the role of temperature on both the 6-hour hydrolysis (initial hydrolysis) rate and the 3-day hydrolysis (extent of digestion). There is no ball-milled bagasse control on the following enzymatic hydrolysis graphs because the ball-milled sample was tested for digestibility during fermentation instead of enzymatic hydrolysis. (The fermentation results of the ball-milled samples are discussed in Chapter VI.)

Overall, the data show that the biomass digestibility is improved by the shock tube treatment. On a percentage basis, the effect is more pronounced with the initial rate (6 h) than the extent of digestion (3 d). This observation is consistent with results obtained from Zhu et al., (2007), which also showed that crystallinity affects the 6-h digestibility more than the 3-day digestibility. The improvement in digestibility is observed with a single shock, so multiple shocks are not necessary. Also, the effect is seen at moderate temperatures (20 to 40°C), so extreme temperatures (0, 60, 80°C) are not required.

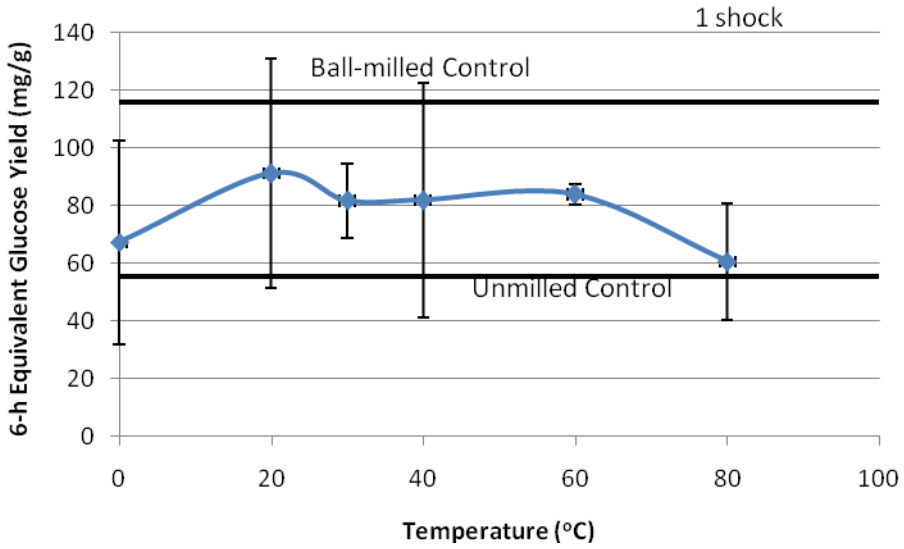

Figure 5.17. Effect of temperature on initial hydrolysis with one shock (error bars = ± 2 standard deviations).

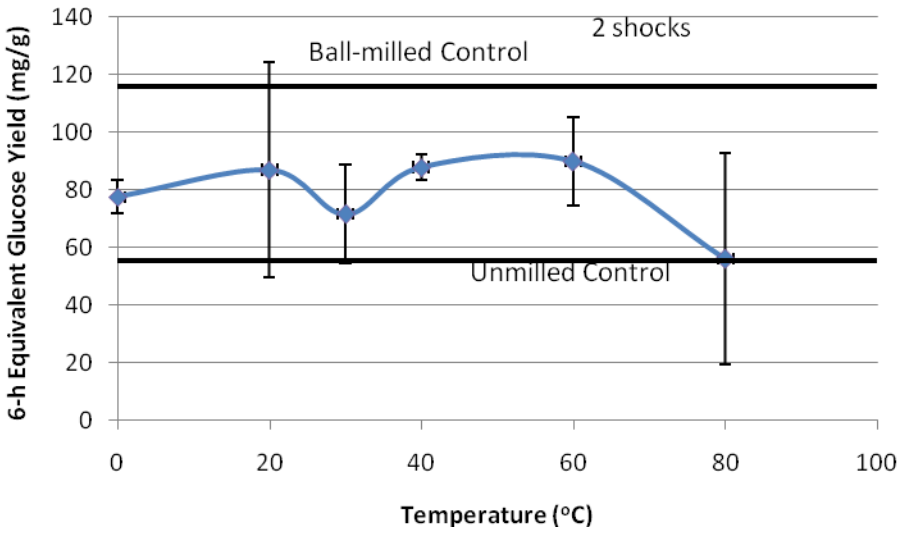

Figure 5.18. Effect of temperature on initial hydrolysis with two shocks (error bars = ± 2 standard deviations).

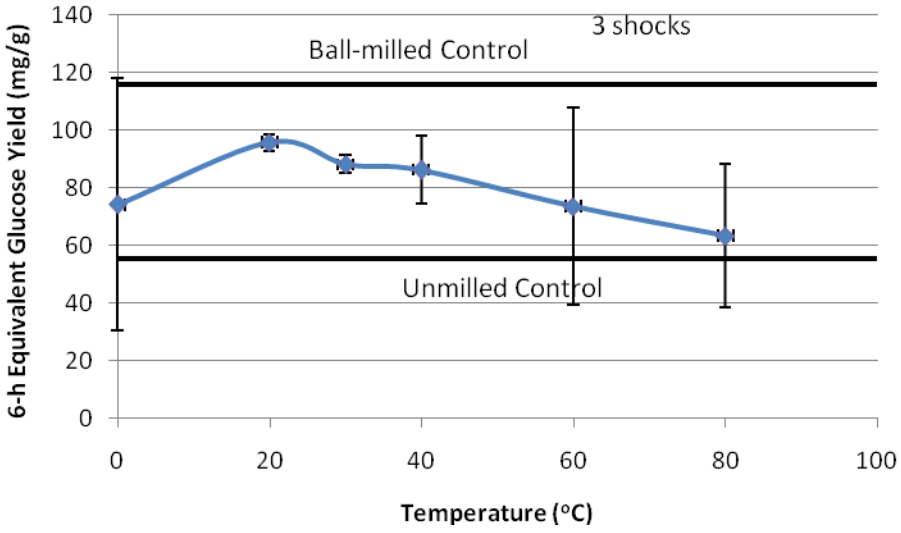

Figure 5.19. Effect of temperature on initial hydrolysis with three shocks (error bars = ± 2 standard deviations).

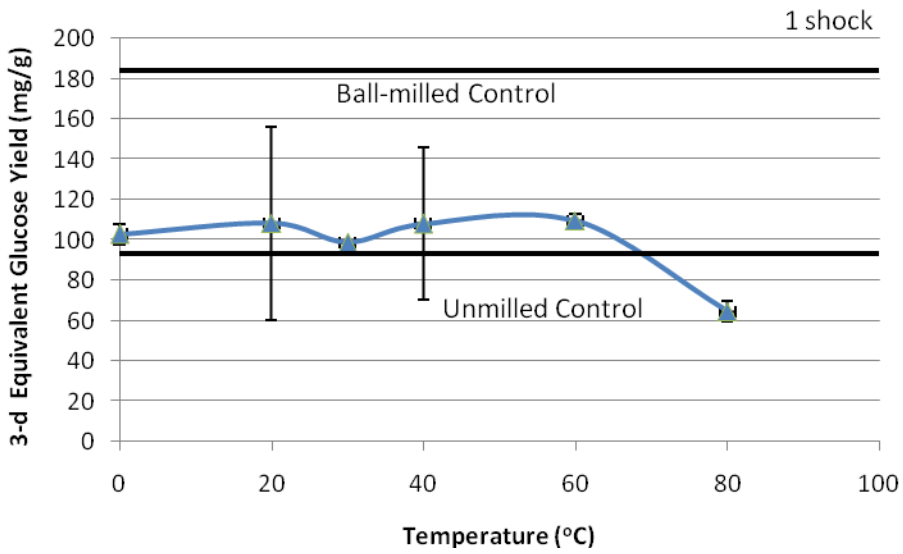

Figure 5.20. Effect of temperature on extent of hydrolysis with one shock (error bars = ± 2 standard deviations).

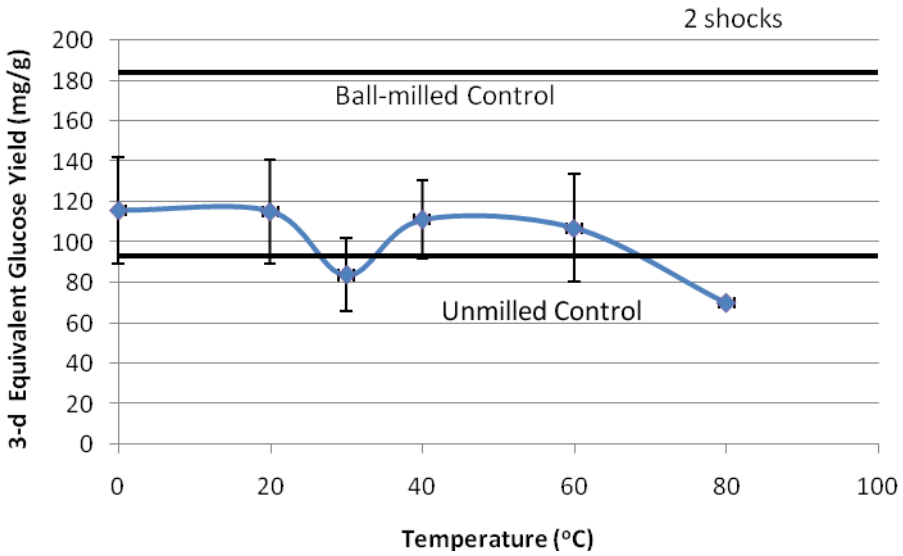

Figure 5.21. Effect of temperature on extent of hydrolysis with two shocks (error bars = ± 2 standard deviations).

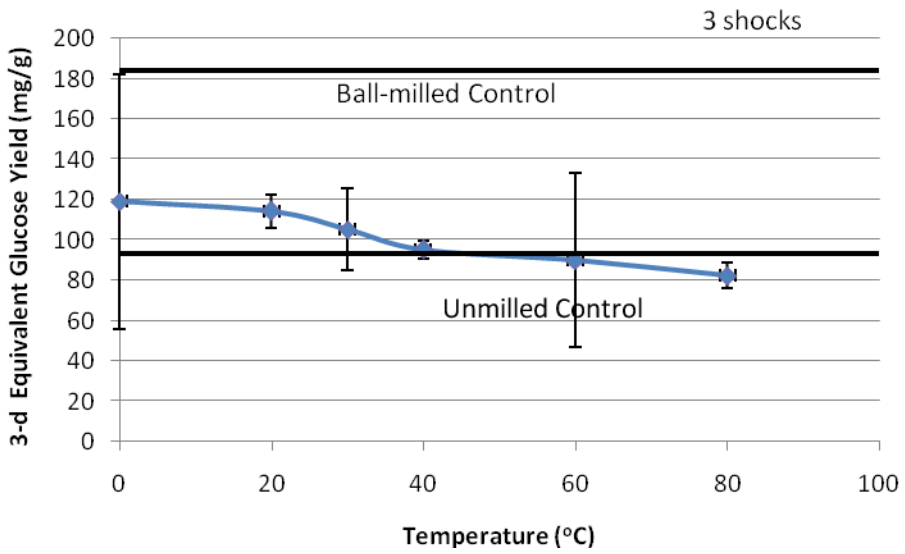

Figure 5.22. Effect of temperature on extent of hydrolysis with three shocks (error bars = ± 2 standard deviations).

The results of reducing the volume of the shock tube in an attempt to improve the effectiveness of the shock pretreatment are given in Figures 5.23 to 5.31. All of the tests involving the spacers were performed at 0°C so that any effects of pretreatment would be contributed to the reduced volume only and not the temperature. Reducing the volume by inserting spacers had no significant effect on either the crystallinity or digestibility.

Figures 5.32 and 5.33 shows that there was no significant correlation between crystallinity and digestibility of bagasse for unmilled bagasse. It should be noted that the crystallinity varied over a narrow range (39.5 to 42.5%) so it would be difficult to see an effect.

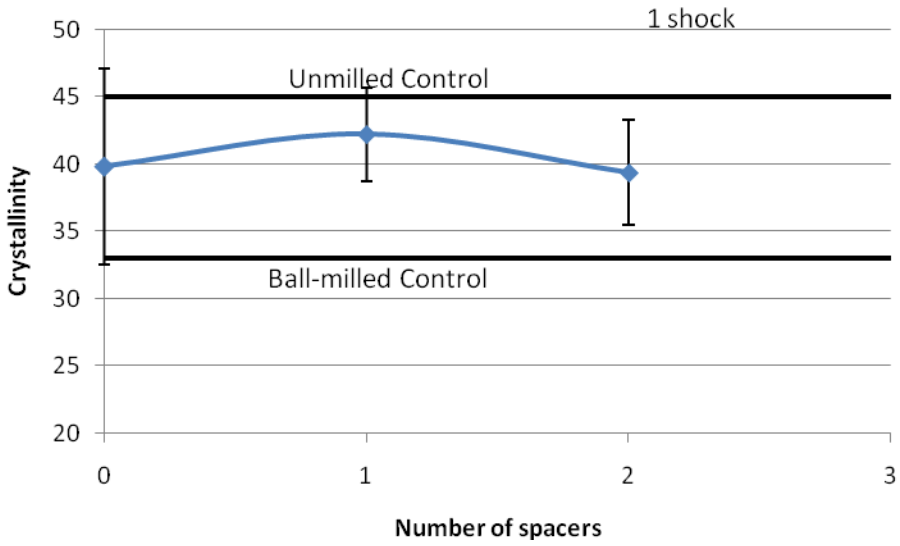

Figure 5.23. Effect of spacers on crystallinity with one shock (error bars = ± 2 standard deviations).

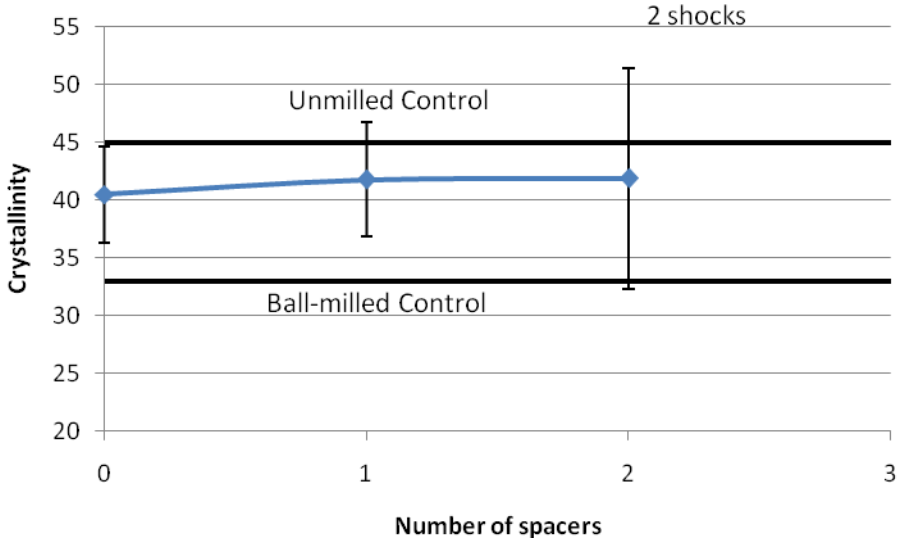

Figure 5.24. Effect of spacers on crystallinity with two shocks (error bars = ± 2 standard deviations).

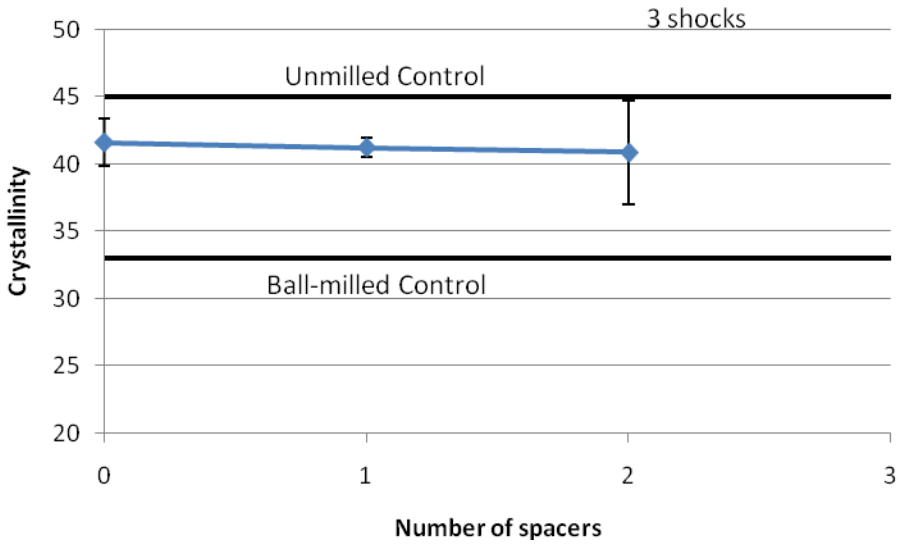

Figure 5.25. Effect of spacers on crystallinity with three shocks (error bars = ± 2 standard deviations).

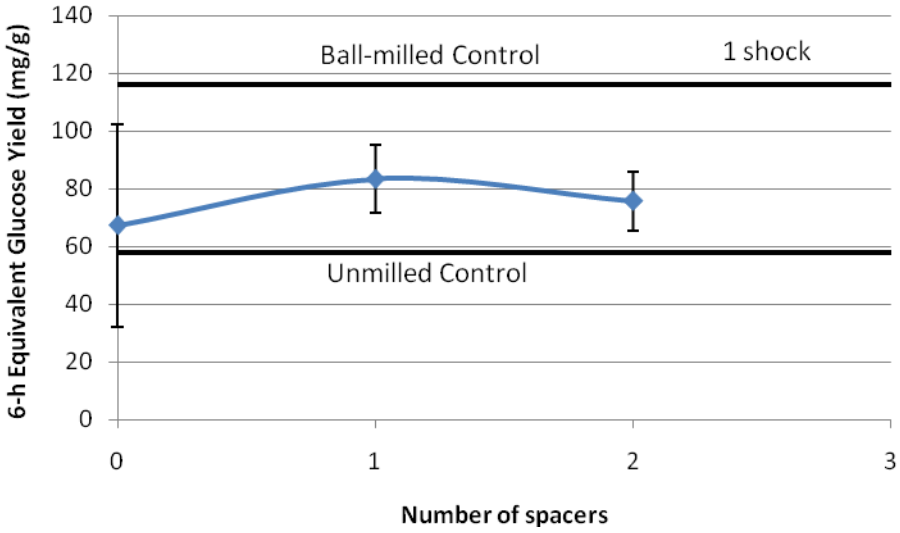

Figure 5.26. Effect of spacers on initial hydrolysis with one shock (error bars = ± 2 standard deviations).

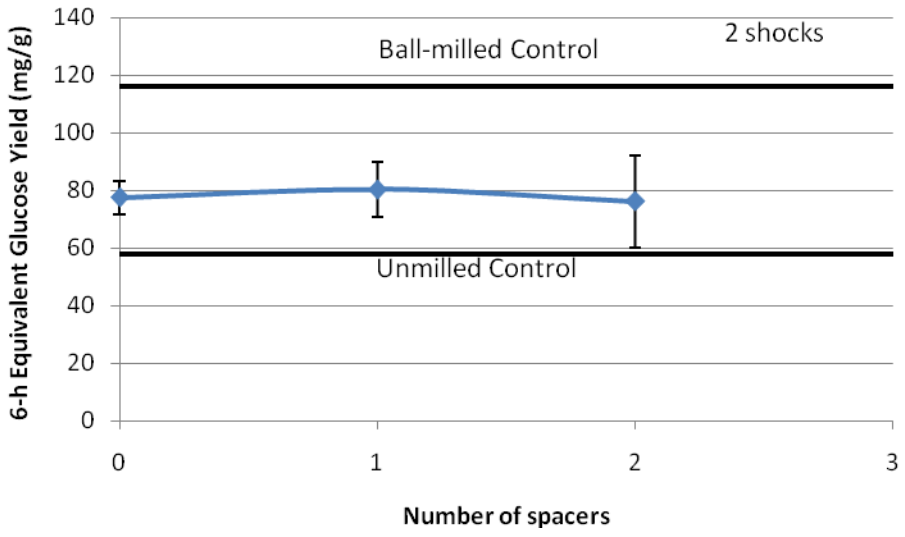

Figure 5.27. Effect of spacers on initial hydrolysis with two shocks (error bars = ± 2 standard deviations).

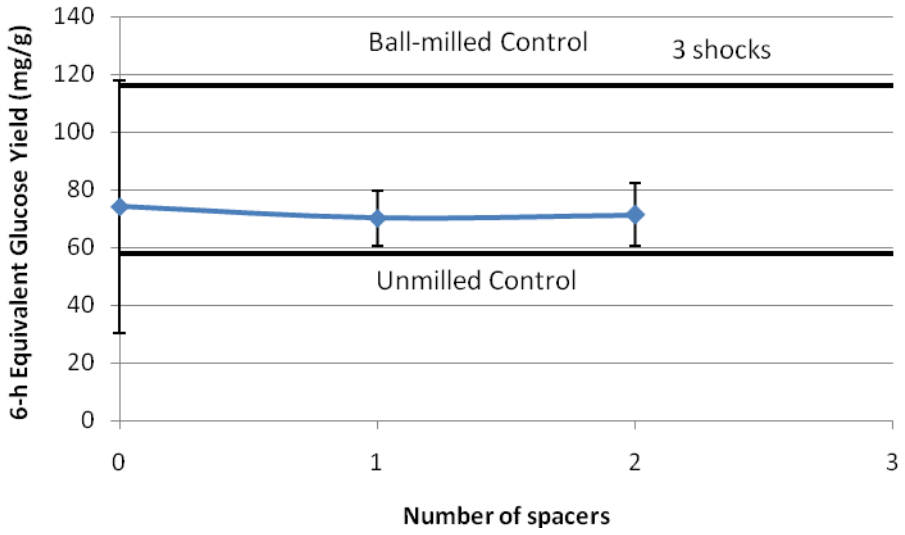

Figure 5.28. Effect of spacers on initial hydrolysis with three shocks (error bars = ± 2 standard deviations).

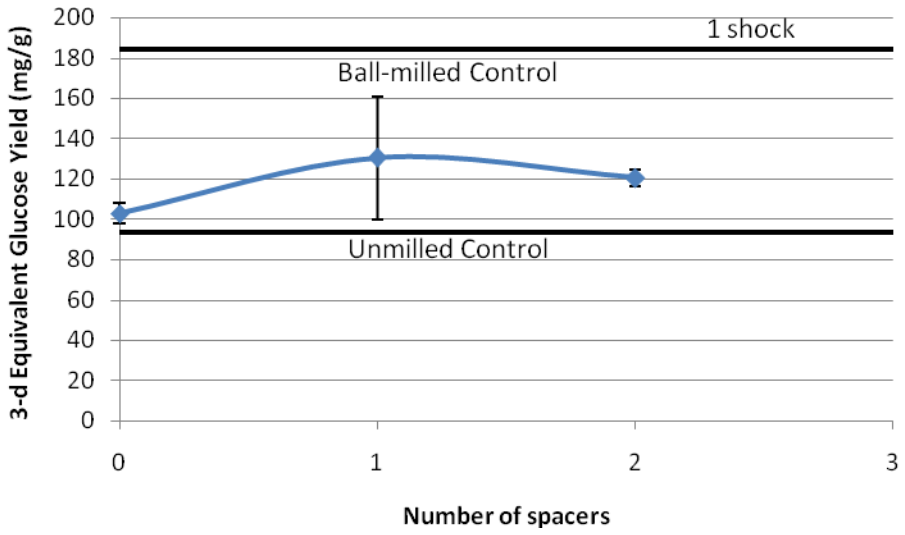

Figure 5.29. Effect of spacers on extent of hydrolysis with one shock (error bars = ± 2 standard deviations).

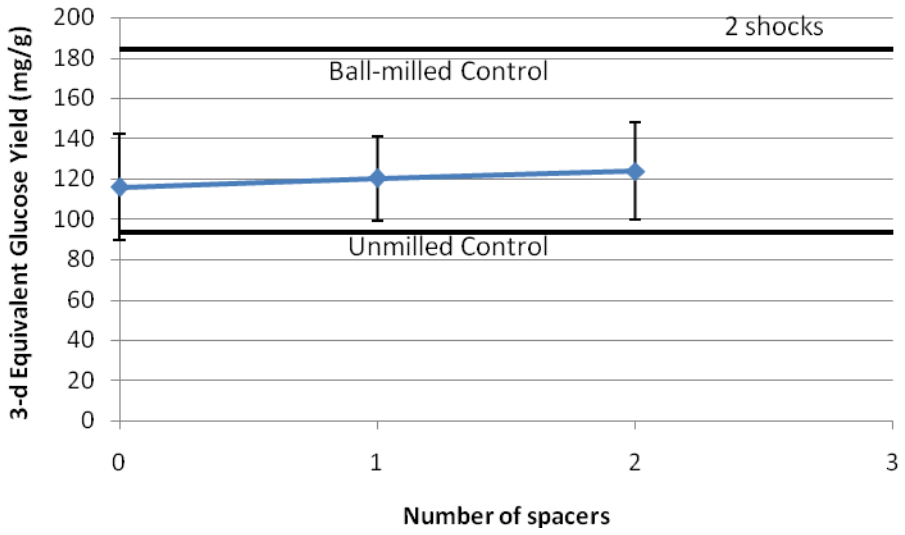

Figure 5.30. Effect of spacers on extent of hydrolysis with two shocks (error bars = ± 2 standard deviations).

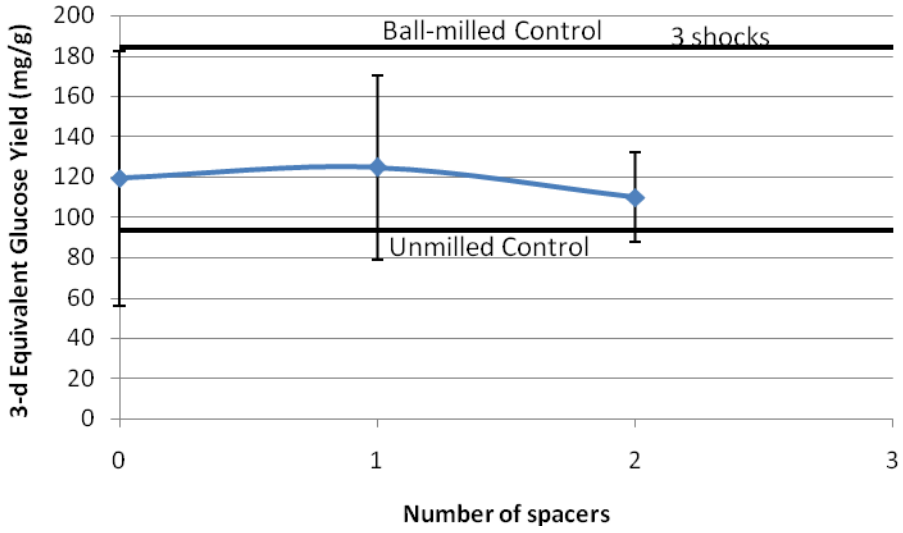

Figure 5.31. Effect of spacers on extent of hydrolysis with three shocks (error bars = ± 2 standard deviations).

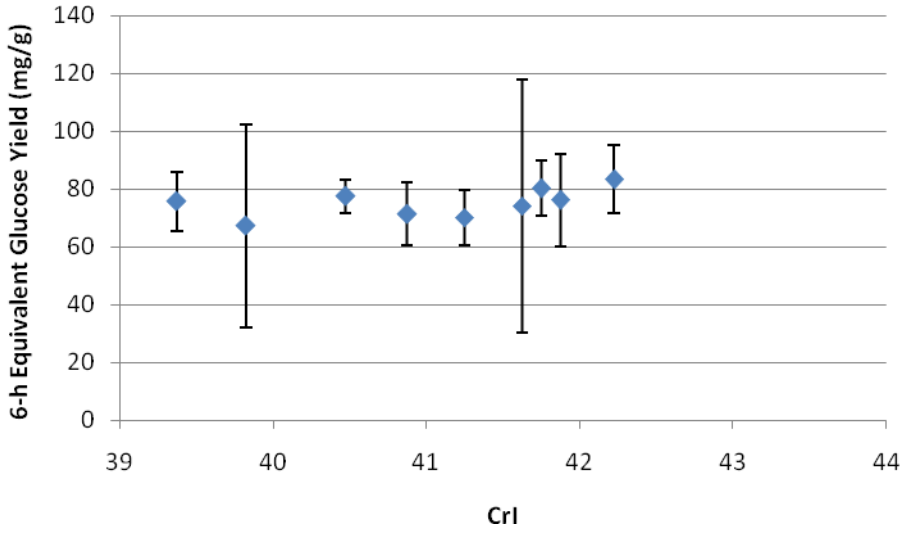

Figure 5.32. Correlation of crystallinity versus 6-h digestibility for unmilled bagasse (error = ± 2 standard deviations).

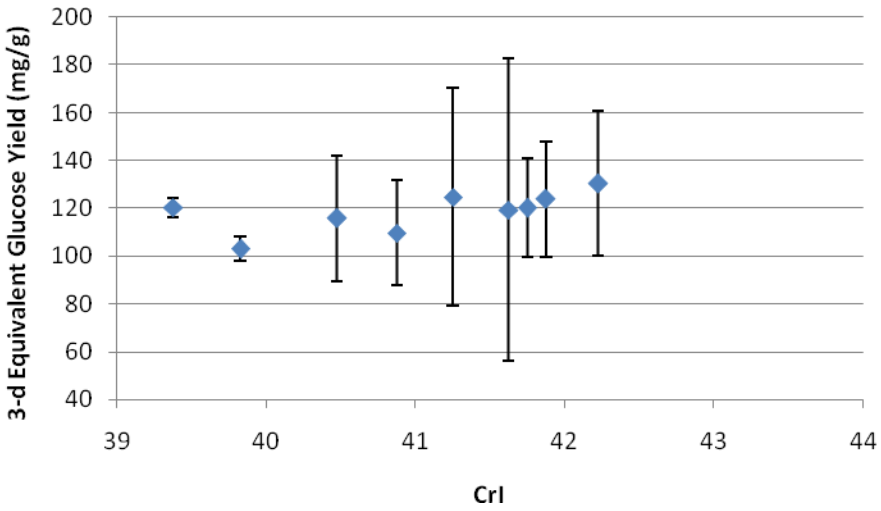

Figure 5.33. Correlation of crystallinity versus 3-d digestibility for unmilled bagasse (error = ± 2 standard deviations).

CONCLUSIONS

Many factors were varied in the shock tube pretreatment study: water loading, bagasse loading, multiple shocks, shock tube volume, and temperature. Each was modified in an attempt to find optimal settings for the shock tube pretreatment. The water loading, bagasse loading, and multiple shock tests were run using Remington Express 12-gauge 2.75-in Magnum shotgun shells. Using these shells, there was no significant effect of water loading on the bagasse crystallinity. Likewise, there was no statistically significant effect of multiple shocks on bagasse crystallinity, and in the case of the unmilled lime-treated bagasse, there was no statistical effect of bagasse loading on crystallinity. However, the raw knife-milled 10-mesh and the unmilled bagasse showed a statistically significant reduction in crystallinity with higher bagasse loadings.

Additional multiple shock tests, as well as the temperature and the shock tube volume tests, were run using the larger Remington Express 12-gauge 3.5-in Magnum shotgun shells. At 0, 60, and 80^{o}C, a single shock was sufficient to significantly reduce

the crystallinity. At 20, 30, and 40^{o}C, two shocks were required to significantly reduce crystallinity, but the third was unnecessary. Also, increasing the size of the shotgun shells from Remington Express 12-gauge, 2.75-in Magnum shells to 3.5-in Magnum shells produced the largest pressure recorded in this study.

Overall, the data showed that the shock tube treatment decreased bagasse crystallinity. The crystallinity of shock-treated samples was approximately half-way between the crystallinity of untreated bagasse and ball-milled bagasse. There was also an improvement in biomass digestibility. On average, the 6-h samples resulted in a 35% improvement in digestibility whereas the 3-d samples resulted in a 22% increase. Therefore, on a percentage basis, the effect is more prominent with the initial rate (6 h) than the extent of digestion (3 d). This observation is consistent with results obtained from Zhu et al., (2007), which also showed that crystallinity affects the 6-h digestibility more than the 3-day digestibility. The improvement in digestibility is observed with a single shock; therefore, multiple shocks are unnecessary. Also, the effect is seen at moderate temperatures (20 to 40^{o}C), so extreme temperatures (0, 60, 80^{o}C) are not required.

CHAPTER VI
CRYSTALLINITY IMPACT ON BATCH FERMENTATION

INTRODUCTION

The anaerobic fermentation of biomass to carboxylic acids has been studied extensively in recent years using various biomass feedstocks as energy sources (Zeikus, 1980; Ross and Holtzapple, 2001; Thanakoses et al., 2003; Agbogbo, 2005; Aiello-Mazzarri et al., 2006). Anaerobic fermentation uses a mixed culture of microorganisms that produce enzymes to hydrolyze the biomass. These microorganisms can be found in swamps and marine ecosystems. The resulting sugars are fermented to mixed carboxylic acids (Ross and Holtzapple, 2001; Thanakoses et al., 2003).

Sugarcane bagasse has an advantage as an energy source over poplar wood and other hardwoods because of its moderate lignin content (Chang and Holtzapple, 2000). Further, it is collected in central locations as a waste product at sugar mills.

Traditionally in the MixAlco process, calcium carbonate was used as a buffer during fermentation to maintain the pH at 5.8. Agbogbo (2005) compared ammonium bicarbonate buffer to calcium carbonate buffer and found that the ammonium bicarbonate buffer gives almost double the product concentrations of the calcium carbonate buffer.

The crystalline structure of biomass is one factor that limits enzyme effectiveness during enzymatic hydrolysis (Fan et al., 1980; Abraham and Kurup, 1997, Mosier et al., 2005, Zhu et al., 2007) and thus it is expected to limit the digestibility of biomass during fermentation. This work entailed performing batch fermentations using ball-milled bagasse, ball-milled lime-treated bagasse, raw knife-milled 80-mesh bagasse, and knife-milled lime-treated 80-mesh bagasse to determine the effect of crystallinity on fermentation. Both physically pretreated and chemically pretreated bagasse were used as represented in Figure 6.1.

Table 6.1. Physical and chemical pretreatments used in batch fermentation.

		CHEMICAL PRETREATMENT	
		None	$Ca(OH)_2$
PHYSICAL PRETREATMENT	Knife-milled	X	X
	Ball-milled	X	X

The crystallinity of each material was determined beforehand, and the total acid concentration in the liquid product was found after fermentation. Each fermentation condition was run in duplicate to ensure repeatability.

RESULTS AND DISCUSSION

Both physically and chemically pretreated bagasse were used in the batch fermentation including the following: unmilled, ball-milled, lime pretreated knife-milled 80-mesh, and lime-treated ball-milled bagasse. 80-mesh bagasse was used to minimize any differences from the ball-milled bagasse fermentation that could be attributed to the different particle sizes. The 80-mesh bagasse is a similar particle size to ball-milled bagasse.

Raw knife-milled 10-mesh bagasse samples were ball-milled for three days as detailed in Chapter II to produced ball-milled bagasse samples. Ball-milled lime-treated and knife-milled lime-treated 80-mesh samples were produced by performing small-scale aerated lime pretreatment (see Chapter II) on ball-milled samples and raw knife-

milled 80-mesh samples, respectively, for 1 month at 55°C. The batch fermentation and carboxylic acid procedures described in Appendices H and K were used for this study.

Figures 6.1 – 6.5 show the acid concentrations produced during the batch fermentation for each substrate after 30 days. The ball-milled lime-treated bagasse gave the highest acid concentrations of 33 g/L followed by the ball-milled bagasse with an acid concentration of 21 g/L. The lowest acid concentrations were produced from the knife-milled lime-treated 80-mesh bagasse (19 g/L) and raw knife-milled 80-mesh bagasse (14 g/L).

On average, ball-milled lime-treated bagasse produced more than twice as much acid than raw knife-milled 80-mesh bagasse and almost twice as much (44%) as knife-milled lime-treated 80-mesh bagasse. Ball-milled bagasse gave about 33% more acid than raw knife-milled 10-mesh bagasse and about 10% more acid than knife-milled lime-treated 80-mesh bagasse.

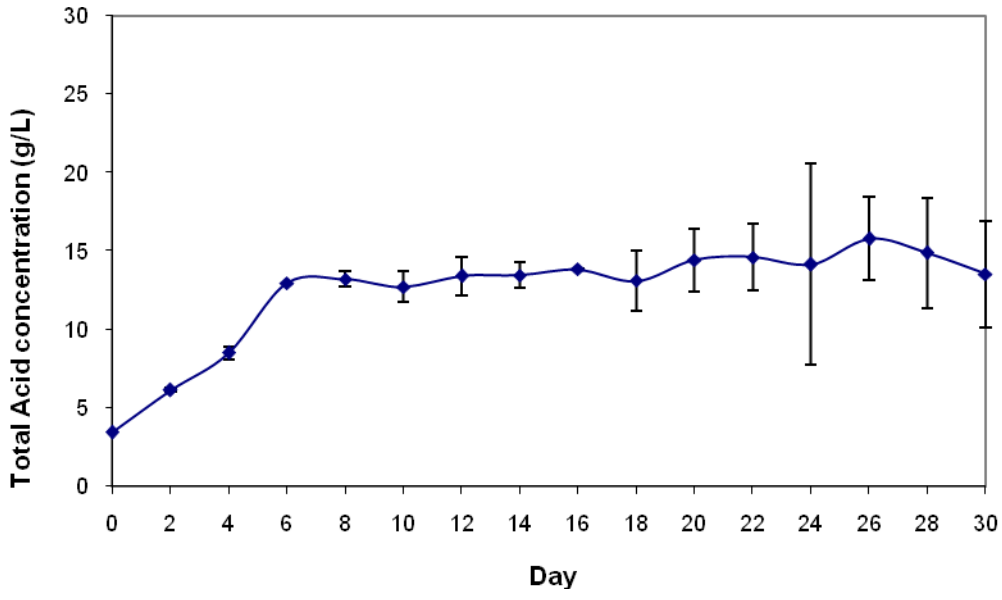

Figure 6.1. Raw knife-milled 80-mesh bagasse total acid production (error bars = ± 2 standard deviations).

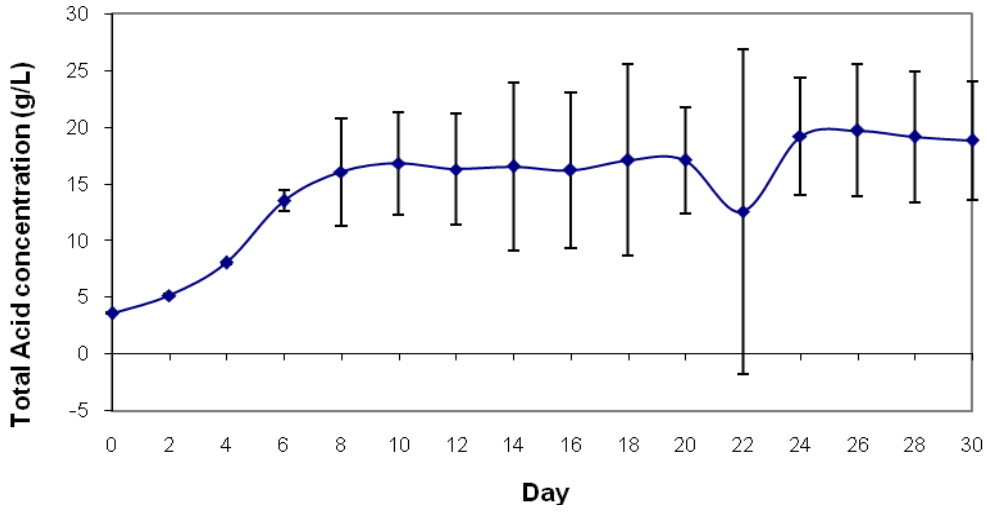

Figure 6.2. Knife-milled lime-treated 80-mesh bagasse total acid production (error bars = ± 2 standard deviations).

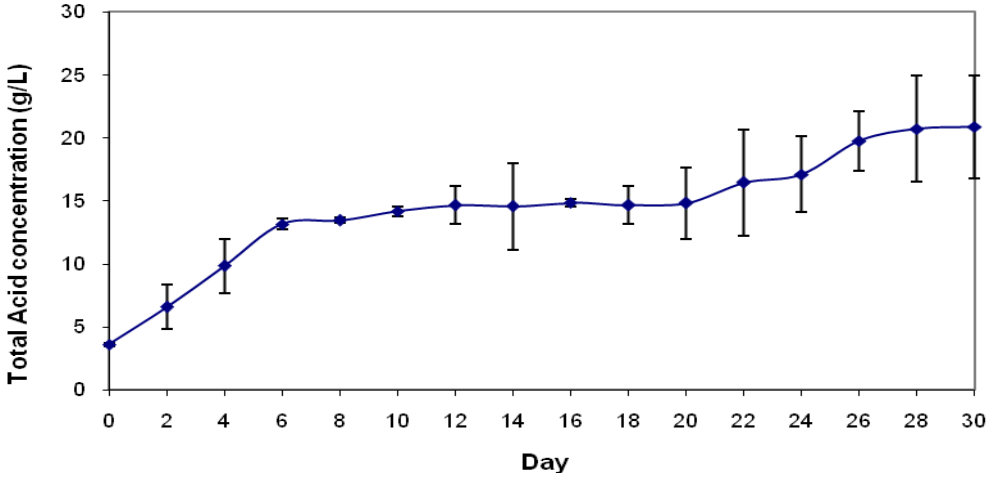

Figure 6.3. Ball-milled bagasse total acid production (error bars = ± 2 standard deviations).

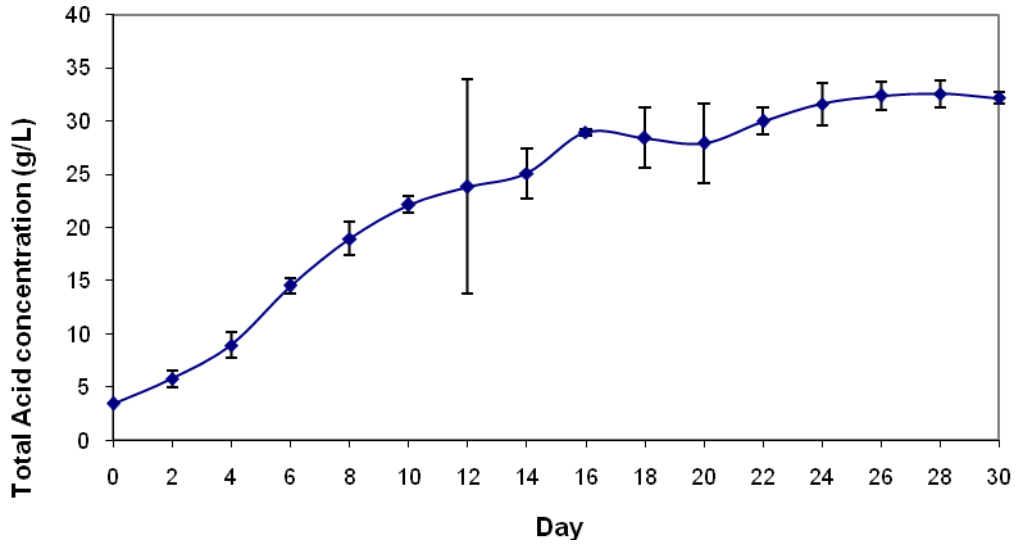

Figure 6.4. Ball-milled lime-treated bagasse total acid production (error bars = ± 2 standard deviations).

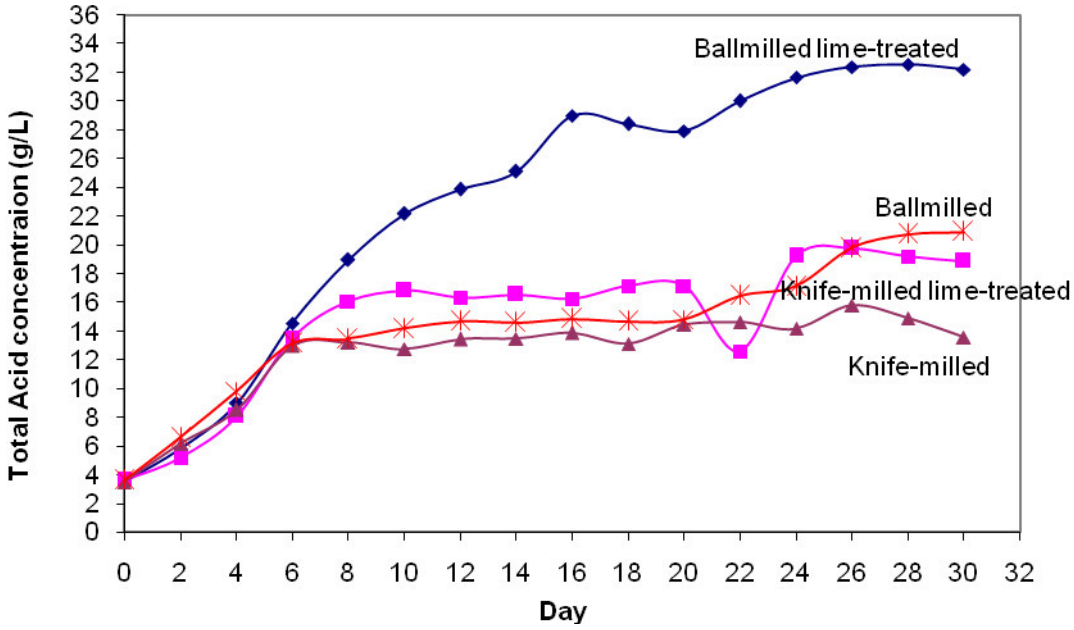

Figure 6.5. Batch fermentation total acid concentrations.

Concentrations of acetic (C2), propionic (C3), and butyric (C4) acids are displayed in Figures 6.6 to 6.9. The ball-milled lime-treated sample produced the highest amounts of both acetic and propionic acid. The largest amount of butyric acid was produced by the raw knife-milled 80-mesh bagasse.

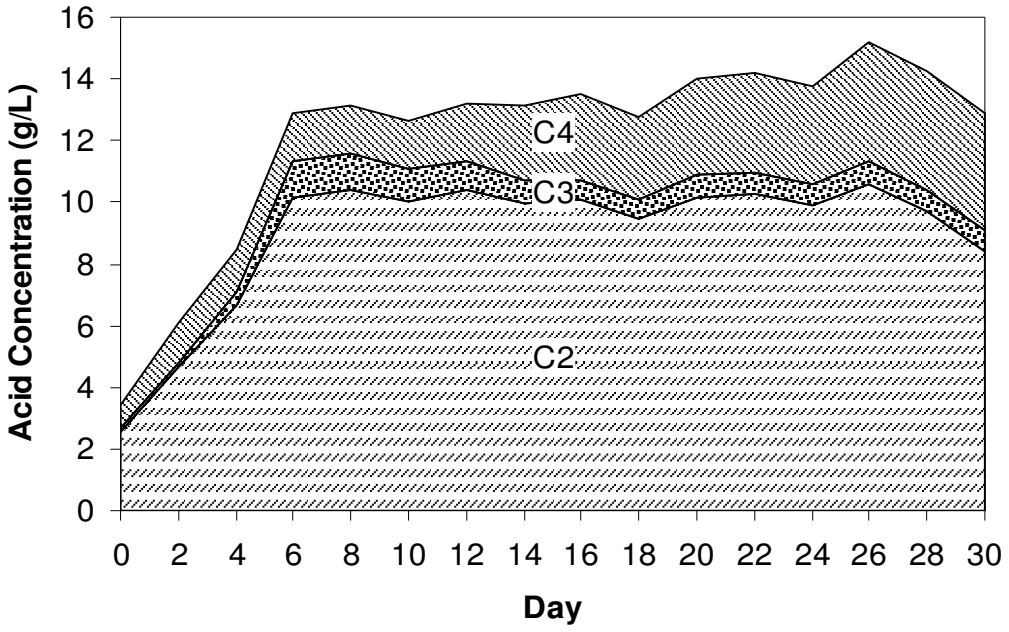

Figure 6.6. Acid composition of raw knife-milled 80-mesh bagasse (average shown). Negligible amounts of heptanoic acid were also produced on Days 26, 28, and 30.

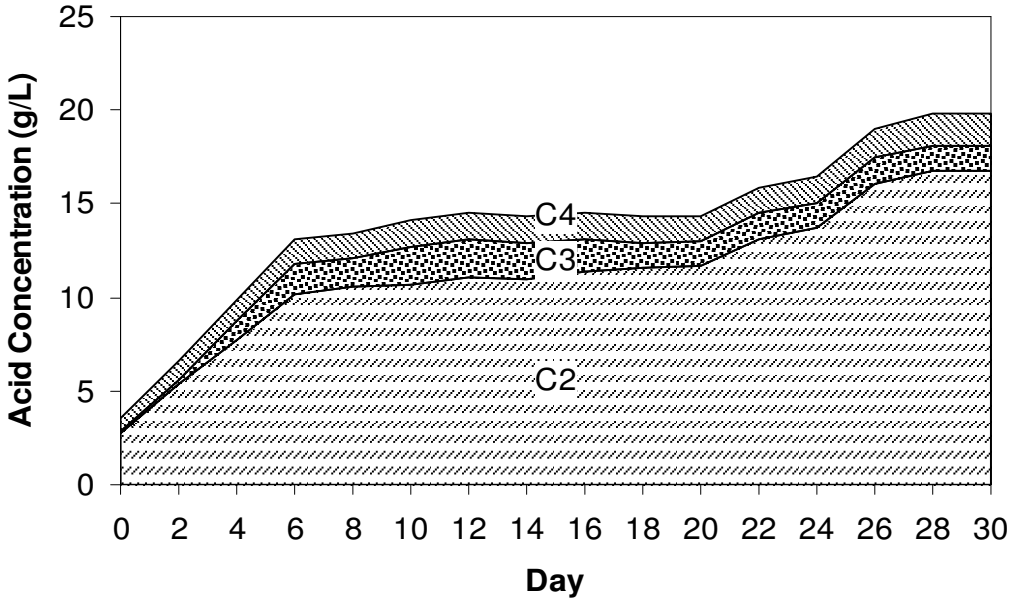

Figure 6.7. Acid composition of ball-milled bagasse (average shown). Negligible amounts of valeric and caprioc acid were also produced after Day 14.

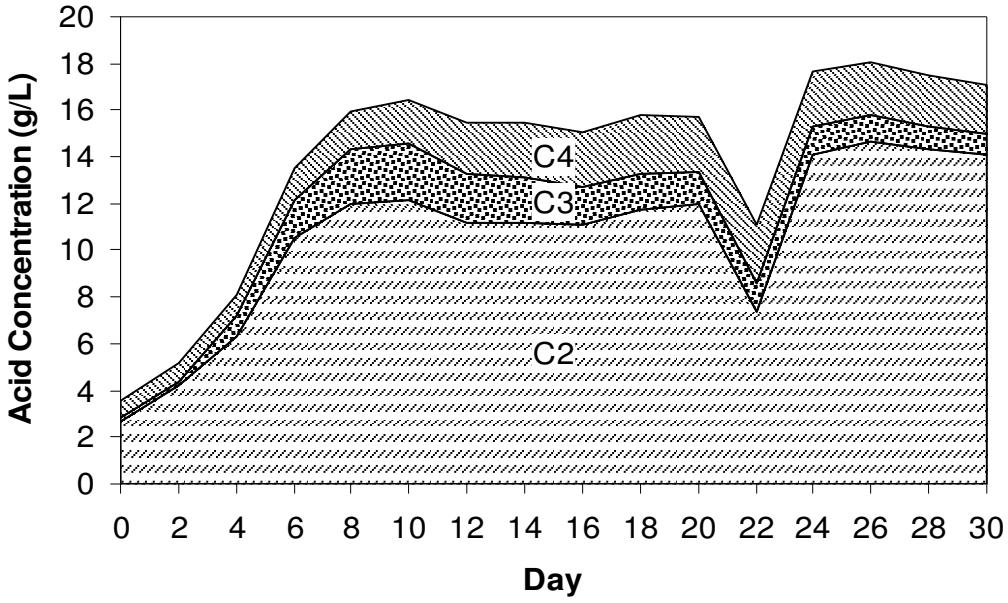

Figure 6.8. Acid composition of knife-milled lime-treated 80-mesh bagasse (average shown). Negligible amounts of valeric, caprioc, and heptanoic acid were also produced after Day 10.

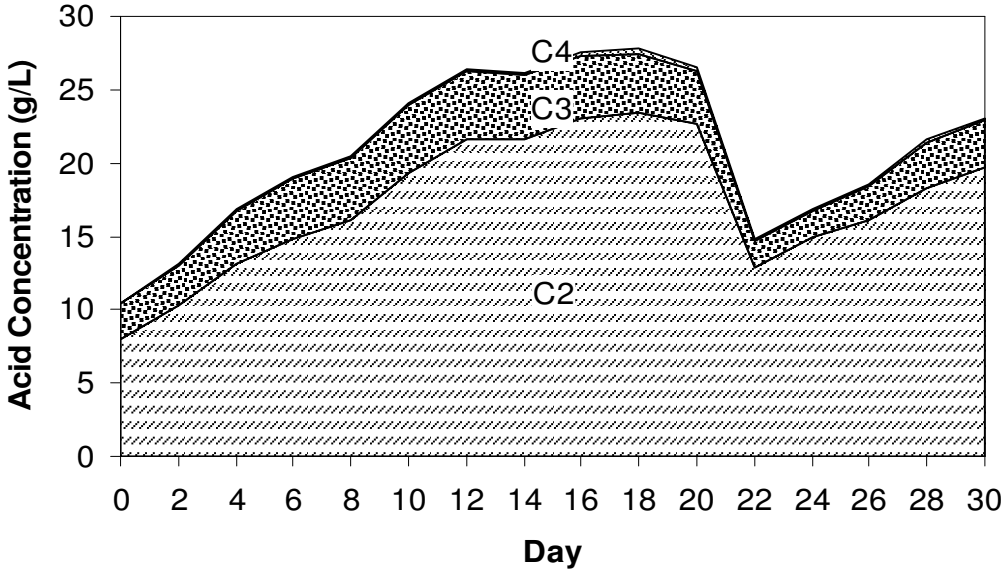

Figure 6.9. Acid composition of lime-treated ball-milled bagasse (average shown). Negligible amounts of valeric and heptonoic acid were also produced after Day 12.

Figures 6.10 to 6.13 show that the daily gas production was high during the first two weeks of fermentation most likely due to the relatively large amounts of amorphous regions present within the bagasse. After the microorganisms consumed this readily digestible portion, the gas production slowed and stabilized during the last two weeks of fermentation.

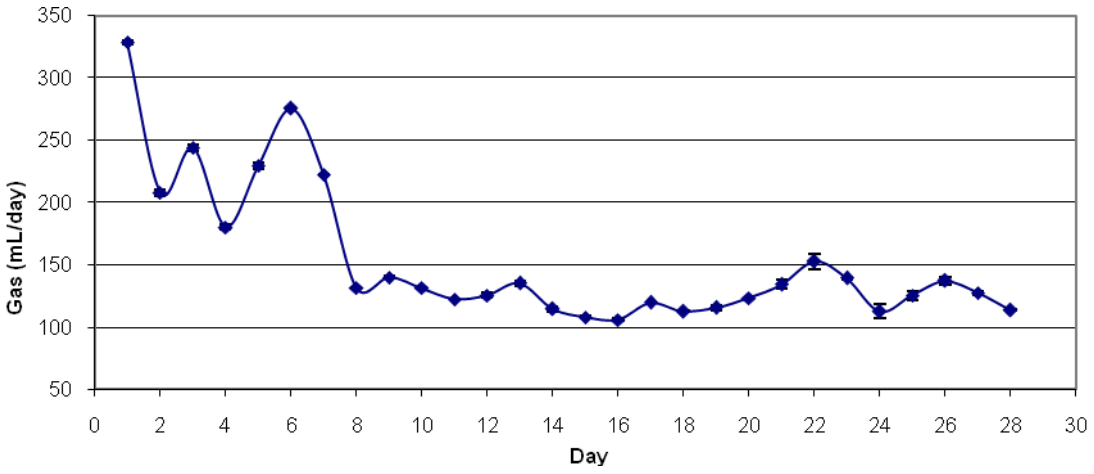

Figure 6.10. Raw knife-milled 80-mesh bagasse daily gas production (error = ± 2 standard deviations).

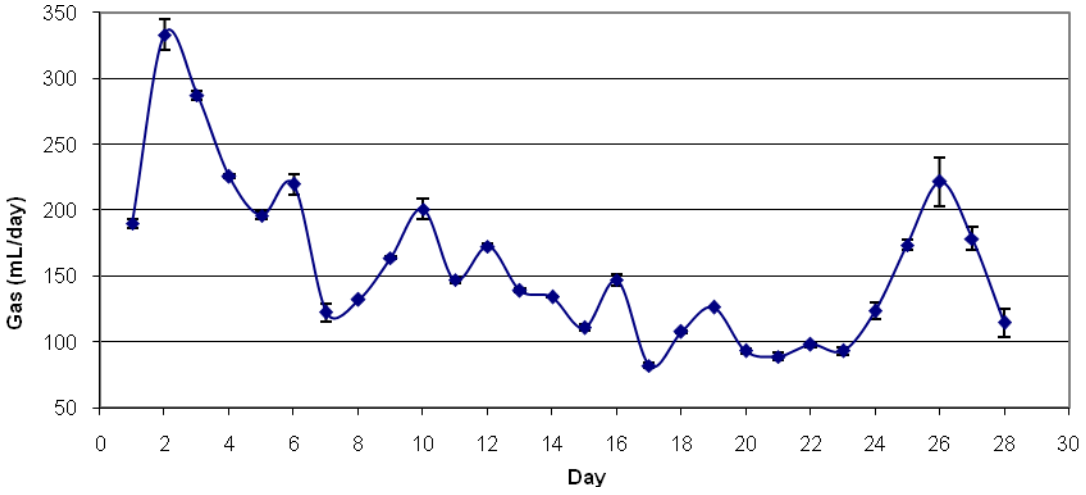

Figure 6.11. Ball-milled bagasse daily gas production (error = ± 2 standard deviations).

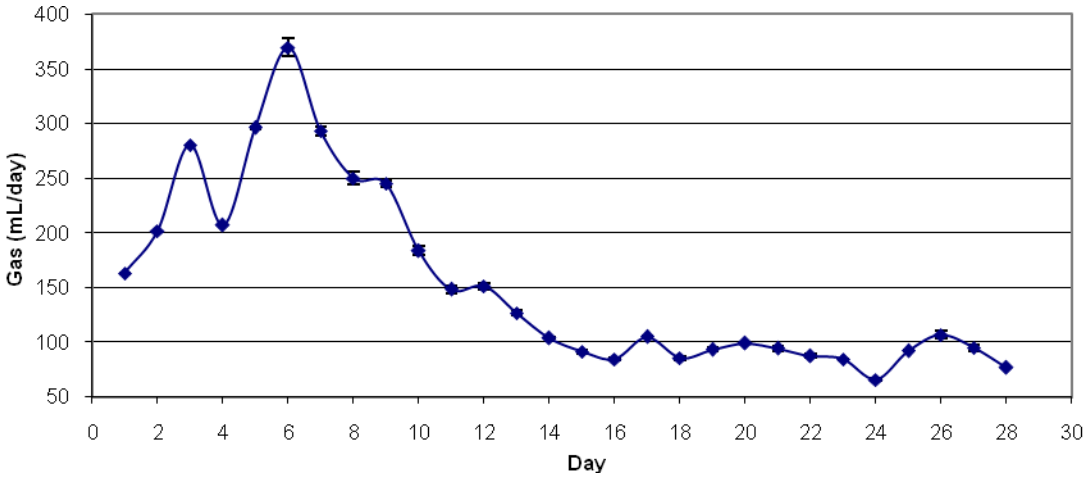

Figure 6.12. Lime pretreated knife-milled 80-mesh bagasse daily gas production (error = ± 2 standard deviations).

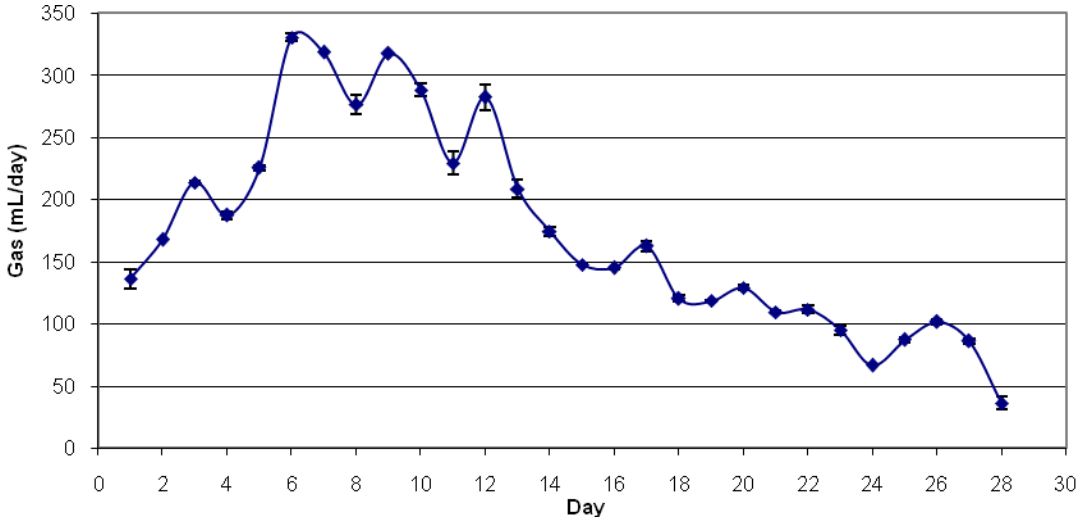

Figure 6.13. Lime-treated ball-milled bagasse daily gas production (error = ± 2 standard deviations).

Gas samples were tested regularly throughout the fermentation for the presence of methane. No methane was detected by the gas chromatograph (GC) in any of the samples taken in this study. Figure 6.14 shows a sample gas chromatogram of raw knife-milled 80-mesh bagasse. Nitrogen gas is detected at 1.97 min and carbon dioxide gas is detected at 3.413 min. No methane gas is detected in this chromatogram; if methane were present in this sample, there would be a peak after ~ 2.4 min.

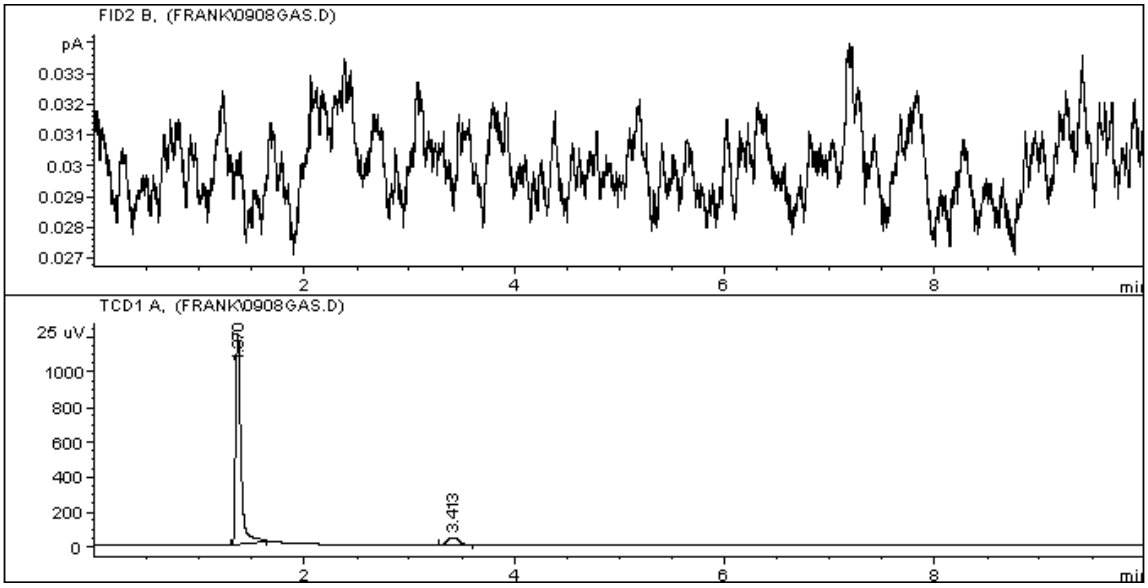

6.14. Sample gas chromatogram of raw knife-milled 80-mesh bagasse.

The pH of each fermentor was monitored daily and controlled to ~7. If the pH was lower than 7, a small amount of ammonium bicarbonate was added to adjust the pH to 7. However, if the pH was 7 or above, no buffer was added.

Figures 6.15 to 6.18 show the daily pH of each fermentor. During the first week of the fermentation, the pH remained at or below 7. By the end of the batch fermentation, the buffer system stabilized, and the pH rose to almost 8 even though acid was still being produced in the fermentors.

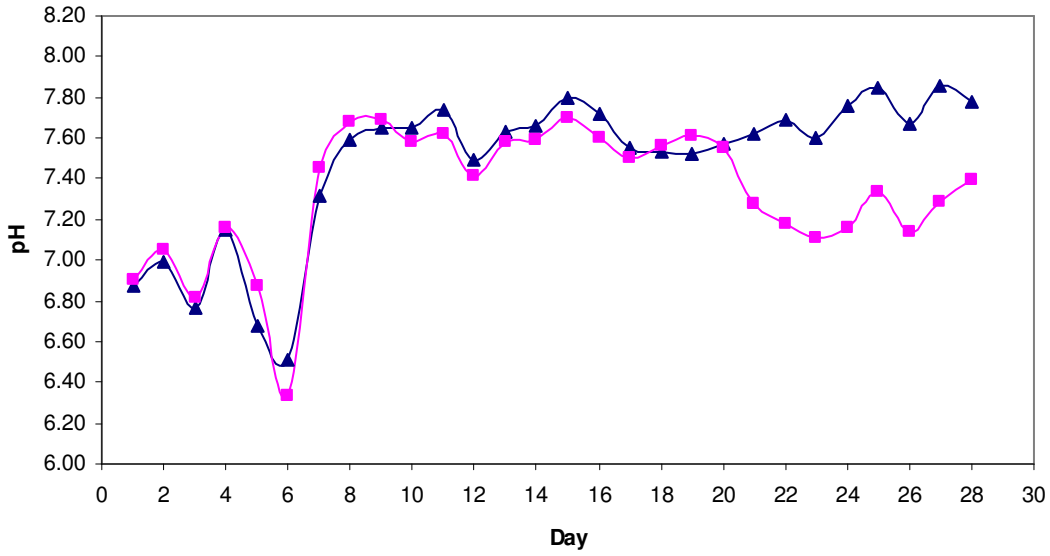

Figure 6.15. Raw knife-milled 80-mesh bagasse pH (duplicates shown).

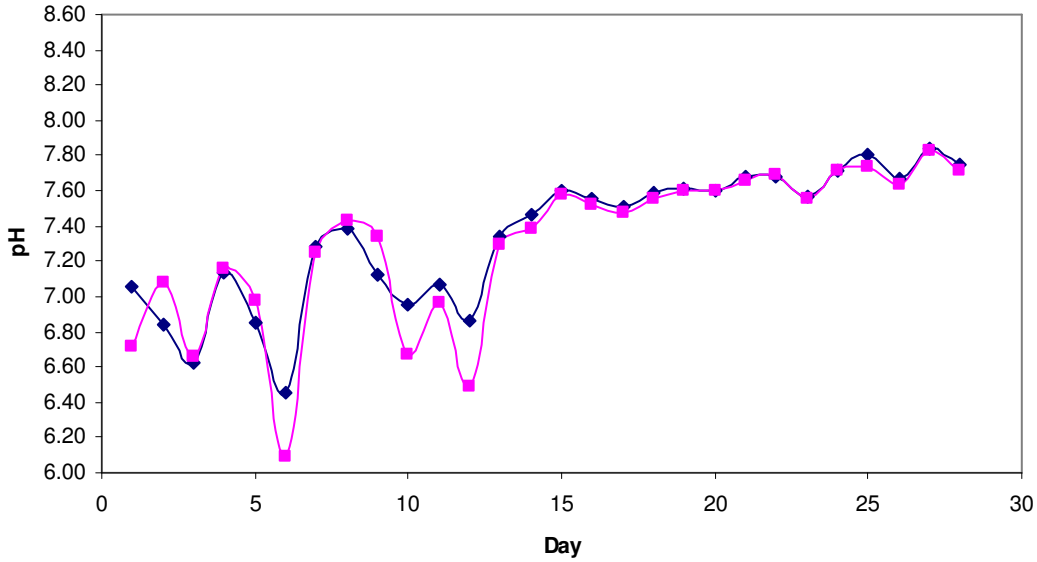

Figure 6.16. Knife-milled lime-treated 80-mesh bagasse pH (duplicates shown).

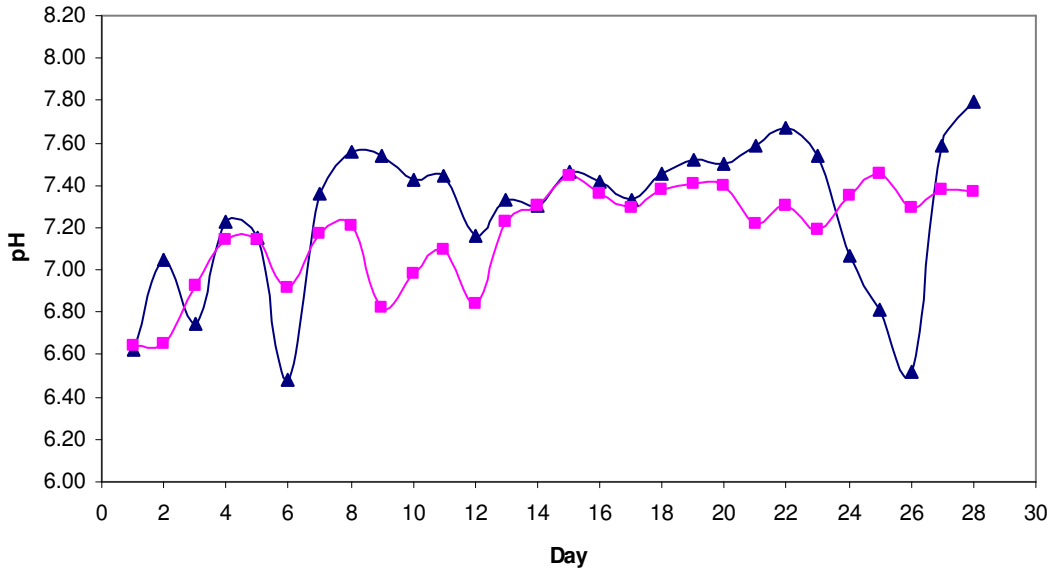

Figure 6.17. Ball-milled bagasse pH (duplicates shown).

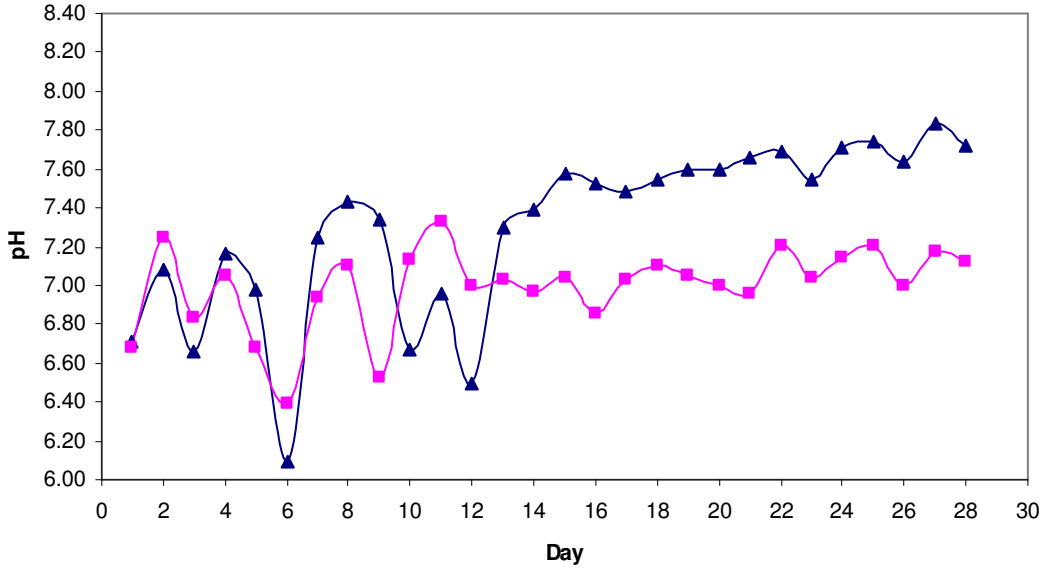

Figure 6.18. Ball-milled lime-treated bagasse pH (duplicates shown).

CONCLUSIONS

Among ball-milled bagasse and raw knife-milled 80-mesh bagasse, the substrates with the lower crystallinities produced higher acid concentrations. This conclusion did not hold with lime pretreatment because it increases the crystallinity due to the removal of amorphous material like lignin and hemicelluloses (Chang and Holtzapple, 2000). However, the removal of lignin increases biomass digestibility by giving the microorganisms greater access to the cellulose in biomass. So the ball-milled lime-treated bagasse produced more acid than the knife-milled lime-treated 80-mesh.

Ball-milling alone was effective in producing relatively high acid concentrations of 21 g/L. Likewise, lime pretreatment alone was effective in producing relatively high acid concentrations of 19 g/L. However, combining the decrystallization pretreatment with the delignification pretreatment resulted in a 42% increase in acid production of 33 g/L, versus lime pretreatment alone, and a 36% increase versus ball-milling alone.

Overall, pretreatment methods that lower the crystallinity of biomass are successful in improving the final acid concentrations produced during fermentation. However, multiple pretreatment methods that both lower the crystallinity of biomass and remove lignin are even more effective in improving the final acid concentrations produced during fermentation.

CHAPTER VII
CONCLUSIONS

This work analyzed the role crystallinity plays in enzymatic digestibility. New physical pilot-scale pretreatments were developed, including hydrodynamic cavitation and shock tube pretreatment, and the resulting biomass crystallinities and digestibilities were determined. A new laboratory-scale lime pretreatment system was also constructed to increase the amount of bagasse that could be pretreated at one time. Furthermore, fermentation was performed to directly correlate the impact of crystallinity and lignin removal in fermentations that used the MixAlco process.

Neither acoustic nor hydrodynamic cavitation was very effective in reducing bagasse crystallinity. Sonication successfully increased Avicel microcrystalline cellulose digestibility; however, there was no effect on lime-treated bagasse most likely due to the presence of amorphous hemicellulose and lignin that protected the crystalline cellulose regions.

Similarly, hydrodynamic cavitation was not effective in reducing the crystallinity or increasing the digestibility of raw knife-milled 10-mesh bagasse or lime-treated knife-milled 10-mesh bagasse. Again, this is partly due to the increased crystallinity of lime-treated bagasse and the recalcitrance of bagasse in general. Furthermore, hydrodynamic cavitation requires a large amount of energy. The energy cost is about $96/tonne, which is too expensive to be economical.

Many factors were varied in the shock tube pretreatment study: water loading, bagasse loading, multiple shocks, shock tube volume, and temperature. Each was modified in an attempt to find optimal settings for the shock tube pretreatment. The water loading, bagasse loading, and multiple shock tests were run using Remington Express 12-gauge 2.75-in Magnum shotgun shells. Using these shells, there was no significant effect of water loading on the bagasse crystallinity. Likewise, there was no statistically significant effect of multiple shocks on bagasse crystallinity, and in the case of the unmilled lime-treated bagasse, there was no statistical effect of bagasse loading on

crystallinity. However, the raw knife-milled 10-mesh and the unmilled bagasse showed a statistically significant reduction in crystallinity with higher bagasse loadings.

Additional multiple shock tests, as well as the temperature and the shock tube volume tests, were run using the larger Remington Express 12-gauge 3.5-in Magnum shotgun shells. At 0, 60, and 80^{o}C, a single shock was sufficient to significantly reduce the crystallinity. At 20, 30, and 40^{o}C, two shocks were required to significantly reduce crystallinity, but the third was unnecessary. Also, increasing the size of the shotgun shells from Remington Express 12-gauge, 2.75-in Magnum shells to 3.5-in Magnum shells produced the largest pressure recorded in this study.

Overall, the data showed that the shock tube treatment decreased bagasse crystallinity. The crystallinity of shock-treated samples was approximately half-way between the crystallinity of untreated bagasse and ball-milled bagasse. The data also showed that the shock tube treatment improved biomass digestibility. On average, the 6-h samples resulted in a 35% improvement in digestibility whereas the 3-d samples resulted in a 22% increase. On a percentage basis, the effect is more prominent with the initial rate (6 h) than the extent of digestion (3 d). This observation is consistent with results obtained from Zhu et al., (2007), which also showed that crystallinity affects the 6-h digestibility more than the 3-day digestibility. The improvement in digestibility is observed with a single shock; therefore, multiple shocks are unnecessary. Also, the effect is seen at moderate temperatures (20 to 40^{o}C), so extreme temperatures (0, 60, 80^{o}C) are not required.

In the batch fermentations, the substrates possessing lower crystallinities (e.g., ball-milled bagasse and raw knife-milled 80-mesh bagasse) produced higher acid concentrations. The lime-treated substrates had higher crystallinities, presumably from the loss of amorphous materials like lignin and acetyl groups (Chang and Holtzapple, 2000), and therefore, their acid concentrations were lower. Ball-milling alone was effective in producing relatively high acid concentrations, 21 g/L. Likewise, lime pretreatment alone was effective in producing relatively high acid concentrations, 19 g/L. However, combining the decrystallization pretreatment with the delignification

pretreatment resulted in a 42% increase in acid production (33 g/L), versus lime pretreatment alone, and a 33% increase versus ball-milling alone. Hence, multiple pretreatment methods that both lower the crystallinity of biomass and remove lignin are useful in improving the final acid concentrations produced during fermentation.

Regarding decrystallization pretreatments, the shock tube shows the most potential for future work. Of all of the variables tested, the temperature and the size of the shotgun shells produced the greatest effects. Future work should focus on finding the optimal operating conditions for the shock tube pretreatment. A bigger shock is likely to reduce the crystallinity even more.

REFERENCES

Abraham, M. and Kurup, G.M., (1997) Pretreatment Studies of Cellulose Wastes for Optimization of Cellulase Enzyme Activity. Applied Biochemistry and Biotechnology 62, 201 – 211.

Agbogbo, F. (2005) Anaerobic Fermentation of Rice Straw and Chicken Manure to Carboxylic Acids. PhD Dissertation, Texas A&M University, College Station, TX

Aiello-Mazzarri, C., Agbogbo, F., and Holtzapple, M. (2006) Conversion of Municipal Solid Waste to Carboxylic Acids Using a Mixed Culture of Mesophilic Microorganisms. Bioresource Technology, 97, 47 – 56.

Balasundaram, B. and Pandit, A.B. (2001) Significance of Location of Enzymes on Their Release during Microbial Cell Disruption. Biotechnology and Bioengineering, 75, 607 – 614.

Bauchop, T. (1967) Inhibition of Rumen Microorganisms by Methane Analogues. Journal of Bacteriology, 94, 171-175.

Bhaskaran, K.A. and Roth, P. (2002). The Shock Tube as Wave Reactor for Kinetic Studies and Material Systems. Progress in Energy and Combustion Science, 28, 151 – 192.

Caldwell, D.R., and Bryant, M.P. (1966) Medium Without Rumen Fluid for Non-selective Enumeration and Isolation of Rumen Bacteria. Applied Microbiology, 14, 794 – 801.

Chang, V.S., Nagwani, M., and Holtzapple, M.T. (1998) Lime Pretreatment of Crop Residues Bagasse and Wheat Straw. Applied Biochemistry and Biotechnology, 74, 135-159.

Chang, V.S. and Holtzapple, M.T. (2000) Fundamental Factors Affecting Biomass Enzymatic Reactivity. Applied Biochemistry and Biotechnology, 84-86, 5 – 37.

Chu, C.P, Lee, D.J., Chang, B., You, C.S., and Tay, J.H. (2002) "Weak" Ultrasonic Pre-treatment on Anaerobic Digestion of Flocculated Activated Biosolids. Water Resources, 36, 2681 – 2688.

Cintas, P. and Luche, J.L. (1999) Green Chemistry: The Sonochemical Approach. Green Chemistry, 1, 115 – 125.

Coughlan, M. (1992) Enzymatic Hydrolysis of Cellulose: An Overview. Bioresource Technology, 39, 107 – 115.

Coward-Kelly, G. (2002) Generating Highly Digestive Animal Feed Via Thermo-chemical and/or Hydrodynamic Cavitation Treatment of Agricultural Feedstocks. PhD dissertation, Texas A&M University, College Station, TX.

Deschamps, F.C., Ramos, L.P., and Fontana, J.D. (1996) Pretreatment of Sugar Cane Bagasse for Enhanced Ruminal Digestion. Applied Biochemistry and Biotechnology, 57/58, 171 – 182.

Fan, L.T., Lee, Y.H, and Beardmore, D.H. (1980) Mechanism of the Enzymatic Hydrolysis of Cellulose: Effects of Major Structural Features of Cellulose on Enzymatic Hydrolysis. Biotechnology and Bioengineering, 22, 177 – 199.

Fan, L.T., Lee, Y.H, and Beardmore, D.H. (1981) The Influence of Major Structural Features of Cellulose on Rate of Enzymatic Hydrolysis. Biotechnology and Bioengineering, 23, 419 – 424.

Fan, L.T. and Lee, Y.H. (1982) Kinetic Studies of Enzymatic Hydrolysis of Insoluble Cellulose: Analysis of the Initial Rates. Biotechnology and Bioengineering, 24, 2383 – 2406.

Fan, L.T. and Lee, Y.H. (1983) Kinetic Studies of Enzymatic Hydrolysis of Insoluble Cellulose: Derivation of a Mechanistic Kinetic Model. Biotechnology and Bioengineering, 25, 2707 – 2733.

Fluent User Guides. (2001) Fluent Inc., www.fluent.com, accessed May 19, 2007.

Fu, Z. (2007) Conversion of Sugarcane Bagasse to Carboxylic Acids under Thermophilic Conditions. PhD dissertation, Texas A&M University, College Station, Texas.

Gandi J., Holtzapple, M.T., Ferrer, A., Byers, F.M., Turner, N., Nagwani, M., and Chang, S. (1997) Lime Treatment of Agricultural Residues to Improve Rumen Digestibility, Animal Feed Science and Technology, 68, 295 – 211.

Genomics GTL. (2007) Transforming Cellulosic Biomass, www.genomicsgtl.energy.gov. accessed May 19, 2007.

Ghosh, P. and Singh, A. (1993) Physicochemical and Biological Treatments for Enzymatic/Microbial Conversion of Lignocellulosic Biomass. Advances in Applied Microbiology, 39, 295 – 333.

Gogate, P.R. and Pandit, A.B. (2005) A Review and Assessment of Hydrodynamic Cavitation as a Technology for the Future. Ultrasonics Sonochemistry, 12. 21-37.

Holtzapple, M. (1993) Cellulose, Hemicellulose, Lignin. In: Macrae, R., Robinson, R.K., Sadler, M.J. (Eds.), Encyclopedia of Food Science, Food Technology, and Nutrition. Vol. 2, 758 – 767, 2324 – 2334, 2731 – 2738. Academic Press, London.

Holtzapple, M.T., Ross, M.K., Chang, N.S., Chang, V.S., Aldelson, S.K., and Brazel, C. (1997). Biomass Conversion to Mixed Alcohols Fuels Using the MixAlco Process. In: Saha, B.C., Woodward, J. (eds), ACS Symposium Series 666. ACS, Washington, DC, pp. 130 – 142.

Holtzapple, M.T., Davison, R.R., Ross, M.K., Aldrett-Lee, S., Nagwani, M., Lee, C.M., Lee, C., Adelson, S., Karr, W., Gaskin, D., Shirage, H., Chang, N., Chang, V.S. and Loescher, M. (1999) Biomass Conversion to Mixed Alcohol Fuels Using the MixAlco Process. Applied Biochemistry and Biotechnology, 77-79, 609 – 631.

Hu, H., Zhou, Z., Xu, Z., and Finch, J.A. (1998) Numerical and Experimental Study of a Hydrodynamic Cavitation Tube. Metallurgical and Materials Transactions, 29B, 911 – 917.

Jyoti, K.K. and Pandit, A.B. (2001) Water Disinfection by Acoustic and Hydrodynamic Cavitation. Biochemical Engineering Journal, 7, 201 – 212.

Kim, S. and Holtzapple, M.T. (2006) Effect of Structural Features on Enzyme Digestibility of Corn Stover. Bioresource Technology, 97, 583 – 591.

Kim, T. H., Kim, J.S., Sunwoo, C. and Lee, Y. Y. (2003) Pretreatment of Corn Stover by Aqueous Ammonia. Bioresource Technology, 90, 39-47.

Krycer, I. and Hersey, J.A. (1980) A Comparative Study of Comminution in Rotary and Vibratory Ball Mills. Powder Technology, **27** 2,137–141.

Kumar, P.S., Kumar, M.S., and Pandit, A.B. (2000) Experimental Quantification of Chemical Effects on Hydrodynamic Cavitation. Chemical Engineering Science, 55,1633 – 1639.

Lonsane, B.K., Ghildyal, N.P, Budiatman S, and Ramakrishna, R.V. (1985) Engineering Aspects of Solid-State Fermentation. Enzyme and Microbial Technology 7, 258 – 265.

Lynd, L. R., Elander, R.T., and Wyman, C.E. (1996) Likely Features and Costs of Mature Biomass Ethanol Technology. Applied Biochemistry and Biotechnology, 57/58, 741-761.

Malherbe, S. and Cloete, T.E. (2002) Lignocellulose Biodegradation: Fundamentals and Applications. Re/Views in Environmental Science and Bio/Technology, 1, 105 – 114.

Mason, T.J. (2003). Sonochemistry and Sonoprocessing: The Link, the Trends, and (Probably) the Future. Ultrasonics Sonochemistry, 10, 175 – 179.

Mosier N, Wyman C, Dale B, Elander, R., Lee, Y.Y., Holtzapple, M., and Ladisch, M. (2005). Features of Promising Technologies for Pretreatment of Lignocellulosic Biomass. Bioresource Technology 96, 673-686.

Pandit, A.B., Kumar, P.S., and Kumar, M.S. (1999) Improve Reactions with Hydrodynamic Cavitation. Chemical Engineering Progress, 95, 43 – 49.

Pandit, A.B. and Gogate, P.R. (2000) Engineering Design Method for Cavitational Reactors: I. Sonochemical Reactors. AICHE Journal, 46, 372 – 379.

Parrot, E.L., (1990) Comminution. In: J. Swarbrick and J.C. Boylan, Editors, Encyclopedia of Pharmaceutical Technology. Vol. 3**,** 101–121.

Philippidis, G.P. and Hatzis, C. (1997. Biochemical Engineering Analysis of Critical Process Factors in the Biomass-to-Ethanol Technology. Biotechnology Progress, 13, 222 – 231.

Puri, Vinod. (1984) Effect of Crystallinity and Degree of Polymerization of Cellulose on Enzymatic Saccharification. Biotechnology and Bioengineering, 26, 1219 – 1222.

Ross, M.K., and Holtzapple, M.T. (2001) Laboratory Method for High-Solids Countercurrent Fermentations. Applied Biochemistry and Biotechnology, 45/46, 111 – 126.

Russell, J.B, and Martin, S.A. (1984) Effects of Various Methane Inhibitors on the Fermentation of Amino Acids by Mixed Rumen Microorganisms. Journal of Animal Science, 59, 1329 – 1338.

Segal, L., Loeb, L., and Creely, J.J. (1954) An X-ray Study of the Decomposition Product of the Ethylamine-Cellulose Complex. Journal of Polymer Science, 13, 193 – 206.

Segal, L., Creely, J.J., Martin, A.E., and Conrad, C.M. (1959) An Empirical Method for Estimating the Degree of Crystallinity of Native Cellulose Using the X-ray Diffractometer. Textile Res. Journal, 29, 786 – 794.

Shah, Y.T., Pandit. A.B., and Moholkar, V.S. (1999) Cavitation Reaction Engineering. Kluwer Academic/Plenum Publishers, New York.

Sinitsyn, A.P., Gusakov, A.V., and Vlasenko, E.Y. (1991) Effect of Structural and Physico-Chemical Features of Cellulosic Substrates on the Efficiency of Enzymatic Hydrolysis. Applied Biochemistry and Biotechnology, 30, 43 – 59.

Suslick, K.S., Mdleleni, M.M., and Ries, J.T. (1997) Chemistry Induced by Hydrodynamic Cavitation. Journal of American Chemical Society, 119, 9303 – 9304.

Thanakoses, P., Mostafa, N.A. A., and Holtzapple, M.T. (2003) Conversion of Sugarcane Bagasse to Mixed Carboxylic Acids Using a Mixed Culture of Mesophilic Microorganisms. Applied Biochemistry and Biotechnology, 105, 523 – 546.

Thompson, D.N. and Chen, H. (1992) Comparison of Pretreatment Methods on the Basis of Available Surface Area, Bioresource Technology, 39, 155 – 163.

United States EPA. (2006) Global Warming. www.epa.gov, accessed October 2006.

Ward, G.H., and Schultz, R.K. (1995) Process-induced Crystallinity Changes in Albuterol Sulfate and Its Effect on Powder Physical Stability, Pharmaceutical Research, 12, 773–779.

Watanawanavet, S. (2005) Optimization of a High-Efficiency Jet Ejector By Computational Fluid Dynamic Software. MS Thesis, Texas A&M University, College Station, TX.

Weimer, P.J., Hackney, J.M, and French, A.D. (1995) Effects of Chemical Treatments and Heating on the Crystallinity of Celluloses and Their Implications for Evaluating the Effect of Crystallinity on Cellulose Biodegradation. Biotechnology and Bioengineering, 48, 169 – 178.

Wyman, C. (2001) Twenty Years of Trials, Tribulations, and Research Progress in Bioethanol Technology. Applied Biochemistry and Biotechnology, 91 – 93, 5 – 21.

Zeikus, J.G. (1980) Chemical and Fuel Production by Anaerobic Bacteria. Annual Review of Microbiology, 34, 423 – 464.

Zhao, H., Kwak, J.H., Wang, Y., Franz, J.A., White, J.M., and Holladay, J.E. (2006) Effects of Crystallinity on Dilute Acid Hydrolysis of Cellulose by Cellulose Ball-Milling Study. Energy & Fuels, 20, 807-811.

Zhu, L., O'Dwyer, J.P., Chang, V.S., Granda, C.B., and Holtzapple, M.T. (2007) Structural Features Affecting Biomass Enzymatic Digestibility. Bioresource Technology. Submitted.

APPENDIX A
MIXALCO LIME PRETREATMENT

A large pile of bagasse was lime pretreated for a maximum of 8 weeks according to conditions recommended by Holtzapple et al. (1999). Approximately 5 kg (equivalent dry weight) of bagasse was placed on top of a rock bed in a large plastic storage bin (L × W × H = 3 ft × 2ft × 2 ft). A water sprayer above the pile kept the bagasse wet, and the water was recycled through a water heater and heat exchanger to maintain a constant temperature of 50^{o}C. Air was scrubbed by a lime slurry and then bubbled through the pile via air diffusers beneath the pile.

Procedure

1. Mix a large amount of raw bagasse (~ 5 kg) with excess lime (30 g/g dry biomass). Mix well to ensure contact between the lime and bagasse.
2. Form a pile on top of the rock bed with the bagasse and lime mixture in the storage bin. (Note: The pile cannot be too large or the dome covering will not seal properly.)
3. Place the dome covering on top of the bin.
4. Screw in the unions connecting the inlet and outlet pipes of the sump.
5. Fill the sump with water to about ¾ the height of the bin.
6. Fill the water tank with water.
7. Open the air valve (~ 20 standard cubic feet per hour) connected to diffusers located beneath the pile.
8. Be sure the return line valve to the sump is open, and the valve to the water sprayer is initially closed.
9. Prime both centrifugal pumps.
10. Turn on pumps. Allow time for air bubbles to be pushed out of the system. This could take a few minutes.
11. Turn on the water heater.

12. Turn on the temperature controller set to control the temperature at 50^{o}C.
13. Open and adjust the sprayer valve to the appropriate position to be sure water is discharging from each sprinkler onto the pile.
14. Add more water to the sump every other day to maintain a constant water level.
15. Monitor the pH of the lime slurry to ensure basic conditions are maintained.
16. Monitor the pH of the sump weekly to determine when to end the pretreatment (ca. pH of 9).

Check the system daily for leaks, and monitor the strainer in the sump pump discharge line weekly to be sure it is not clogged. The pretreatment is finished when the lignin content is reduced to 10% (digestibility is not improved further below 10% lignin content, Chang and Holtzapple, 2000) or when the pH drops below 9, whichever comes first. End the pretreatment after 8 weeks if neither of these conditions occurs before then. Flush the system thoroughly with fresh water before using it again.

APPENDIX B
ACOUSTIC CAVITATION TREATMENT

Bagasse, first pretreated by the small-scale MixAlco pile pretreatment, was ground using a Thomas-Wiley laboratory knife mill (Arthur H. Thomas Company, Philadelphia, PA) and sieved to pass through a 10-mesh screen. The moisture content, lignin, ash, glucan, and xylan content were determined beforehand.

Acoustic cavitation was performed using bagasse and Avicel cellulose in a Fisher Ultrasonic Dismembrator Model 300 at 60% operating power for varying lengths of time. Enzymatic hydrolysis was determined after each cavitation treatment.

Procedure

1. Find the moisture content of the bagasse samples according to NREL standard procedure No. 001.
2. Add 2.5 grams dry weight bagasse and 30 mL of distilled water into a 125-mL centrifuge tube.
3. Place the tube in an ice bath (beaker) for several minutes before sonicating.
4. Immerse the sonicator probe inside the mixture in the tube.
5. Adjust the power setting if needed and turn on the sonicator for the desired time period.
6. Perform enzymatic hydrolysis after sonication using Steps 3 – 15 in the Enzymatic Hydrolysis Procedure (Appendix E).
7. Repeat this procedure for each material.

APPENDIX C
HYDRODYNAMIC CAVITATION TREATMENT

Bagasse, first pretreated by the laboratory-scale lime pretreatment, was ground using a Thomas-Wiley laboratory knife mill (Arthur H. Thomas Company, Philadelphia, PA) and sieved to pass through a 10-mesh screen. The moisture content, lignin, ash, glucan, and xylan content were determined beforehand.

Hydrodynamic cavitation experiments were performed in an open 200-L jacketed reactor with a mixer powered by a variable-speed motor, a centrifugal pump, and a venturi cavitator that was constructed in the chemical engineering workshop (Figures C.1 and C.2). A low mixing rate of 60 rpm was needed to keep the solid particles suspended in the liquid.

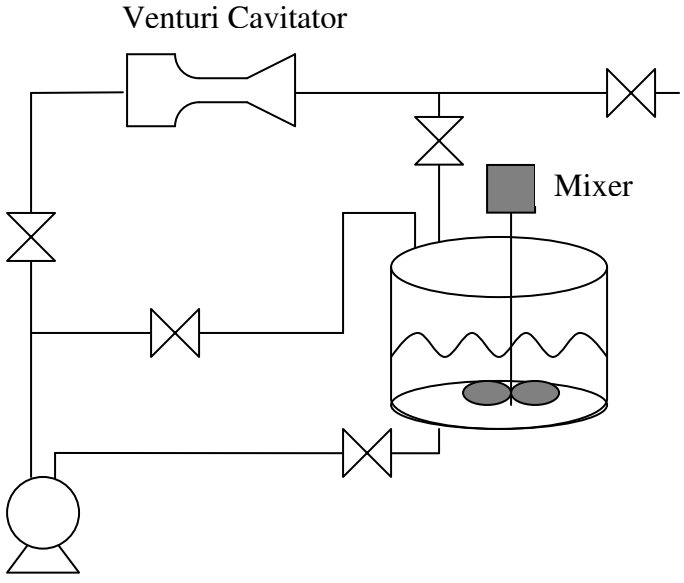

Figure C.1. Hydrodynamic cavitation illustration.

Figure C.2. Hydrodynamic cavitation photograph.

Samples were cavitated for various lengths of time and afterwards filtered to separate the liquid phase from the solid phase. The samples were allowed to air-dry for two days, and part of the sample was used for crystallinity measurements.

The moisture content was then measured so an appropriate dry weight could be determined before performing enzymatic hydrolysis. Then enzymatic hydrolysis was performed on the samples, and finally, the DNS assay was performed to attain the equivalent glucose sugar measurement resulting from the enzymatic hydrolysis.

Procedure

1. Add a known volume of water to the tank (130 L).
2. Turn on the pump and adjust the valves until the desired flow is reached that causes cavitation to occur (tiny bubbles form in the throat of the cavitator) in the venturi cavitator. See Figure C.3 below.

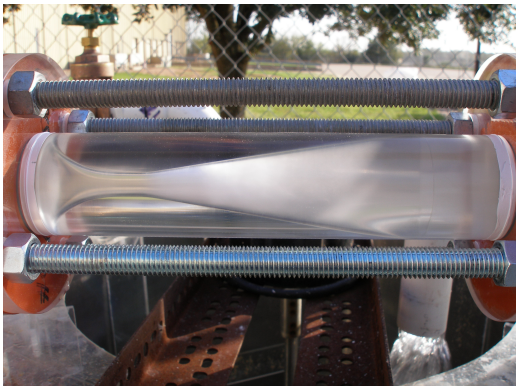

Figure C.3. Cavitation occurring in the throat of the cavitator.

3. Measure flow several times by determining the volume collected in a side container during a known time interval.
4. Turn on the mixer at ~100 rpm.
5. Measure the water temperature.
6. Add 1% bagasse to the water (1.3 kg)
7. After the desired time period, take 1-L samples and separate the solids for crystallinity determination and enzymatic hydrolysis.
8. Repeat the procedure for each material.

APPENDIX D
SHOCK TUBE TREATMENT

Shock tube treatment was studied to determine if it decrystallizes biomass. The biomass used in this experiment included unground bagasse, unground lime-pretreated bagasse, and knife-milled 10-mesh bagasse.

The bagasse was mixed with various amounts of water and placed inside the shock tube (Figure D-1). In the initial testing of the shock tube, the water loading, bagasse loading, and multiple shock tests were performed using Remington Express 12-gauge, 2.75-in shotgun shells. In subsequent tests, it was hypothesized that a larger shell would produce a greater decrystallization effect and further improve digestibility. Therefore, Remington Express Buckshot 12-guage 3.5-in magnum shotgun shells were used, which were more effective in reducing crystallinity and improving digestibility. The shotgun shell was then loaded into the trigger mechanism and released by pulling a cord connected to it from 10 feet away. The maximum pressure was recorded by a pressure gauge located at the top of the shock tube.

After each treatment, the biomass was unloaded and allowed to air-dry for several days. The samples were then ground in a coffee grinder to reduce the particle size and obtain a homogenous sample for the determination of the crystallinity. Crystallinity measurements were then made in the crystallinity lab in the Chemistry Department at Texas A&M University using a Brukar D8 Powder X-ray Diffractometer Short Arm (XRD). The crystallinity was determined before and after the shock tube treatment.

Figure D-1. Shock tube.

Procedure

1. Unbolt the cover flange of the shock tube.
2. Load the desired amount of biomass and water into the shock tube.
3. Rebolt the cover flange of the shock tube.
4. Load the shot gun shell into the shell holder on top of the shock tube.
5. Lift the trigger release on the trigger mechanism and hold it in place by inserting a pin into the top of the mechanism.
6. Tie a cord around the pin in the trigger mechanism.
7. Stand behind a protecting wall approximately 10 feet away and pull the cord to release the trigger mechanism.
8. Record the pressure from the pressure gauge.
9. Open the pressure release valve to release pressure from inside the tube.
10. Unload the shotgun shell.
11. Unbolt the cover flange of the shock tube.
12. Remove the biomass sample from the shock tube and let it air dry for several days under a fume hood.
13. Grind the samples if needed to achieve homogeneity.
14. Perform crystallinity tests on biomass using an X-ray diffactometer.

APPENDIX E
ENZYMATIC HYDROLYSIS (3-DAY DIGESTIBILITY TEST)

Untreated bagasse and lime pretreated bagasse were ground to pass through a 10-mesh sieve. Biomass composition was analyzed before and after each pretreatment. Pure cellulose (Avicel PH-101) was also used in this test.

Enzymatic hydrolysis experiments were run to determine the increase in biomass digestion as a result of each pretreatment. The decreased lignin content after the alkali pretreatments made the cellulose more readily available to the enzymes during hydrolysis. During hydrolysis, citrate buffer (pH of 4.8), sodium azide (microbial inhibitor), and cellulase enzymes were added to the biomass and water mixture. The samples were incubated in a 50^{o}C shaking incubator to ensure the reaction temperature was optimal for the cellulase enzymes and the samples were thoroughly mixed.

Samples were taken at time zero, 1-h, and 72-h to determine the concentration of glucose in the sample, the initial digestion rate, and the extent of digestion, respectively, for the acoustic cavitation pretreatment. The enzymatic procedure was modified for the cavitation pretreatment samples and shock tube pretreatment samples. Zhu et al., (2007) recently discovered that crystallinity greatly affects the initial hydrolysis rate, whereas lignin content plays a more important role in the extent of digestion. So, instead of taking the initial hydrolysis rate samples at 1-h, samples were taken at 6-h because the 1-h sample released too little sugar to obtain accurate, reliable measurements.

After the incubation period, the samples were boiled to denature the enzymes and to stop the hydrolysis. Then, the dinitrosalicylic (DNS) assay was performed and the equivalent glucose sugars were measured with a spectrophotometer.

Procedure

1. Determine the moisture content of the bagasse.
2. Place 2.5 g dry weight of bagasse and add 30 mL of distilled water into a 125-mL centrifuge tube.
3. Add 2.5 mL of citrate buffer (1-M) and 1.5 mL of sodium azide solution (0.01 g/mL).
4. Adjust pH to 4.8 by adding glacial acetic acid or sodium hydroxide. Stir well while adjusting the pH.
5. Rinse the pH probe with ~2 mL of distilled water.
6. Place the tube inside the shaking air incubator at 50^{o}C until it reaches thermal equilibrium.
7. Measure 10 mL of distilled water in a graduated cylinder.
8. Add 0.192 mL of cellulase (loading ~5 FPU/g dry biomass) and 0.29 mL of cellobiase (loading ~30 CBU/ g dry biomass).
9. Rinse the cellulase pipette tip several times with the water, discharging the water into the centrifuge tube. Pour the remaining water into the centrifuge tube.
10. Withdraw 3 mL of the mixture using a 5-mL pipette with a cut-off tip. Shake tube well to obtain a homogeneous sample.
11. Screw top back on and place into a 100-rpm shaking air incubator at 50^{o}C,
12. Boil samples for 15 min in screw-capped tubes to denature the enzymes and cool down in an ice bath.
13. Transfer the contents of each tube into a labeled centrifuge tube and store in freezer for analysis later by the DNS assay.
14. Repeat Steps 10 – 13 for the 1-h sample.
15. After 3 days, measure the final volume of the slurry in each tube. Record the volumes. Repeat Steps 12 – 13 for a 6-mL sample of each final slurry.
    The total volume for the initial slurry is calculated as:

$$V_{\text{initial}}\,(\text{mL}) = V_{\text{final}}\,(\text{mL}) + V_{\text{samples}}\,(\text{mL}) \qquad \text{(E.1)}$$

APPENDIX F
GLUCOSE EQUIVALENT BY THE DINITROSALICYLIC ACID ASSAY (DNS)

The glucose equivalent (reducing sugars) was measured by the DNS assay. Glucose standards (5 mg/mL) were used for the calibration curve in the measurement of the reducing sugars. *Note: The spectrophotometer should be turned on at least 1 h before use.*

Procedure

Standard preparation

1. Dry ~1 g of glucose in 45^{o}C oven for at least 24 h.
2. Remove sample from oven and let it cool in a desiccator until it reaches room temperature.
3. Weigh 0.5 g of glucose and transfer to a 100-mL volumetric flask. Fill the flask to the 100-mL mark with distilled water.
4. Transfer the standard solution to 50-mL centrifuge tubes and store in the freezer until needed.

DNS reagent preparation

1. Dissolve 10.6 g of 3, 5-dinitrosalicylic acid and 19.8 g of NaOH in 1416 mL of distilled water in a tinted 5-gallon glass bottle.
2. Add stir bar and place bottle on stir plate. Continue stirring throughout the rest of the preparation.
3. Add 306 g of Rochelle salt (sodium potassium tartrate).
4. Fill a small dilution tube halfway with phenol crystals, and melt them under a fume hood at 50^{o}C in a water bath. Add 7.6 mL to the above mixture.
5. Add 8.3 g of sodium meta-bisulfite.
6. Adjust the pH of the mixture to 12.6 by adding NaOH.

DNS Reagent Calibration

1. Prepare dilutions of known glucose concentration in test tubes according to Table 1 using the glucose standard (room temperature, well shaken).
2. Add 0.5 mL of each dilution to 1 mL of distilled water into test tubes.
3. Add 3 mL of DNS reagent into each test tube using a 5-mL pipette.
4. Place the caps on the test tubes and vortex.
5. Place samples in a vigorously boiling water bath for exactly 5 minutes.
6. Cool the test tubes to room temperature in an ice bath for several minutes.
7. Add 10 mL of distilled water to each test tube.
8. Zero the spectrophotometer at 540 nm with distilled water.
9. Measure the absorbance of each sample.
10. Prepare the calibration curve.

Table F.1. Dilutions used for DNS calibration curve.

Glucose Concentration (mg/mL)	**Distilled Water (mL)**	**Glucose Standard (mL)**
0.2	4.8	0.2
0.4	4.6	0.4
0.6	4.4	0.6
0.8	4.2	0.8
1.0	4.0	1.0
2.0	3.0	2.0
3.0	2.0	3.0
4.0	1.0	4.0
5.0	0.0	5.0

Glucose Equivalent Measurement

1. Thaw frozen samples and vortex.
2. Centrifuge samples at 4000 rpm for 5 minutes.
3. Dilute samples into test tubes so that the sugar concentration lies between 0.2 and 5.0 mg/mL. Vortex the diluted samples.
4. Repeat Steps 3 – 9 in "DNS Reagent Calibration."
5. Calculate the glucose equivalent concentration from the absorbance of the sample using the calibration curve.
6. Calculate the glucose equivalent yield with the formula:

$$Y = \frac{G \times D \times V}{W} \tag{F.1}$$

where,

Y = mg equivalent glucose/g dry biomass

G = equivalent glucose concentration in diluted sample (mg/mL)

D = dilution factor

V = total volume in 3-day digestibility mixture (mL)

W = dry weight of biomass used in 3-day digestibility test (g)

Figure F.1. Calibration curve for the DNS assay.

APPENDIX G
CRYSTALLINITY ANALYSIS

The crystallinity of the samples was measured before and after pretreatment to determine the effect of each pretreatment. A Brukar D8 Powder X-ray Diffractometer Short Arm located in the Chemistry Building, Room 2407, at Texas A&M University was used to measure the crystallinity of each sample.

The samples were filled flush to the top of an aluminum sample holder. The samples were scanned at 2^{o}/min from $2\theta = 10^{o}$ to 26^{o} with a step size of 0.05^{o}. The crystallinity index was determined from the formula given by Segal et al. (1954, 1959)

$$CrI = \frac{I_{002} - I_{am}}{I_{002}} \times 100 \qquad \text{(G.1)}$$

where I_{002} is the maximum intensity of the 002 peak at $2\theta = 22.5^{o}$ and I_{am} is the intensity at $2\theta = 18.7^{o}$.

Procedure

1. Air-dry the homogenous bagasse sample.
2. Load the sample flush to the top of the sample tray.
3. Use a microscope slide to slide away the excess bagasse and to smooth the top of the sample. The sample must be smooth and flat to ensure accurate readings.
4. Load the sample tray into the XRD by placing it on the holder while pushing up the latch beneath the holder to lock it in place.
5. Close the doors by pulling them together firmly until they lock in place.
6. Input the sample description into the computer connected to the XRD. Follow the instructions given in the Step-by-Step Tutorial located next to the computer.
7. Start the analysis by clicking Execute Job.

8. After the sample finishes, open the doors and remove the tray by pushing the release latch behind the holder. *Note: Be sure the red light indicating the laser is operating is not on before opening the doors.*
9. Repeat this process for each sample.

APPENDIX H
BATCH FERMENTATION

Batch fermentation was performed using bagasse samples of different crystallinities to determine the effects of crystallinity on fermentation. Knife-milled 80-mesh bagasse, ball-milled bagasse, knife-milled 80-mesh lime-pretreated bagasse, and ball-milled lime-pretreated bagasse were used.

Ammonium bicarbonate was used as buffer in the system. Dried chicken manure was added as a nutrient source along with a dry nutrient mix. Fermentation proceeded for 28 days. At the end of the batch fermentation, the volume of the remaining liquid was measured as well as the weight of the solids. Then the solids were ashed to determine the final volatile solid content.

Procedure

Preparation

1. Find the moisture content of the biomass and the chicken manure.
2. Find the volatile solids content (see procedure below).
3. Weigh the empty reactors to be used during fermentation without the caps. This will be used to calculate the final weight of the biomass slurry after fermentation.
4. Test the reactors for leaks by filling them with water and incubating them overnight.

Fermentation

1. Thaw inocula (if needed) and centrifuge to clarify the liquid.
2. Weigh 16 g (dry weight) of biomass and 4 g of dry manure (80:20 ratio).
3. Add the biomass and manure to each reactor.
4. Add 0.3 grams of nutrients to each reactor.
5. Add 1 gram of buffer (ammonium bicarbonate) to each reactor.

6. Add 230 mL of deoxygenated water with cysteine hydrochloride and sodium sulfide (Appendix I) into each reactor.
7. Add 20 mL of inocula into each reactor.
8. Add 120 μL of iodoform solution into each reactor to prohibit methane production. (Note: Iodoform solution consisted of 20 g iodoform in 1 L ethanol.)
9. Centrifuge the reactors at 4000 rpm for 15 minutes.
10. Take a 2-mL t_o sample from each reactor.
11. Measure the initial pH of each reactor.
12. Purge the reactors with nitrogen and place the rubber stopper tops on each reactor. Screw the reactor bottle caps firmly around the rubber stoppers.
13. Incubate the reactors and monitor regularly for leaks.
14. Record the gas production daily of each reactor using the water displacement apparatus to measure the gases. Replace the septum of each fermentor when there are visible holes in the septum as a result of regular gas sampling.
15. Measure pH daily. If the pH is lower than 7, add an appropriate amount of buffer to raise the pH to 7.
16. Add 120 μL of iodoform every two days.
17. Take samples every two days after adjusting pH and recording gas production. Follow Steps 8 – 9 above.
18. Add 0.3 grams of nutrients to each reactor every 4 days.
19. Take gas samples weekly and analyze the gas in the gas chromatograph (GC) to ensure methane is not being produced.
20. End fermentation when the acid production levels off (~ 28 days).

APPENDIX I
LIQUID MEDIA PREPARATION

The liquid media used in the batch fermentations was prepared as follows:

1. Boil 5 L of distilled water in a 6-L Erlenmeyer flask.
2. Boil distilled water under a nitrogen purge for 10 minutes.
3. Allow the water to cool to room temperature. Cap the top of the container to prevent air from getting inside it.
4. Add 0.275% cysteine hydrochloride and 0.275% sodium sulfide per liter of boiled water.
5. Insert a stir rod into the flask and stir for 10 minutes under a nitrogen purge.
6. Quickly pour the liquid into storage bottles, filling them completely and closing the lids tightly.

APPENDIX J
CARBOXYLIC ACIDS ANALYSIS

For carboxylic acid analysis, at least 3 mL of liquid should be withdrawn from the fermentor and placed in a 15-mL conical bottom centrifuge tube. If not used immediately, the samples may be stored at –15°C. At the moment of the analysis, if the sample has been stored in the freezer, thaw and vortex the sample before beginning the procedure.

GC LIQUID SAMPLE PREPARATION

1. Centrifuge the liquid sample for 5 min at 3500 rpm.
2. Pipette 1 mL of the liquid clear broth into a 15-mL round-bottom ultracentrifuge tube.
3. Add to the same tube, 1 mL of 10-mM of internal stand 4-methyl-valeric acid (1.162 g/L internal standard, ISTD).
4. Add to the same tube, 1 mL of 3-M phosphoric acid to acidify the sample and allow the carboxylic acids to be released in the GC injection port.
5. Cap the tube and vortex.
6. Centrifuge the mixture at 15,000 rpm (40,000 × g) in the IEC B-20A centrifuge (Industrial Equipment Co., Needham Hts., MA). Due to the poor refrigeration system in the centrifuge, simply accelerate the centrifuge to 15,000 rpm and immediately to zero rpm. (Be sure that the temperature is lower than 25°C before using it.)
7. Pipette 1 mL of the centrifugated mixture into a glass GC vial and cap. The sample in the vial is ready to be analyzed. If the sample will not be analyzed immediately, it can be stored in the freezer. If frozen, care should be taken to thaw and vortex the sample before the GC analysis.

GC OPERATION

1. Before starting the GC, check the gas supply cylinders (compressed hydrogen, zero-grade helium, and compressed zero-grade air from Praxair, Bryan, TX) to insure at least 100 psig pressure in each. If there is not enough gas, switch cylinders and place an order for new ones.
2. Establish gas flow by setting the regulators in the 40 psig for hydrogen, 60 psig for helium, and 50 psig for air.
3. Check the solvent and waste bottles on the injection tower. Fill the solvent bottles with methanol, and be sure the waste bottles are empty.
4. Make sure the column head pressure gauge on the GC indicates the proper pressure (15 psig). Low head pressure usually indicates a worn-out septum. Replace the septum before starting the GC.
5. Up to 100 samples can be loaded into the autosampler plate. Place the samples in the autosampler racks without leaving empty spaces between samples. Place volatile acid standard mix (Matreya, Inc. #1075) solution every 50 samples for calibration.
6. Check the setting conditions in the method:
    a. Oven temperature = 50 ^{o}C
    b. Ramp = 20 ^{o}C/min
    c. Inlet temperature = 230 ^{o}C
    d. Detector temperature = 250 ^{o}C
    e. H_2 flow = 40 mL/min
    f. He flow = 180 mL/min
    g. Air flow = 400 mL/min
7. Start the GC on the computer by selecting the method with the setting conditions mentioned above. Set and load the sequence of samples to run. Once the conditions are reached and the green start signal is on the screen, start the run sequence. Details about operation, setting sequence and calibration are in the Agilent 6890 instrument manual.

8. Periodically check back to ensure that the equipment is working properly. Be sure to indicate the number of samples and any maintenance performed (changes of septum, gas cylinders, liner, etc.) in the GC logbook.
9. When finished running the sequence, turn the GC on standby and close the air and hydrogen cylinder valves.

APPENDIX K
BIOMASS DRYING PROCEDURE

This procedure was used to air-dry all of the biomass samples in this work. Before starting the procedure, excess water was carefully pressed out of the samples by hand.

1. Spread out the biomass evenly in a long rectangular stainless steel pan. Do not spread the biomass deeper than 4 cm.
2. Place the pans beneath in a hood to air dry (controlled air velocity of 100 ft/min).
3. Turn the biomass once per day to ensure even drying.
4. The sample is considered dry when the moisture content is 10% or less (measured using NREL Standard Procedure 001), which is usually after a minimum of two days.

	Abs	Sonication Treatment time (min)	Equiv. Glucose Conc. (mg/mL)	Final Volume	Total volume (ml)	Y0 (mg/g)	Y1 (mg/g)	Y3 (mg/g)	1-hr Yield (mg/g)	3-day yield* (mg/g)
Initial :										
1	0.074	15	0.646	38.5	44.5	23.007				
2	0.072	15	0.631	38.5	44.5	22.469				
3	0.068	15	0.601	39.0	45.0	21.633				
4	0.074	30	0.646	37.0	43.0	22.231				
5	0.076	30	0.661	38.5	44.5	23.545				
6	0.072	30	0.631	38.5	44.5	22.469				
1-hr:										
1	0.171	15	1.379	38.5	44.5		122.770			
2	0.162	15	1.311	38.5	44.5		116.716			
3	0.178	15	1.432	39.0	45.0		128.912			
4	0.183	30	1.470	37.0	43.0		126.432			
5	0.185	30	1.485	38.5	44.5		132.188			
6	0.170	30	1.372	38.5	44.5		122.098			
3-day:										
1	0.390	15	3.035	38.5	44.5			540.189	99.763	517.182
2	0.384	15	2.989	38.5	44.5			532.116	94.247	509.648
3	0.380	15	2.959	39.0	45.0			532.653	107.279	511.020
4	0.396	30	3.080	37.0	43.0			529.781	104.201	507.550
5	0.384	30	2.989	38.5	44.5			532.116	108.643	508.571
6	0.386	30	3.005	38.5	44.5			534.807	107.279	513.175
Initial :										
1	0.076	45	0.653	39.5	45.5	23.756				
2	0.076	45	0.653	38.5	44.5	23.234				
3	0.077	45	0.660	38.5	44.5	23.501				

	Abs	Sonication Treatment time (min)	Equiv. Glucose Conc. (mg/mL)	Final Volume	Total volume (ml)	Y0 (mg/g)	Y1 (mg/g)	Y3 (mg/g)	1-hr Yield (mg/g)	3-day yield* (mg/g)
4	0.068	60	0.592	39.5	45.5	21.566				
5	0.080	60	0.683	39.0	45.0	24.577				
6	0.078	60	0.668	39.0	45.0	24.036				
1-hr:										
1	0.188	45	1.495	39.5	45.5		136.021			
2	0.190	45	1.510	38.5	44.5		134.370			
3	0.190	45	1.510	38.5	44.5		134.370			
4	0.189	60	1.502	39.5	45.5		136.705			
5	0.196	60	1.555	39.0	45.0		139.940			
6	0.193	60	1.532	39.0	45.0		137.910			
3-day:										
1	0.418	45	3.224	39.5	45.5			586.779	112.265	563.023
2	0.412	45	3.179	38.5	44.5			565.853	111.136	542.619
3	0.426	45	3.284	38.5	44.5			584.589	110.869	561.088
4	0.429	60	3.307	39.5	45.5			601.832	115.139	580.265
5	0.442	60	3.405	39.0	45.0			612.812	115.362	588.235
6	0.447	60	3.442	39.0	45.0			619.579	110.869	596.078
Initial :										
1	0.044	0	0.402	36.0	43.0	13.831				
2	0.045	0	0.409	38.5	45.5	14.904				
3	0.046	0	0.417	36.0	43.0	14.340				
1-hr:										
1	0.174	0	1.363	36.0	43.0		117.209			
2	0.172	0	1.348	38.5	45.5		122.678			
3	0.168	0	1.319	36.0	43.0		113.395			
3-day:	.									
1	0.396	0	3.004	36.0	43.0			516.636	103.378	502.804
2	0.371	0	2.819	38.5	45.5			513.044	107.774	498.139

	Abs	Sonication Treatment time (min)	Equiv. Glucose Conc. (mg/mL)	Final Volume	Total volume (ml)	Y0 (mg/g)	Y1 (mg/g)	Y3 (mg/g)	1-hr Yield (mg/g)	3-day yield* (mg/g)
3	0.403	0	3.055	36.0	43.0			525.534	99.056	511.195
Initial :										
1	0.080	90	0.704	37.5	44.5	25.059				
2	0.073	90	0.648	38.0	45.0	23.330				
3	0.075	90	0.664	39.5	46.5	24.701				
4	0.078	120	0.688	36.5	43.5	23.941				
5	0.071	120	0.632	38.0	45.0	22.755				
6	0.082	120	0.720	38.0	48.0	27.643				
7	0.067	300	0.600	36.0	46.0	22.086				
1-hr:										
1	0.211	90	1.749	37.5	44.5		155.697			
2	0.206	90	1.709	38.0	45.0		153.855			
3	0.203	90	1.686	39.5	46.5		156.757			
4	0.217	120	1.797	36.5	43.5		156.364			
5	0.224	120	1.853	38.0	45.0		166.784			
6	0.228	120	1.885	38.0	48.0		180.967			
7	0.240	300	1.981	36.0	46.0		182.238			
3-day:										
1	0.505	90	4.096	37.5	44.5			729.047	130.638	703.988
2	0.476	90	3.864	38.0	45.0			695.579	130.525	672.249
3	0.468	90	3.800	39.5	46.5			706.889	132.056	682.188
4	0.505	120	4.096	36.5	43.5			712.664	132.423	688.723
5	0.478	120	3.880	38.0	45.0			698.452	144.029	675.697
6	0.469	120	3.808	38.0	48.0			731.224	153.324	703.581
7	0.516	300	4.184	36.0	46.0			769.775	132.056	745.074
Initial :										
1	0.088	135	0.708	36.5	42.5	24.084				
2	0.091	135	0.732	37.5	43.5	25.467				

	Abs	Sonication Treatment time (min)	Equiv. Glucose Conc. (mg/mL)	Final Volume	Total volume (ml)	Y0 (mg/g)	Y1 (mg/g)	Y3 (mg/g)	1-hr Yield (mg/g)	3-day yield* (mg/g)
3	0.094	135	0.755	37.5	43.5	26.284				
4	0.103	150	0.826	37.0	43.0	28.402				
5	0.081	150	0.654	37.0	43.0	22.485				
6	0.096	150	0.771	37.5	43.5	26.828				
1-hr:										
1	0.208	135	1.647	36.5	42.5		139.961			
2	0.200	135	1.584	37.5	43.5		137.812			
3	0.199	135	1.576	37.5	43.5		137.132			
4	0.207	150	1.639	37.0	43.0		140.935			
5	0.191	150	1.514	37.0	43.0		130.177			
6	0.222	150	1.756	37.5	43.5		152.777			
3-day:										
1	0.478	135	3.758	36.5	42.5			638.796	115.876	614.711
2	0.290	135	2.288	37.5	43.5			398.064	112.345	372.597
3	0.498	135	3.914	37.5	43.5			681.035	110.848	654.752
4	0.515	150	4.047	37.0	43.0			696.069	112.533	667.667
5	0.507	150	3.984	37.0	43.0			685.310	107.692	662.825
6	0.522	150	4.102	37.5	43.5			713.686	125.949	686.858
Initial :	*Bagasse*									
1	0.056	60	0.507	44.0	56.0	22.719				
2	0.060	60	0.537	46.0	58.0	24.923				
3	0.042	0	0.402	48.0	60.0	19.301				
4	0.040	0	0.387	48.0	60.0	18.581				
5	0.020	raw	0.237	42.0	54.0	10.241				
6	0.020	raw	0.237	42.0	54.0	10.241				

	Abs	Sonication Treatment time (min)	Equiv. Glucose Conc. (mg/mL)	Final Volume	Total volume (ml)	Y0 (mg/g)	Y1 (mg/g)	Y3 (mg/g)	1-hr Yield (mg/g)	3-day yield* (mg/g)
1-hr:										
1	0.218	60	1.722	44.0	56.0		192.912			
2	0.218	60	1.722	46.0	58.0		199.802			
3	0.210	0	1.662	48.0	60.0		199.490			
4	0.200	0	1.587	48.0	60.0		190.488			
5	0.072	raw	0.627	42.0	54.0		67.733			
6	0.073	raw	0.635	42.0	54.0		68.543			
3-day:										
1	0.294	60	2.293	44.0	56.0			513.536	170.193	490.817
2	0.273	60	2.135	46.0	58.0			495.328	174.879	470.405
3	0.270	0	2.113	48.0	60.0			507.007	180.189	487.706
4	0.256	0	2.008	48.0	60.0			481.800	171.907	463.220
5	0.063	raw	0.560	42.0	54.0			120.882	57.492	110.641
6	0.041	raw	0.395	42.0	54.0			85.233	58.302	74.992
Initial :										
1	0.036	75	0.357	45.0	58.0	16.569				
2	0.042	75	0.402	45.0	58.0	18.657				
3	0.049	90	0.455	45.0	58.0	21.094				
4	0.048	90	0.447	46.0	59.0	21.104				
5	0.044	120	0.417	45.0	58.0	19.354				
6	0.049	120	0.455	45.5	58.5	21.276				
7	0.047	15	0.440	46.0	59.0	20.750				
8	0.046	15	0.432	46.0	59.0	20.395				
9	0.044	30	0.417	43.0	56.0	18.686				
10	0.051	30	0.470	46.0	59.0	22.166				
11	0.054	105	0.492	43.0	56.0	22.047				
12	0.051	105	0.470	45.0	58.0	21.790				
13	0.055	45	0.500	45.5	58.5	23.382				

	Abs	Sonication Treatment time (min)	Equiv. Glucose Conc. (mg/mL)	Final Volume	Total volume (ml)	Y0 (mg/g)	Y1 (mg/g)	Y3 (mg/g)	1-hr Yield (mg/g)	3-day yield* (mg/g)
14	0.056	45	0.507	47.0	60.0	24.342				
1-hr:										
1	0.188	75	1.497	45.0	58.0		173.695			
2	0.198	75	1.572	45.0	58.0		182.398			
3	0.189	90	1.505	45.0	58.0		174.566			
4	0.217	90	1.715	46.0	59.0		202.362			
5	0.210	120	1.662	45.0	58.0		192.840			
6	0.199	120	1.580	45.5	58.5		184.848			
7	0.195	15	1.550	46.0	59.0		182.887			
8	0.193	15	1.535	46.0	59.0		181.116			
9	0.199	30	1.580	43.0	56.0		176.948			
10	0.201	30	1.595	46.0	59.0		188.198			
11	0.216	105	1.707	43.0	56.0		191.232			
12	0.220	105	1.737	45.0	58.0		201.542			
13	0.224	45	1.767	45.5	58.5		206.791			
14	0.216	45	1.707	47.0	60.0		204.891			
3-day:										
1	0.260	75	2.038	45.0	58.0			472.702	157.126	456.133
2	0.262	75	2.053	45.0	58.0			476.183	163.740	457.526
3	0.282	90	2.203	45.0	58.0			510.992	153.472	489.898
4	0.306	90	2.383	46.0	59.0			562.293	181.258	541.189
5	0.302	120	2.353	45.0	58.0			545.800	173.487	526.447
6	0.274	120	2.143	45.5	58.5			501.353	163.572	480.077
7	0.310	15	2.413	46.0	59.0			569.374	162.137	548.625
8	0.285	15	2.225	46.0	59.0			525.113	160.721	504.718
9	0.277	30	2.165	43.0	56.0			484.969	158.262	466.283
10	0.307	30	2.390	46.0	59.0			564.063	166.032	541.897
11	0.307	105	2.390	43.0	56.0			535.382	169.185	513.335

	Abs	Sonication Treatment time (min)	Equiv. Glucose Conc. (mg/mL)	Final Volume	Total volume (ml)	Y0 (mg/g)	Y1 (mg/g)	Y3 (mg/g)	1-hr Yield (mg/g)	3-day yield* (mg/g)
12	0.321	105	2.495	45.0	58.0			578.869	179.752	557.078
13	0.293	45	2.285	45.5	58.5			534.707	183.408	511.324
14	0.306	45	2.383	47.0	60.0			571.823	180.549	547.481

Sample	Abs	# of Shocks	Temp	Equiv. Glucose Conc. (mg/mL)	Final Volume	Total volume (ml)	Y0 (mg/g)	Y1 (mg/g)	Y3 (mg/g)	6-hr Yield (mg/g)	3-day yield (mg/g)
Initial :	***Bagasse***										
1	0.016	1	40	0.206	38.0	47.0	7.752				
2	0.025	1	40	0.276	37.0	46.0	10.145				
3	0.025	2	40	0.276	37.0	46.0	10.145				
4	0.021	2	40	0.245	38.0	47.0	9.204				
5	0.022	3	40	0.253	37.0	46.0	9.292				
6	0.041	3	40	0.399	36.0	45.0	14.372				
7	0.038	1	30	0.376	38.0	47.0	14.140				
8	0.020	1	30	0.237	37.0	46.0	8.724				
9	0.027	2	30	0.291	36.0	45.0	10.480				
10	0.031	2	30	0.322	36.0	45.0	11.592				
11	0.022	3	30	0.253	37.0	46.0	9.292				
12	0.032	3	30	0.330	37.0	46.0	12.134				
13	0.036	1	20	0.361	38.0	47.0	13.559				
14	0.043	1	20	0.415	38.0	47.0	15.592				
15	0.032	2	20	0.330	38.0	47.0	12.398				
16	0.024	2	20	0.268	38.0	47.0	10.075				
17	0.030	3	20	0.314	37.0	46.0	11.566				
18	0.022	3	20	0.253	39.0	48.0	9.696				
6-hr:											
1	0.093	1	40	0.801	38.0	47.0		75.273			
2	0.139	1	40	1.156	37.0	46.0		106.351			
3	0.125	2	40	1.048	37.0	46.0		96.405			
4	0.125	2	40	1.048	38.0	47.0		98.500			
5	0.118	3	40	0.994	37.0	46.0		91.432			
6	0.140	3	40	1.164	36.0	45.0		104.734			
7	0.115	1	30	0.971	38.0	47.0		91.242			
8	0.123	1	30	1.032	37.0	46.0		94.984			

Sample	Abs	# of Shocks	Temp	Equiv. Glucose Conc. (mg/mL)	Final Volume	Total volume (ml)	Y0 (mg/g)	Y1 (mg/g)	Y3 (mg/g)	6-hr Yield (mg/g)	3-day yield (mg/g)
9	0.090	2	30	0.778	36.0	45.0		69.985			
10	0.109	2	30	0.924	36.0	45.0		83.189			
11	0.128	3	30	1.071	37.0	46.0		98.536			
12	0.129	3	30	1.079	37.0	46.0		99.246			
13	0.153	1	20	1.264	38.0	47.0		118.825			
14	0.117	1	20	0.986	38.0	47.0		92.693			
15	0.108	2	20	0.917	38.0	47.0		86.161			
16	0.141	2	20	1.171	38.0	47.0		110.114			
17	0.139	3	20	1.156	37.0	46.0		106.351			
	0.133	3	20	1.110	39.0	48.0		106.527			
3-day:											
1	0.060	1	40	0.546	38.0	47.0			102.638	67.520	94.886
2	0.082	1	40	0.716	37.0	46.0			131.713	96.206	121.568
3	0.070	2	40	0.623	37.0	46.0			114.663	86.260	104.518
4	0.077	2	40	0.677	38.0	47.0			127.317	89.296	118.113
5	0.064	3	40	0.577	37.0	46.0			106.137	82.139	96.845
6	0.067	3	40	0.600	36.0	45.0			108.000	90.361	93.628
7	0.067	1	30	0.600	38.0	47.0			112.800	77.102	98.660
8	0.065	1	30	0.585	37.0	46.0			107.558	86.260	98.834
9	0.048	2	30	0.453	36.0	45.0			81.591	59.504	71.110
10	0.058	2	30	0.531	36.0	45.0			95.490	71.597	83.898
11	0.075	3	30	0.662	37.0	46.0			121.767	89.244	112.474
12	0.067	3	30	0.600	37.0	46.0			110.400	87.112	98.266
13	0.085	1	20	0.739	38.0	47.0			138.931	105.265	125.372
14	0.063	1	20	0.569	38.0	47.0			106.993	77.102	91.401
15	0.071	2	20	0.631	38.0	47.0			118.607	73.763	106.209
16	0.082	2	20	0.716	38.0	47.0			134.576	100.039	124.501
17	0.080	3	20	0.700	37.0	46.0			128.871	94.785	117.305

Sample	Abs	# of Shocks	Temp	Equiv. Glucose Conc. (mg/mL)	Final Volume	Total volume (ml)	Y0 (mg/g)	Y1 (mg/g)	Y3 (mg/g)	6-hr Yield (mg/g)	3-day yield (mg/g)
18	0.071	3	20	0.631	39.0	48.0			121.131	96.830	111.434
Initial :											
1	0.039	1	60	0.384	38.0	47.0	14.430				
2	0.017	1	60	0.214	38.0	47.0	8.043				
3	0.020	2	60	0.237	38.0	47.0	8.914				
4	0.022	2	60	0.253	38.0	47.0	9.494				
5	0.024	3	60	0.268	37.0	46.0	9.861				
6	0.025	3	60	0.276	39.0	48.0	10.586				
7	0.026	1	80	0.283	39.0	48.0	10.882				
8	0.030	1	80	0.314	38.0	47.0	11.817				
9	0.027	2	80	0.291	37.0	46.0	10.713				
10	0.023	2	80	0.260	36.0	45.0	9.368				
11	0.016	3	80	0.206	38.0	47.0	7.752				
12	0.034	3	80	0.345	38.0	47.0	12.979				
6-hr:											
1	0.139	1	60	1.156	33.0	42.0		97.103			
2	0.144	1	60	1.195	30.0	39.0		93.178			
3	0.150	2	60	1.241	33.0	42.0		104.238			
4	0.134	2	60	1.117	33.0	42.0		93.859			
5	0.102	3	60	0.870	32.0	41.0		71.362			
6	0.145	3	60	1.202	31.0	40.0		96.185			
7	0.099	1	80	0.847	29.0	38.0		64.380			
8	0.115	1	80	0.971	32.0	41.0		79.594			
9	0.115	2	80	0.971	32.0	41.0		79.594			
10	0.072	2	80	0.639	32.0	41.0		52.366			
11	0.122	3	80	1.025	30.0	39.0		79.927			
12	0.096	3	80	0.824	32.0	41.0		67.563			

Sample	Abs	# of Shocks	Temp	Equiv. Glucose Conc. (mg/mL)	Final Volume	Total volume (ml)	Y0 (mg/g)	Y1 (mg/g)	Y3 (mg/g)	6-hr Yield (mg/g)	3-day yield (mg/g)
3-day:						9.0					
1	0.084	1	60	0.731	33.0	42.0			122.854	82.672	108.424
2	0.088	1	60	0.762	30.0	39.0			118.897	85.136	110.855
3	0.086	2	60	0.747	33.0	42.0			125.449	95.324	116.535
4	0.072	2	60	0.639	33.0	42.0			107.286	84.365	97.792
5	0.056	3	60	0.515	32.0	41.0			84.469	61.501	74.609
6	0.083	3	60	0.724	31.0	40.0			115.768	85.599	105.182
7	0.052	1	80	0.484	29.0	38.0			73.594	53.497	62.711
8	0.051	1	80	0.476	32.0	41.0			78.137	67.777	66.320
9	0.053	2	80	0.492	32.0	41.0			80.670	68.881	69.957
10	0.052	2	80	0.484	32.0	41.0			79.404	42.998	70.036
11	0.066	3	80	0.592	30.0	39.0			92.395	72.175	84.643
12	0.063	3	80	0.569	32.0	41.0			93.334	54.584	80.356
Initial :											
1	0.027	1	0, no spacer	0.291	37.0	46.0	10.713				
2	0.027	1	0, no spacer	0.291	38.0	47.0	10.946				
3	0.027	2	0, no spacer	0.291	38.0	47.0	10.946				
4	0.023	2	0, no spacer	0.260	37.0	46.0	9.577				
5	0.030	3	0, no spacer	0.314	38.0	47.0	11.817				
6	0.024	3	0, no spacer	0.268	38.0	47.0	10.075				
7	0.037	1	0, 1 spacer	0.368	38.0	47.0	13.850				
8	0.026	1	0, 1 spacer	0.283	38.0	47.0	10.656				
9	0.034	2	0, 1 spacer	0.345	37.0	46.0	12.702				
10	0.037	2	0, 1 spacer	0.368	36.0	45.0	13.260				
11	0.036	3	0, 1 spacer	0.361	37.0	46.0	13.271				
12	0.048	3	0, 1 spacer	0.453	38.0	47.0	17.043				
13	0.038	1	0, 2 spacer	0.376	38.0	47.0	14.140				
14	0.038	1	0, 2 spacer	0.376	38.0	47.0	14.140				

Sample	Abs	# of Shocks	Temp	Equiv. Glucose Conc. (mg/mL)	Final Volume	Total volume (ml)	Y0 (mg/g)	Y1 (mg/g)	Y3 (mg/g)	6-hr Yield (mg/g)	3-day yield (mg/g)
15	0.056	2	0, 2 spacer	0.515	38.0	47.0	19.366				
16	0.032	2	0, 2 spacer	0.330	38.0	47.0	12.398				
17	0.029	3	0, 2 spacer	0.307	37.0	46.0	11.282				
18	0.041	3	0, 2 spacer	0.399	36.0	45.0	14.372				
6-hr:				0.083							
1	0.064	1	0, no spacer	0.577	37.0	46.0		53.069			
2	0.097	1	0, no spacer	0.832	38.0	47.0		78.176			
3	0.114	2	0, no spacer	0.963	38.0	47.0		90.516			
4	0.109	2	0, no spacer	0.924	37.0	46.0		85.038			
5	0.129	3	0, no spacer	1.079	38.0	47.0		101.404			
6	0.084	3	0, no spacer	0.731	38.0	47.0		68.740			
7	0.129	1	0, 1 spacer	1.079	38.0	47.0		101.404			
8	0.113	1	0, 1 spacer	0.955	38.0	47.0		89.790			
9	0.125	2	0, 1 spacer	1.048	37.0	46.0		96.405			
10	0.119	2	0, 1 spacer	1.002	36.0	45.0		90.139			
11	0.102	3	0, 1 spacer	0.870	37.0	46.0		80.065			
12	0.114	3	0, 1 spacer	0.963	38.0	47.0		90.516			
13	0.118	1	0, 2 spacer	0.994	38.0	47.0		93.419			
14	0.108	1	0, 2 spacer	0.917	38.0	47.0		86.161			
15	0.113	2	0, 2 spacer	0.955	38.0	47.0		89.790			
16	0.119	2	0, 2 spacer	1.002	38.0	47.0		94.145			
11	0.111	3	0, 2 spacer	0.940	37.0	46.0		86.459			
12	0.107	3	0, 2 spacer	0.909	36.0	45.0		81.799			
3-day:											
1	0.068	1	0, no spacer	0.608	37.0	46.0			111.821	42.356	101.108
2	0.069	1	0, no spacer	0.615	38.0	47.0			115.703	67.230	104.757
3	0.083	2	0, no spacer	0.724	38.0	47.0			136.028	79.570	125.082
4	0.071	2	0, no spacer	0.631	37.0	46.0			116.083	75.461	106.507

Sample	Abs	# of Shocks	Temp	Equiv. Glucose Conc. (mg/mL)	Final Volume	Total volume (ml)	Y0 (mg/g)	Y1 (mg/g)	Y3 (mg/g)	6-hr Yield (mg/g)	3-day yield (mg/g)
5	0.095	3	0, no spacer	0.816	38.0	47.0			153.449	89.587	141.632
6	0.063	3	0, no spacer	0.569	38.0	47.0			106.993	58.665	96.918
7	0.096	1	0, 1 spacer	0.824	38.0	47.0			154.900	87.554	141.051
8	0.079	1	0, 1 spacer	0.693	38.0	47.0			130.221	79.134	119.565
9	0.088	2	0, 1 spacer	0.762	37.0	46.0			140.238	83.702	127.535
10	0.080	2	0, 1 spacer	0.700	36.0	45.0			126.069	76.879	112.809
11	0.075	3	0, 1 spacer	0.662	37.0	46.0			121.767	66.794	108.496
12	0.098	3	0, 1 spacer	0.839	38.0	47.0			157.804	73.472	140.760
13	0.083	1	0, 2 spacer	0.724	38.0	47.0			136.028	79.279	121.888
14	0.081	1	0, 2 spacer	0.708	38.0	47.0			133.124	72.021	118.984
15	0.082	2	0, 2 spacer	0.716	38.0	47.0			134.576	70.424	115.210
16	0.089	2	0, 2 spacer	0.770	38.0	47.0			144.738	81.747	132.340
11	0.080	3	0, 2 spacer	0.700	37.0	46.0			128.871	75.177	117.589
12	0.073	3	0, 2 spacer	0.646	36.0	45.0			116.340	67.427	101.968

Sample	Abs	Treatment Time (min)	Equiv. Glucose Conc. (mg/mL)	Final Volume	Total volume (ml)	Y0 (mg/g)	Y1 (mg/g)	Y3 (mg/g)	1-hr Yield (mg/g)	3-day yield (mg/g)
Initial :	***20%***									
1	0.008	0	0.144	38.0	47.0	5.429				
2	0.008	0	0.144	39.0	48.0	5.545				
3	0.007	20	0.137	38.0	47.0	5.139				
4	0.008	20	0.144	39.0	48.0	5.545				
5	0.008	40	0.144	39.0	48.0	5.545				
6	0.007	40	0.137	38.0	47.0	5.139				
7	0.009	60	0.152	38.0	47.0	5.720				
8	0.006	60	0.129	38.0	47.0	4.849				
9	0.015	120	0.198	38.0	47.0	7.462				
10	0.006	120	0.129	36.0	45.0	4.642				
6-hr:										
1	0.077	0	0.677	38.0	47.0		63.659			
2	0.068	0	0.608	39.0	48.0		58.341			
3	0.070	20	0.623	38.0	47.0		58.578			
4	0.110	20	0.928	39.0	48.0		89.106			
5	0.081	40	0.708	39.0	48.0		67.978			
6	0.073	40	0.646	38.0	47.0		60.755			
7	0.071	60	0.631	38.0	47.0		59.303			
8	0.079	60	0.693	38.0	47.0		65.110			
9	0.088	120	0.762	38.0	47.0		71.643			
10	0.109	120	0.924	36.0	45.0		83.189			
3-day:					9.0					
1	0.046	0	0.438	38.0	47.0			82.314	58.229	76.884
2	0.045	0	0.430	39.0	48.0			82.582	52.796	77.037
3	0.043	20	0.415	38.0	47.0			77.958	53.438	72.819
4	0.066	20	0.592	39.0	48.0			113.717	83.561	108.172
5	0.051	40	0.476	39.0	48.0			91.478	62.433	85.933

Sample	Abs	Treatment Time (min)	Equiv. Glucose Conc. (mg/mL)	Final Volume	Total volume (ml)	Y0 (mg/g)	Y1 (mg/g)	Y3 (mg/g)	1-hr Yield (mg/g)	3-day yield (mg/g)
6	0.047	40	0.446	38.0	47.0			83.765	55.616	78.626
7	0.043	60	0.415	38.0	47.0			77.958	53.584	72.238
8	0.054	60	0.500	38.0	47.0			93.927	60.262	89.079
9	0.054	120	0.500	38.0	47.0			93.927	64.181	86.465
10	0.071	120	0.631	36.0	45.0			113.560	78.547	108.917
Initial :	***15%***									
1	0.015	0	0.198	38.0	47.0	7.462				
2	0.011	0	0.168	38.0	47.0	6.301				
3	0.007	20	0.137	38.0	47.0	5.139				
4	0.008	20	0.144	38.0	47.0	5.429				
5	0.007	40	0.137	37.0	46.0	5.030				
6	0.009	40	0.152	39.0	48.0	5.842				
7	0.008	60	0.144	39.0	48.0	5.545				
8	0.008	60	0.144	38.0	47.0	5.429				
9	0.007	120	0.137	37.0	46.0	5.030				
10	0.012	120	0.175	36.0	45.0	6.310				
6-hr:										
1	0.117	0	0.986	38.0	47.0		92.693			
2	0.114	0	0.963	38.0	47.0		90.516			
3	0.072	20	0.639	38.0	47.0		60.029			
4	0.125	20	1.048	38.0	47.0		98.500			
5	0.120	40	1.009	37.0	46.0		92.853			
6	0.099	40	0.847	39.0	48.0		81.322			
7	0.127	60	1.063	39.0	48.0		102.079			
8	0.087	60	0.754	38.0	47.0		70.917			
9	0.137	120	1.141	37.0	46.0		104.930			
10	0.129	120	1.079	36.0	45.0		97.089			

Sample	Abs	Treatment Time (min)	Equiv. Glucose Conc. (mg/mL)	Final Volume	Total volume (ml)	Y0 (mg/g)	Y1 (mg/g)	Y3 (mg/g)	1-hr Yield (mg/g)	3-day yield (mg/g)
3-day:										
1	0.067	0	0.600	38.0	47.0			112.800	85.232	105.338
2	0.073	0	0.646	38.0	47.0			121.510	84.215	115.210
3	0.045	20	0.430	38.0	47.0			80.862	54.890	75.723
4	0.082	20	0.716	38.0	47.0			134.576	93.071	129.147
5	0.064	40	0.577	37.0	46.0			106.137	87.823	101.108
6	0.063	40	0.569	39.0	48.0			109.269	75.480	103.428
7	0.072	60	0.639	39.0	48.0			122.613	96.534	117.068
8	0.072	60	0.639	38.0	47.0			120.059	65.488	114.629
9	0.093	120	0.801	37.0	46.0			147.342	99.900	142.312
10	0.084	120	0.731	36.0	45.0			131.629	90.778	125.319
Initial :	***100%***									
1	0.009	0	0.155	28.0	40.0	4.945				
2	0.007	0	0.140	30.0	42.0	4.688				
3	0.013	20	0.185	29.0	41.0	6.053				
4	0.009	20	0.155	27.0	39.0	4.822				
5	0.008	40	0.147	27.0	39.0	4.588				
6	0.010	40	0.162	29.0	41.0	5.315				
7	0.013	60	0.185	30.0	42.0	6.201				
8	0.008	60	0.147	32.0	44.0	5.176				
9	0.010	120	0.162	30.0	42.0	5.445				
10	0.007	120	0.140	33.0	45.0	5.023				
6-hr:										
1	0.112	0	0.927	28.0	40.0		74.179			
2	0.132	0	1.077	30.0	42.0		90.491			
3	0.142	20	1.152	29.0	41.0		94.488			
4	0.138	20	1.122	27.0	39.0		87.538			
5	0.143	40	1.160	27.0	39.0		90.464			

Sample	Abs	Treatment Time (min)	Equiv. Glucose Conc. (mg/mL)	Final Volume	Total volume (ml)	Y0 (mg/g)	Y1 (mg/g)	Y3 (mg/g)	1-hr Yield (mg/g)	3-day yield (mg/g)
6	0.116	40	0.957	29.0	41.0		78.494			
7	0.177	60	1.415	30.0	42.0		118.848			
8	0.129	60	1.055	32.0	44.0		92.819			
9	0.139	120	1.130	30.0	42.0		94.902			
10	0.154	120	1.242	33.0	45.0		111.808			
3-day:										
1	0.071	0	0.620	28.0	40.0			99.145	69.233	94.200
2	0.072	0	0.627	30.0	42.0			105.362	85.802	100.674
3	0.073	20	0.635	29.0	41.0			104.084	88.435	98.031
4	0.060	20	0.537	27.0	39.0			83.793	82.716	78.971
5	0.078	40	0.672	27.0	39.0			104.858	85.876	100.271
6	0.069	40	0.605	29.0	41.0			99.163	73.179	93.848
7	0.101	60	0.845	30.0	42.0			141.911	112.647	135.711
8	0.086	60	0.732	32.0	44.0			128.864	87.644	123.689
9	0.076	120	0.657	30.0	42.0			110.404	89.457	104.959
10	0.082	120	0.702	33.0	45.0			126.392	106.785	121.368
Initial :	***100%***									
1	0.008	0	0.147	33.0	45.0	5.293				
2	0.008	0	0.147	30.0	42.0	4.940				
3	0.010	20	0.162	33.0	45.0	5.833				
4	0.018	20	0.222	33.0	45.0	7.994				
5	0.009	40	0.155	32.0	44.0	5.440				
6	0.008	40	0.147	31.0	43.0	5.058				
7	0.009	60	0.155	29.0	41.0	5.069				
8	0.009	60	0.155	32.0	44.0	5.440				
9	0.010	120	0.162	30.0	42.0	5.445				
10	0.015	120	0.200	32.0	44.0	7.024				

Sample	Abs	Treatment Time (min)	Equiv. Glucose Conc. (mg/mL)	Final Volume	Total volume (ml)	Y0 (mg/g)	Y1 (mg/g)	Y3 (mg/g)	1-hr Yield (mg/g)	3-day yield (mg/g)
6-hr:										
1	0.131	0	1.070	33.0	45.0		96.279			
2	0.125	0	1.025	30.0	42.0		86.080			
3	0.137	20	1.115	33.0	45.0		100.330			
4	0.130	20	1.062	33.0	45.0		95.604			
5	0.141	40	1.145	32.0	44.0		100.741			
6	0.144	40	1.167	31.0	43.0		100.387			
7	0.133	60	1.085	29.0	41.0		88.951			
8	0.136	60	1.107	32.0	44.0		97.440			
9	0.126	120	1.032	30.0	42.0		86.710			
10	0.106	120	0.882	32.0	44.0		77.635			
3-day:										
1	0.070	0	0.612	33.0	45.0			110.188	90.986	104.894
2	0.072	0	0.627	30.0	42.0			105.362	81.139	100.422
3	0.068	20	0.597	33.0	45.0			107.487	94.497	101.653
4	0.072	20	0.627	33.0	45.0			112.888	87.610	104.894
5	0.081	40	0.695	32.0	44.0			122.263	95.301	116.823
6	0.079	40	0.680	31.0	43.0			116.903	95.329	111.845
7	0.062	60	0.552	29.0	41.0			90.551	83.882	85.482
8	0.060	60	0.537	32.0	44.0			94.536	92.001	89.096
9	0.066	120	0.582	30.0	42.0			97.800	81.265	92.356
10	0.046	120	0.432	32.0	44.0			76.051	70.611	69.027

Sample	Treatment	# of Shocks	Loading (g)	Water (L)	CrI	Date	CrI Duplicate	Date	Average	Std. Dev.
Bagasse Loading										
	Raw(unground)	1	100	1	54	6/8/2006	55	6/8/2006	55	0.707107
	Raw(unground)	1	125	1	47	9/6/2006	37	9/6/2006	42	7.071068
	Raw(unground)	1	150	1	46	9/6/2006	48	9/6/2006	47	1.414214
	Raw(unground)	1	175	1	49	9/6/2006	48	9/6/2006	49	0.707107
	Raw(unground)	1	200	1	45	6/22/2006	44	6/22/2006	45	0.707107
	10-mesh	1	100	3	59	6/8/2006	57	6/8/2006	58	1.414214
	10-mesh	1	150	3	57	9/20/2006	57	9/20/2006	57	0
	10-mesh	1	175	3	57	9/20/2006	62	9/20/2006	60	3.535534
	10-mesh	1	200	3	54	6/22/2006	47	6/22/2006	51	4.949747
	10-mesh	1	225	3	45	9/20/2006	42	9/20/2006	44	2.12132
	10-mesh	1	250	3	46	9/20/2006	44	9/20/2006	45	1.414214
	10-mesh	1	300	3	55	6/8/2006	50	6/8/2006	53	3.535534
	Lime/Air	1	50	1	62	9/6/2006	66	9/6/2006	64	2.828427
	Lime/Air	1	75	1	64	9/20/2006	63	9/20/2006	64	0.707107
	Lime/Air	1	100	1	62	9/15/2006	65	9/15/2006	64	2.12132
	Lime/Air	1	125	1	64	9/26/2006	59	9/26/2006	62	3.535534
	Lime/Air	1	150	1	63	9/15/2006	64	9/6/2006	64	0.707107
	Lime/Air	1	200	1	67	6/8/2006	64	6/8/2006	66	2.12132
Water Loading										
	Raw(unground)	1	200	0	51	5/24/2006	50	11/16/2005	51	0.707107
	Raw(unground)	1	200	1	47	5/24/2006	46	11/16/2005	47	0.707107
	Raw(unground)	1	200	2	50	5/24/2006	50	11/16/2005	50	0
	Raw(unground)	1	200	3	52	5/24/2006	51	11/16/2005	52	0.707107
	10-mesh	1	200	0	53	5/24/2006	53	11/16/2005	53	0
	10-mesh	1	200	1	54	5/24/2006	54	11/16/2005	54	0
	10-mesh	1	200	2	52	5/24/2006	52	11/16/2005	52	0
	10-mesh	1	200	3	51	5/24/2006	51	11/16/2005	51	0
	Lime/Air	1	200	0	67	6/8/2006	64	6/22/2006	66	2.12132
	Lime/Air	1	200	1	64	6/8/2006	62	6/22/2006	63	1.414214
	Lime/Air	1	200	2	65	6/8/2006	65	6/22/2006	65	0
	Lime/Air	1	200	3	69	6/8/2006	59	6/22/2006	64	7.071068

Sample	Treatment	# of Shocks	Loading (g)	Water (L)	CrI	Date	CrI Duplicate	Date	Average	Std. Dev.
Number of Shocks										
	Raw(unground)	0	125	1	50	11/16/2005	46	9/26/2006	48	2.828427
	Raw(unground)	1	125	1	43	9/26/2006	49	10/3/2006	46	4.242641
	Raw(unground)	2	125	1	55	10/3/2006	57	10/3/2006	56	1.414214
	Raw(unground)	3	125	1	50	10/3/2006	51	10/3/2006	51	0.707107
	10-mesh	0	200	3	49	6/22/2006	52	11/16/2005	51	2.12132
	10-mesh	1	200	3	54	6/22/2006	47	6/22/2006	51	4.949747
	10-mesh	2	200	3	55	6/22/2006	56	6/22/2006	56	0.707107
	10-mesh	3	200	3	49	9/26/2006	55	9/26/2006	52	4.242641
	Lime/Air	0	125	1	67	9/15/2006	64	9/26/2006	66	2.12132
	Lime/Air	1	125	1	62	9/26/2006	68	10/3/2006	65	4.596194
	Lime/Air	2	125	1	65	10/3/2006	61	10/3/2006	63	2.828427
	Lime/Air	3	125	1	60	10/3/2006	61	10/3/2006	61	0.707107

Sample	Description	Temp	CrI
Control	*no shock*	*room temp*	*46*
1	1 shock	40	42
2	1 shock	40	44
3	2 shock	40	40
4	2 shock	40	39
5	3 shock	40	39
6	3 shock	40	39
7	1 shock	30	43
8	1 shock	30	43
9	2 shock	30	41
10	2 shock	30	37
11	3 shock	30	39
12	3 shock	30	38
13	1 shock	20	42
14	1 shock	20	42
15	2 shock	20	38
16	2 shock	20	37
17	3 shock	20	38
18	3 shock	20	37
1	1 shock, 60 degrees	60	39
2	1 shock, 60 degrees	60	38
3	2 shock, 60 degrees	60	39
4	2 shock, 60 degrees	60	42
5	3 shock, 60 degrees	60	41
6	3 shock, 60 degrees	60	40
7	1 shock, 80 degrees	80	40
8	1 shock, 80 degrees	80	39
9	2 shock, 80 degrees	80	37
10	2 shock, 80 degrees	80	39
11	3 shock, 80 degrees	80	39
12	3 shock, 80 degrees	80	39

Sample	Description	Temp	CrI
1	1shock, 0 degrees	0	38
2	1 shock,0 degrees	0	37
3	2 shock,0 degrees	0	40
4	2 shock,0 degrees	0	38
5	3 shock,0 degrees	0	44
6	3 shock,0 degrees	0	38
1	1 shock, no spacer	0	42
2	2 shock, no spacer	0	42
3	3 shock, no spacer	0	42
4	1 shock, 1 spacer	0	43
5	2 shock, 1 spacer	0	44
6	3 shock, 1 spacer	0	42
7	1 shock, 2 spacers	0	41
8	2 shock, 2 spacers	0	45
9	3 shock, 2 spacers	0	42
Hydrodynamic Cavitation			
15%	0 min	Raw	52
15%	20 min	Raw	52
15%	40 min	Raw	51
15%	60 min	Raw	52
15%	120 min	Raw	50
20%	0 min	Raw	50
20%	20 min	Raw	50
20%	40 min	Raw	50
20%	60 min	Raw	51
20%	120 min	Raw	47
100%	0 min	Raw	52
100%	20 min	Raw	51

Sample	Description	Temp	CrI
100%	40 min	Raw	50
100%	60 min	Raw	50
100%	120 min	Raw	51
15%	0 min	Lime-treated	61
15%	20 min	Lime-treated	64
15%	40 min	Lime-treated	63
15%	60 min	Lime-treated	62
15%	120 min	Lime-treated	62
20%	0 min	Lime-treated	65
20%	20 min	Lime-treated	65
20%	40 min	Lime-treated	64
20%	60 min	Lime-treated	65
20%	120 min	Lime-treated	66

Acid Conc. Day	Raw 80 mesh	Raw 80 mesh	Bottle 1&2 Average	Std. Dev.	Raw Ball-milled	Raw Ball-milled	Bottle 3&4 Average	Std. Dev.
0	3.45	3.45	3.45	0.00	3.55	3.64	3.60	0.059
2	6.17	6.08	6.13	0.06	7.19	5.95	6.57	0.876
4	8.37	8.66	8.51	0.20	10.57	9.05	9.81	1.080
6	12.97	12.98	12.98	0.01	13.02	13.30	13.16	0.197
8	13.38	13.02	13.20	0.25	13.36	13.52	13.44	0.117
10	13.09	12.38	12.73	0.50	14.29	14.01	14.15	0.198
12	12.97	13.84	13.41	0.62	15.18	14.11	14.65	0.758
14	13.16	13.73	13.44	0.41	15.78	13.34	14.56	1.722
16	13.82	13.86	13.84	0.03	14.95	14.72	14.83	0.161
18	12.43	13.78	13.10	0.96	15.18	14.12	14.65	0.753
20	13.70	15.13	14.42	1.01	15.81	13.79	14.80	1.427
22	13.87	15.37	14.62	1.06	17.93	14.93	16.43	2.119
24	11.90	16.42	14.16	3.20	18.15	16.03	17.09	1.503
26	14.84	16.72	15.78	1.33	18.94	20.60	19.77	1.178
28	13.63	16.12	14.88	1.76	19.21	22.21	20.71	2.121
30	12.35	14.74	13.54	1.69	19.44	22.33	20.88	2.044

Acid Conc. Day	Lime pretrt. 80 mesh	Lime pretrt. 80 mesh	Bottle 5&6 Average	Std. Dev.	Lime pretrt. Ball-milled	Lime pretrt. Ball-milled	Bottle 7&8 Average	Std. Dev.
0	3.60	3.57	3.58	0.02	3.47	3.48	3.47	0.004
2	5.12	5.19	5.15	0.05	6.07	5.50	5.78	0.403
4	8.10	8.02	8.06	0.06	9.39	8.54	8.97	0.606
6	13.85	13.18	13.52	0.48	14.29	14.80	14.54	0.361
8	17.73	14.35	16.04	2.39	19.50	18.39	18.95	0.784
10	18.40	15.22	16.81	2.25	21.90	22.43	22.16	0.379
12	18.03	14.58	16.30	2.44	20.27	27.41	23.84	5.048
14	19.17	13.89	16.53	3.73	24.23	25.92	25.08	1.193
16	18.63	13.79	16.21	3.42	29.07	28.84	28.95	0.167

Acid Conc.	Lime pretrt. 80 mesh	Lime pretrt. 80 mesh	Bottle 5&6 Average	Std. Dev.	Lime pretrt. Ball-milled	Lime pretrt. Ball-milled	Bottle 7&8 Average	Std. Dev.
18	20.09	14.13	17.11	4.21	27.40	29.40	28.40	1.414
20	18.76	15.45	17.10	2.34	26.61	29.22	27.91	1.848
22	7.51	17.61	12.56	7.15	30.44	29.53	29.99	0.641
24	21.02	17.37	19.20	2.58	30.92	32.33	31.63	0.992
26	21.79	17.67	19.73	2.91	31.88	32.86	32.37	0.688
28	21.23	17.13	19.18	2.90	32.09	33.01	32.55	0.651
30	20.67	16.99	18.83	2.60	32.00	32.37	32.18	0.264

Bottle 1 **Bottle 2**

Day	1	2	3	4	5	6	7	8	9	10	11	12
Fermentor 1	6.87	6.99	6.77	7.15	6.68	6.51	7.32	7.59	7.65	7.65	7.74	7.49
Fermentor 2	6.90	7.05	6.82	7.16	6.87	6.33	7.45	7.68	7.69	7.58	7.62	7.41
Fermentor 3	6.64	6.65	6.93	7.14	7.14	6.92	7.17	7.21	6.82	6.98	7.10	6.84
Fermentor 4	6.62	7.05	6.75	7.23	7.15	6.48	7.36	7.56	7.54	7.43	7.44	7.16
Fermentor 5	7.02	6.79	6.72	7.14	6.84	6.41	6.97	6.80	6.96	7.00	7.12	6.91
Fermentor 6	7.06	6.84	6.63	7.13	6.85	6.45	7.28	7.38	7.12	6.95	7.07	6.86
Fermentor 7	6.68	7.25	6.83	7.05	6.68	6.39	6.94	7.10	6.53	7.13	7.33	7.00
Fermentor 8	6.71	7.08	6.66	7.16	6.98	6.09	7.25	7.43	7.34	6.67	6.96	6.49

Day	13	14	15	16	17	18	19	20	21	22	23	24
Fermentor 1	7.63	7.66	7.80	7.72	7.55	7.53	7.52	7.57	7.62	7.69	7.60	7.76
Fermentor 2	7.58	7.59	7.70	7.60	7.50	7.56	7.61	7.55	7.28	7.18	7.11	7.16
Fermentor 3	7.23	7.30	7.44	7.36	7.29	7.38	7.41	7.40	7.22	7.30	7.19	7.35
Fermentor 4	7.33	7.30	7.46	7.42	7.33	7.45	7.52	7.50	7.59	7.67	7.54	7.07
Fermentor 5	7.22	7.32	7.47	7.39	7.35	7.45	7.49	7.52	7.55	7.62	7.44	7.43
Fermentor 6	7.34	7.46	7.60	7.55	7.51	7.59	7.61	7.60	7.68	7.68	7.57	7.72
Fermentor 7	7.03	6.97	7.04	6.85	7.03	7.10	7.05	7.00	6.96	7.21	7.04	7.14
Fermentor 8	7.30	7.39	7.58	7.52	7.48	7.55	7.60	7.60	7.66	7.69	7.55	7.71

Day	25	26	27	28	Avg. pH	Std. Dev.
Fermentor 1	7.85	7.67	7.86	7.78	7.20	0.43002
Fermentor 2	7.34	7.14	7.29	7.39	7.21	0.428535
Fermentor 3	7.45	7.29	7.38	7.37	6.96	0.196877
Fermentor 4	6.81	6.52	7.59	7.79	7.15	0.360936
Fermentor 5	7.51	7.41	7.57	7.54	6.89	0.199089
Fermentor 6	7.80	7.67	7.84	7.75	6.97	0.26288
Fermentor 7	7.21	7.00	7.17	7.12	6.91	0.291094
Fermentor 8	7.74	7.64	7.83	7.72	6.90	0.390544

Day	Initial	Final	Delta	**Avg.**	**Gas (mL)**	**2 Std. Dev.**	Day	Initial	Final	Delta
1	10.3	27.5	17.2	16.75	328.3	1.27	1	14	30.3	16.3
2	10.3	20	9.7	10.6	207.76	2.55	2	10.5	22	11.5
3	10	21.5	11.5	12.45	244.02	2.69	3	15.6	29	13.4
4	9.6	18	8.4	9.2	180.32	2.26	4	17.4	27.4	10
5	11.3	22	10.7	11.7	229.32	2.83	5	10.8	23.5	12.7
6	9.8	24.3	14.5	14.05	275.38	1.27	6	11.8	25.4	13.6
7	10.5	22	11.5	11.35	222.46	0.42	7	10.4	21.6	11.2
8	9.5	16.4	6.9	6.7	131.32	0.57	8	13.7	20.2	6.5
9	9.5	16.3	6.8	7.15	140.14	0.99	9	9.5	17	7.5
10	9.5	16	6.5	6.7	131.32	0.57	10	16.5	23.4	6.9
11	10.4	16.6	6.2	6.25	122.5	0.14	11	12.3	18.6	6.3
12	10.6	16.2	5.6	6.4	125.44	2.26	12	12	19.2	7.2
13	10	16.2	6.2	6.9	135.24	1.98	13	9.9	17.5	7.6
14	10.3	15.5	5.2	5.85	114.66	1.84	14	10.5	17	6.5
15	10.7	15.8	5.1	5.5	107.8	1.13	15	10.4	16.3	5.9
16	10.3	15.3	5	5.4	105.84	1.13	16	16.4	22.2	5.8
17	10.3	16.4	6.1	6.1	119.56	0.00	17	9.1	15.2	6.1
18	9.8	15.8	6	5.75	112.7	0.71	18	9.5	15	5.5
19	10.6	17.3	6.7	5.9	115.64	2.26	19	10.9	16	5.1
20	10.6	16.8	6.2	6.3	123.48	0.28	20	11	17.4	6.4
21	10.1	15.6	5.5	6.85	134.26	3.82	21	9.1	17.3	8.2
22	9.9	15.5	5.6	7.8	152.88	6.22	22	9.3	19.3	10
23	11.8	18.4	6.6	7.1	139.16	1.41	23	19	26.6	7.6
24	12.4	16.2	3.8	5.75	112.7	5.52	24	18.3	26	7.7
25	10.3	15.4	5.1	6.4	125.44	3.68	25	10.8	18.5	7.7
26	11.2	17.2	6	7	137.2	2.83	26	12	20	8
27	10.5	16.5	6	6.5	127.4	1.41	27	10.8	17.8	7
28	11.4	16.5	6	5.8	113.68	0.57	28	15.4	21	5.6

	Bottle 3							Bottle 4		
Day	Initial	Final	Delta	**AVG**	**Gas (mL)**	**2 Std. Dev**	Day	Initial	Final	Delta
1	27.5	36	8.5	9.7	190.12	3.39	1	30.3	41.2	10.9
2	20	41	21	17	333.2	11.31	2	23	36	13
3	21.5	37.3	15.8	14.65	287.14	3.25	3	29	42.5	13.5
4	18	30	12	11.5	225.4	1.41	4	27.4	38.4	11
5	22	31	9	10	196	2.83	5	23.5	34.5	11
6	24.3	32.7	8.4	11.2	219.52	7.92	6	26	40	14
7	22	30.6	8.6	6.25	122.5	6.65	7	21.8	25.7	3.9
8	16.4	23.1	6.7	6.75	132.3	0.14	8	20.2	27	6.8
9	16.3	25	8.7	8.35	163.66	0.99	9	17	25	8
10	16	29	13	10.25	200.9	7.78	10	23.5	31	7.5
11	16.6	25.1	8.5	7.5	147	2.83	11	18.6	25.1	6.5
12	16.2	25.7	9.5	8.8	172.48	1.98	12	19.6	27.7	8.1
13	16.2	22.7	6.5	7.1	139.16	1.70	13	17.5	25.2	7.7
14	15.5	22.5	7	6.85	134.26	0.42	14	17	23.7	6.7
15	16.5	21.3	4.8	5.65	110.74	2.40	15	16.5	23	6.5
16	15.3	21.1	5.8	7.5	147	4.81	16	22.2	31.4	9.2
17	16.4	20	3.6	4.2	82.32	1.70	17	15.2	20	4.8
18	15.8	21	5.2	5.5	107.8	0.85	18	15	20.8	5.8
19	17.3	22	6.5	6.45	126.42	0.14	19	16	22.4	6.4
20	16.8	22.7	4.2	4.75	93.1	1.56	20	17.4	22.7	5.3
21	15.6	17.3	3.4	4.55	89.18	3.25	21	17.3	23	5.7
22	15.5	20.9	4.3	5	98	1.98	22	19.3	25	5.7
23	18.4	24.9	3.8	4.75	93.1	2.69	23	26.6	32.3	5.7
24	16.2	20	4.1	6.3	123.48	6.22	24	26	34.5	8.5
25	15.4	20.1	7.5	8.85	173.46	3.82	25	18.5	28.7	10.2
26	17.2	23.2	4.9	11.3	221.48	18.10	26	20	37.7	17.7
27	17	21.5	6	9.1	178.36	8.77	27	17.8	30	12.2
28	16.5	25.5	2	5.85	114.66	10.89	28	21	30.7	9.7

	Bottle 5							Bottle 6		
Day	Initial	Final	Delta	**Avg.**	**Gas (mL)**	**2 Std. Dev.**	Day	Initial	Final	Delta
1	36	44.2	8.2	8.3	162.68	0.283	1	41.6	50	8.4
2	41	51.2	10.2	10.3	201.88	0.283	2	36	46.4	10.4
3	37.3	51.7	14.4	14.3	280.28	0.283	3	42.5	56.7	14.2
4	30	40.5	10.5	10.55	206.78	0.141	4	38.4	49	10.6
5	31	45.7	14.7	15.1	295.96	1.131	5	34.5	50	15.5
6	32.7	48.6	15.9	18.85	369.46	8.344	6	41.2	63	21.8
7	30.6	47.1	16.5	14.95	293.02	4.384	7	25.7	39.1	13.4
8	23.1	38	14.9	12.75	249.9	6.081	8	27	37.6	10.6
9	25	36.5	11.5	12.5	245	2.828	9	25	38.5	13.5
10	29	36.9	7.9	9.35	183.26	4.101	10	31.3	42.1	10.8
11	25.1	31.3	6.2	7.55	147.98	3.818	11	25.1	34	8.9
12	25.7	32.3	6.6	7.7	150.92	3.111	12	27.7	36.5	8.8
13	22.7	28.3	5.6	6.45	126.42	2.404	13	25.2	32.5	7.3
14	22.5	27.5	5	5.3	103.88	0.849	14	23.7	29.3	5.6
15	21.3	25.5	4.2	4.65	91.14	1.273	15	23.7	28.8	5.1
16	21.1	25	3.9	4.3	84.28	1.131	16	31.4	36.1	4.7
17	20	25	5	5.35	104.86	0.990	17	20	25.7	5.7
18	21	24.8	3.8	4.35	85.26	1.556	18	20.8	25.7	4.9
19	22	26.2	4.2	4.75	93.1	1.556	19	22.4	27.7	5.3
20	22.7	27.8	5.1	5.05	98.98	0.141	20	22.7	27.7	5
21	22.5	26.6	4.1	4.8	94.08	1.980	21	23	28.5	5.5
22	20.9	25.9	5	4.45	87.22	1.556	22	25	28.9	3.9
23	24.9	29.4	4.5	4.3	84.28	0.566	23	32.3	36.4	4.1
24	20	23	3	3.35	65.66	0.990	24	34.5	38.2	3.7
25	20.1	25	4.9	4.7	92.12	0.566	25	28.7	33.2	4.5
26	23.2	29.8	6.6	5.45	106.82	3.253	26	37.7	42	4.3
27	21.7	25.5	3.8	4.85	95.06	2.970	27	33.1	39	5.9
28	34.8	38.5	3.7	3.9	76.44	0.566	28	30.7	34.8	4.1

	Bottle 7							Bottle 8		
Day	Initial	Final	Delta	**AVG**	**Gas (mL)**	**2 Std. Dev.**	Day	Initial	Final	Delta
1	44.2	48.5	4.3	6.95	136.22	7.50	1	50	59.6	9.6
2	51.2	59.7	8.5	8.55	167.58	0.14	2	46.4	55	8.6
3	51.7	62	10.3	10.9	213.64	1.70	3	56.7	68.2	11.5
4	40.5	49	8.5	9.55	187.18	2.97	4	49	59.6	10.6
5	62.3	73	10.7	11.5	225.4	2.26	5	50	62.3	12.3
6	48.6	64.3	15.7	16.85	330.26	3.25	6	63	81	18
7	47.1	63.3	16.2	16.25	318.5	0.14	7	39.1	55.4	16.3
8	38	54.8	16.8	14.1	276.36	7.64	8	37.6	49	11.4
9	36.5	52.7	16.2	16.2	317.52	0.00	9	38.5	54.7	16.2
10	36.9	49.7	12.8	14.7	288.12	5.37	50	42.1	58.7	16.6
11	31.3	39.7	8.4	11.7	229.32	9.33	11	34	49	15
12	32.3	43	10.7	14.4	282.24	10.47	12	36.5	54.6	18.1
13	28.3	36.4	8.1	10.65	208.74	7.21	13	32.5	45.7	13.2
14	27.5	35.2	7.7	8.9	174.44	3.39	14	29.3	39.4	10.1
15	25.5	33.4	7.9	7.55	147.98	0.99	15	28.8	36	7.2
16	25	32.7	7.7	7.4	145.04	0.85	16	36.1	43.2	7.1
17	25	34.8	9.8	8.3	162.68	4.24	17	25.7	32.5	6.8
18	24.8	32	7.2	6.15	120.54	2.97	18	25.7	30.8	5.1
19	26.2	32.5	6.3	6.05	118.58	0.71	19	27.7	33.5	5.8
20	27.8	35.1	7.3	6.6	129.36	1.98	20	27.7	33.6	5.9
21	26.6	32.7	6.1	5.6	109.76	1.41	21	28.5	33.6	5.1
22	25.9	32.7	6.8	5.7	111.72	3.11	22	30.2	34.8	4.6
23	29.4	35.5	6.1	4.85	95.06	3.54	23	36.4	40	3.6
24	38.2	41.5	3.3	3.4	66.64	0.28	24	41.5	45	3.5
25	25	30.1	5.1	4.45	87.22	1.84	25	33.2	37	3.8
26	29.8	35.7	5.9	5.2	101.92	1.98	26	42	46.5	4.5
27	47	50.8	3.8	4.4	86.24	1.70	27	34.3	39.3	5
28	30	34.5	0	1.85	36.26	5.23	28	34.8	38.5	3.7

Throat Diameter 50%		Throat Diameter 10%		Throat Diameter 20%		Throat Diameter 30%	
Pressure	Velocity	Pressure	Velocity	Pressure	Velocity	Pressure	Velocity
flow_inlet 1872.4449	flow_inlet 1.1477411	flow_inlet 1160332	flow_inlet 1.1477411	flow_inlet 66107.969	flow_inlet 1.1477411	flow_inlet 11509.98	flow_inlet 1.1477411
inlet 1831.7168	inlet 1.1782812	inlet 1160291	inlet 1.1782805	inlet 66067.203	inlet 1.1782795	inlet 11469.229	inlet 1.1782846
outlet - 2.1699977	outlet 1.1782846	outlet 49.534939	outlet 1.1782589	outlet 50.814278	outlet 1.1783103	outlet 49.382465	outlet 1.1783119
pressure_inlet -55.597565	pressure_inlet 0.33199498	pressure_inlet -1.6501914	pressure_inlet 0.057124145	pressure_inlet -1.4004385	pressure_inlet 0.05262439	pressure_inlet -1.4297119	pressure_inlet 0.053174023
pressure_outle t 0	pressure_outlet 0.34218585	pressure_outlet -0.010078697	pressure_outl et 0.074292891	pressure_outl et - 0.010030673	pressure_outl et 0.069982946	pressure_outl et - 0.0099383239	pressure_outl et 0.070507817
throat_inlet -9108.7129	throat_inlet 4.7082171	throat_inlet -6117871	throat_inlet 117.1826	throat_inlet -395028.91	throat_inlet 29.450434	throat_inlet -78062.938	throat_inlet 13.06965
throat_outlet -9262.1992	throat_outlet 4.7098637	throat_outlet -6424783.5	throat_outlet 117.24334	throat_outlet -408821.81	throat_outlet 29.474518	throat_outlet -80148.625	throat_outlet 13.074626
Net - 32.053986	Net 0.36297345	Net 12151.197	Net 0.097130582	Net 553.06079	Net 0.09277112	Net 47.768681	Net 0.093234219

Throat Diameter 40%		Throat Diameter 50%		Throat Diameter 60%		Throat Diameter 23	
Pressure	Velocity	Pressure	Velocity	Pressure	Velocity	Pressure	Velocity
flow_inlet 3517.1787	flow_inlet 1.1477411	flow_inlet 1510.7394	low_inlet 1.1477411	flow_inlet 878.21265	flow_inlet 1.1477411	flow_inlet 136840.05	flow_inlet 1.1477411
inlet 3476.4297	inlet 1.1782846	inlet 1469.9875	inlet 1.1782846	inlet 837.44989	inlet 1.1782795	inlet 136799.3	inlet 1.1782842
outlet 56.067669	outlet 1.1783806	outlet 40.258209	outlet 1.1783601	outlet 24.452332	outlet 1.1783613	outlet 101375.48	outlet 1.1783144
pressure_inlet -1.3730416	pressure_inlet 0.052106533	pressure_inlet -1.371706	pressure_inlet 0.052090477	pressure_inlet -1.3838848	pressure_inlet 0.052325439	pressure_inlet 101323.52	pressure_inlet 0.053885952
pressure_outlet - 0.0093191797	pressure_outlet 0.069284126	pressure_outlet - 0.008541435	pressure_outlet 0.069036871	pressure_outlet - 0.0079369824	pressure_outlet 0.06905517	pressure_outlet 101324.99	pressure_outlet 0.071017258
throat_inlet -24188.287	throat_inlet 7.3453727	throat_inlet -9481.2812	throat_inlet 4.7086892	throat_inlet -4197.3789	throat_inlet 3.2732708	throat_inlet -126785.7	throat_inlet 22.289614
throat_outlet -24689.703	throat_outlet 7.3472319	throat_outlet -9705.3633	throat_outlet 4.7101736	throat_outlet -4290.6855	throat_outlet 3.2735987	throat_outlet -133486.61	throat_outlet 22.292837
Net - 5.0660906	Net 0.092038006	Net - 10.50897	Net 0.091813579	Net - 7.9399219	Net 0.091827214	Net 101581.69	Net 0.093900137

Throat Diameter 25		Throat Diameter 27		Throat Diameter 30%		Throat Diameter 28%	
Pressure	Velocity	Pressure	Velocity	Pressure	Velocity	Pressure	Velocity
flow_inlet 126544.51	flow_inlet 1.1477411	flow_inlet 119621.44	flow_inlet 1.1477411	flow_inlet 112911.08	flow_inlet 1.1477411	flow_inlet 116952.88	flow_inlet 1.1477411
inlet 126503.75	inlet 1.1782848	inlet 119580.68	inlet 1.1782844	inlet 112870.33	inlet 1.178285	inlet 116912.14	inlet 1.1782844
outlet 101375.39	outlet 1.178314	outlet 101375.05	outlet 1.1783134	outlet 101374.23	outlet 1.1783156	outlet 101374.69	outlet 1.1783136
pressure_inlet 101323.53	pressure_inlet 0.053826965	pressure_inlet 101323.54	pressure_inlet 0.053707406	pressure_inlet 101323.48	pressure_inlet 0.054795977	pressure_inlet 101323.52	pressure_inlet 0.0539454
pressure_outlet 101324.99	pressure_outlet 0.071101233	pressure_outlet 101324.99	pressure_outlet 0.070867129	pressure_outlet 101324.99	pressure_outlet 0.071987279	pressure_outlet 101324.99	pressure_outlet 0.07124044
throat_inlet -62133.211	throat_inlet 18.87282	throat_inlet -18889.615	throat_inlet 16.185087	throat_inlet 23355.705	throat_inlet 13.069651	throat_inlet -2617.0713	throat_inlet 15.052102
throat_outlet -66794.922	throat_outlet 18.878351	throat_outlet -22049.477	throat_outlet 16.189301	throat_outlet 21260.016	throat_outlet 13.074647	throat_outlet -5367.79	throat_outlet 15.055713
Net 101488.91	Net 0.093871668	Net 101428.7	Net 0.09368562	Net 101373.66	Net 0.094757281	Net 101406.01	Net 0.093985111

Throat Diameter 29%		Throat Diameter 40%		Throat Diameter 28.10%		Throat Diameter 28.20%	
Pressure	Velocity	Pressure	Velocity	Pressure	Velocity	Pressure	Velocity
flow_inlet 114536.52	flow_inlet 1.1477411	flow_inlet 104881.6	flow_inlet 1.1477411	flow_inlet 116955.2	flow_inlet 1.1477411	flow_inlet 116380.52	flow_inlet 1.1477411
inlet 114495.77	inlet 1.178285	inlet 104840.85	inlet 1.1782846	inlet 116914.45	inlet 1.1782845	inlet 116339.76	inlet 1.1782846
outlet 101373.95	outlet 1.1783155	outlet 101375.23	outlet 1.1783165	outlet 101373.35	outlet 1.1783168	outlet 101377.73	outlet 1.1782941
pressure_inlet 101323.52	pressure_inlet 0.053886771	pressure_inlet 101323.59	pressure_inlet 0.052756947	pressure_inlet 101323.45	pressure_inlet 0.055266108	pressure_inlet 101323.55	pressure_inlet 0.053348888
pressure_outlet 101324.99	pressure_outlet 0.071173504	pressure_outlet 101324.99	pressure_outlet 0.070291601	pressure_outlet 101324.99	pressure_outlet 0.072235309	pressure_outlet 101324.99	pressure_outlet 0.070626117
throat_inlet 11870.069	throat_inlet 13.982649	throat_inlet 77176.008	throat_inlet 7.3453727	throat_inlet -957.19635	throat_inlet 14.939444	throat_inlet 475.63101	throat_inlet 14.828673
throat_outlet 9409.292	throat_outlet 13.990233	throat_outlet 76675.969	throat_outlet 7.34723	throat_outlet -3567.251	throat_outlet 14.944407	throat_outlet -2133.156	throat_outlet 14.832592
Net 101385.95	Net 0.093915254	Net 101320.39	Net 0.092852362	Net 101406.84	Net 0.095117182	Net 101401.14	Net 0.093384743

	Throat Diameter 28.30%		Throat Diameter 28.40%	Throat Length 1 cm	Throat Diameter 28.15	Throat Length 0.5 cm	Throat Diameter 28.15
Pressure	Velocity	Pressure	Velocity	Pressure	Velocity	Pressure	Velocity
flow_inlet 115994.98	flow_inlet 1.1477411	low_inlet 115728.85	flow_inlet 1.1477411	flow_inlet 116516.56	flow_inlet 1.1477411	flow_inlet 115052.08	flow_inlet 1.1477411
inlet 115954.23	inlet 1.1782849	inlet 115688.09	inlet 1.1782843	inlet 116475.81	inlet 1.1782844	inlet 115011.33	inlet 1.1782845
outlet 101374.99	outlet 1.1783137	outlet 101379.11	outlet 1.178347	outlet 101377.3	outlet 1.1782939	outlet 101374.67	outlet 1.1783122
pressure_inlet 101323.54	pressure_inlet 0.053618502	pressure_inlet 101323.52	pressure_inlet 0.05412114	pressure_inlet 101323.52	pressure_inlet 0.05391245	pressure_inlet 101323.52	pressure_inlet 0.05414167
pressure_outlet 101324.99	pressure_outlet 0.070957385	pressure_outlet 101324.99	pressure_outlet 0.07116463	pressure_outlet 101324.99	pressure_outlet 0.071006618	pressure_outlet 101324.99	pressure_outlet 0.071350843
throat_inlet 2056.6077	throat_inlet 14.719139	throat_inlet 3477.6321	throat_inlet 14.610422	throat_inlet -278.59125	throat_inlet 14.884055	throat_inlet -934.00177	throat_inlet 14.82865
throat_outlet -629.55469	throat_outlet 14.722404	throat_outlet 869.63269	throat_outlet 14.613465	throat_outlet -2911.3394	throat_outlet 14.887587	throat_outlet -2485.6323	throat_outlet 14.832289
Net 101397.55	Net 0.093679599	Net 101395.25	Net 0.094026886	Net 101402.3	Net 0.093848132	Net 101385.43	Net 0.094157986

	Throat Length 2 cm		Throat Length 3 cm		Throat Length 4 cm		Throat Length 1.1 cm
Pressure	Velocity	Pressure	Velocity	Pressure	Velocity	Pressure	Velocity
flow_inlet 121583.26	flow_inlet 1.1477411	flow_inlet 123706.96	flow_inlet 1.1477411	flow_inlet 127587.13	flow_inlet 1.1477411	flow_inlet 117257.06	flow_inlet 1.1477411
inlet 121542.52	inlet 1.1782842	inlet 123666.22	inlet 1.1782848	inlet 127546.38	inlet 1.1782846	inlet 117216.32	inlet 1.1782844
outlet 101375.16	outlet 1.1783123	outlet 101373.59	outlet 1.178317	outlet 101378.85	outlet 1.1782475	outlet 101377.01	outlet 1.1782513
pressure_inlet 101323.62	pressure_inlet 0.052113611	pressure_inlet 101323.48	pressure_inlet 0.054596461	pressure_inlet 101323.49	pressure_inlet 0.054515235	pressure_inlet 101323.54	pressure_inlet 0.053653359
pressure_outlet 101324.99	pressure_outlet 0.069896184	pressure_outlet 101324.99	pressure_outlet 0.071803711	pressure_outlet 101324.99	pressure_outlet 0.071841702	pressure_outlet 101324.99	pressure_outlet 0.071151249
throat_inlet 5533.6138	throat_inlet 14.828396	throat_inlet 7653.8931	throat_inlet 14.828696	throat_inlet 11571.543	throat_inlet 14.828691	throat_inlet 462.71228	throat_inlet 14.884024
throat_outlet 913.22559	throat_outlet 14.824341	throat_outlet 1188.1719	throat_outlet 14.834124	throat_outlet 3188.3447	throat_outlet 14.836697	throat_outlet -2160.1226	throat_outlet 14.887116
Net 101462.3	Net 0.0924161	Net 101486.78	Net 0.094576731	Net 101532.36	Net 0.094556563	Net 101411.11	Net 0.093797721

	Throat Length 1.2		Throat Length 1.3	D	Throat Length 0.8 cm		Throat Length 1.1
Pressure	Velocity	Pressure	Velocity	Pressure	Velocity	Pressure	Velocity
flow_inlet 117130.36	flow_inlet 1.1477411	flow_inlet 117418.53	flow_inlet 1.1477411	flow_inlet 115846	flow_inlet 1.1477411	flow_inlet 116749.1	flow_inlet 1.1477411
inlet 117089.6	inlet 1.1782846	inlet 117377.77	inlet 1.1782849	inlet 115805.24	inlet 1.1782846	inlet 116708.34	inlet 1.178285
outlet 101377.86	outlet 1.1782576	outlet 101376.81	outlet 1.1782929	outlet 101377.11	outlet 1.1782936	outlet 101375.39	outlet 1.1782941
pressure_inlet 101323.54	pressure_inlet 0.053640246	pressure_inlet 101323.55	pressure_inlet 0.053555977	pressure_inlet 101323.53	pressure_inlet 0.05385058	pressure_inlet 101323.51	pressure_inlet 0.054242685
pressure_outlet 101324.99	pressure_outlet 0.070735916	pressure_outlet 101324.99	pressure_outlet 0.07075727	pressure_outlet 101324.99	pressure_outlet 0.070938863	pressure_outlet 101324.99	pressure_outlet 0.071443543
throat_inlet 329.80432	throat_inlet 14.884071	throat_inlet 634.48914	throat_inlet 14.88406	throat_inlet -100.58768	throat_inlet 14.828668	throat_inlet 755.37201	throat_inlet 14.828691
throat_outlet -2729.293	throat_outlet 14.888296	throat_outlet -2633.686	throat_outlet 14.888742	throat_outlet -2311.7173	throat_outlet 14.832469	throat_outlet -2085.7715	throat_outlet 14.833121
Net 101409.45	Net 0.093581542	Net 101412.8	Net 0.093551815	Net 101394.88	Net 0.093784697	Net 101405.32	Net 0.094225958

	Throat Length 0.5		Throat Length 0.9		Throat Length 1		Throat Length 1.2
Pressure	Velocity	Pressure	Velocity	Pressure	Velocity	Pressure	Velocity
flow_inlet 115104.92	flow_inlet 1.1477411	flow_inlet 96959.125	flow_inlet 1.1477411	flow_inlet 116382.02	flow_inlet 1.1477411	flow_inlet 139233.95	flow_inlet 1.1477411
inlet 115064.17	inlet 1.1782845	inlet -426818.34	inlet 15.249861	inlet 116341.27	inlet 1.1782845	inlet 139193.22	inlet 1.1782851
outlet 101375.62	outlet 1.1782984	outlet -765290.25	outlet 1.6673292	outlet 101377.79	outlet 1.1782949	outlet 101455.84	outlet 1.1782982
pressure_inlet 101323.53	pressure_inlet 0.053798415	pressure_inlet -367388.44	pressure_inlet 30.484243	pressure_inlet 101323.57	pressure_inlet 0.053055767	pressure_inlet 101309.02	pressure_inlet 0.1777834
pressure_outlet 101324.99	pressure_outlet 0.070822574	pressure_outlet 101325	pressure_outlet 30.181112	pressure_outlet 101324.99	pressure_outlet 0.070417427	pressure_outlet 101324.83	pressure_outlet 0.22207361
throat_inlet -1748.8547	throat_inlet 14.88403	throat_inlet -885527.88	throat_inlet 17.398153	throat_inlet 475.89963	throat_inlet 14.828668	throat_inlet 10804.818	throat_inlet 14.828777
throat_outlet -3297.3652	throat_outlet 14.88732	throat_outlet -1605869.1	throat_outlet 14.846809	throat_outlet -2134.5947	throat_outlet 14.832586	throat_outlet 677.55029	throat_outlet 14.833838
Net 101385.84	Net 0.093703724	Net -136564.97	Net 29.915771	Net 101401.16	Net 0.093138456	Net 101653.09	Net 0.22898991

Throat Length 1.3		Throat Length 1 cm		Set Pressure 1 Pa		Set Pressure 2 Pa	
Pressure	Velocity	Pressure	Velocity	Pressure	Velocity	Pressure	Velocity
flow_inlet -3.6798787e+08	flow_inlet 1.1477411	flow_inlet 1.1834657e+10	flow_inlet 1.1477411	flow_inlet 116520.58	flow_inlet 1.1477411	flow_inlet 217848.47	flow_inlet 1.1477411
inlet -4.055319e+08	inlet 83.117462	inlet -6.4359773e+11	inlet 23630.498	inlet 116479.82	inlet 1.1782845	inlet 217807.7	inlet 1.1782842
outlet -165206.33	outlet 2.6133254	outlet -1.6447152e+08	outlet 108.13474	outlet 101377.52	outlet 1.178293	outlet 202703.03	outlet 1.1782582
pressure_inlet 101325	pressure_inlet 118.33878	pressure_inlet -1.6672694e+08	pressure_inlet 574.82495	pressure_inlet 101323.56	pressure_inlet 0.053208571	pressure_inlet 202648.53	pressure_inlet 0.053577021
pressure_outlet -6760268.5	pressure_outlet 116.39278	pressure_outlet 0	pressure_outlet 568.55658	pressure_outlet 101324.99	pressure_outlet 0.07048668	pressure_outlet 202650	pressure_outlet 0.070964351
throat_inlet -47300832	throat_inlet 120.82037	throat_inlet 4.8751109e+09	throat_inlet 42.206264	throat_inlet -278.88873	throat_inlet 14.884054	throat_inlet 101048.88	throat_inlet 14.884057
throat_outlet -18221198	throat_outlet 98.122871	throat_outlet 4.8822968e+09	throat_outlet 14.966187	throat_outlet -2915.3125	throat_outlet 14.887589	throat_outlet 98426.047	throat_outlet 14.887576
Net -7600210	Net 115.88588	Net -3.5739177e+09	Net 693.0705	Net 101402.35	Net 0.093247414	Net 202727.39	Net 0.093663186

	Set Pressure 3 Pa		Set Pressure 4 Pa		Set Pressure 5 Pa		Set Pressure 0.5 Pa	
Pressure	Velocity	Pressure	Velocity	Pressure	Velocity	Pressure	Velocity
				flow_inlet 714259.31	flow_inlet 1.1477411	flow_inlet 66207.344	flow_inlet 1.1477411
flow_inlet 319164.56	flow_inlet 1.1477411	flow_inlet 421198.06	flow_inlet 1.1477411				
inlet 319123.78	inlet 1.1782838	inlet 421157.31	inlet 1.1782837	inlet 714218.62	inlet 1.1782844	inlet 66166.594	inlet 1.1782848
outlet 304028.22	outlet 1.1782606	outlet 405344.97	outlet 1.1783214	outlet 506917.19	outlet 1.1783284	outlet 50709.551	outlet 1.1783321
pressure_inlet 303973.5	pressure_inlet 0.054337762	pressure_inlet 405298.03	pressure_inlet 0.061916877	pressure_inlet 506595.06	pressure_inlet 0.24364878	pressure_inlet 50661.434	pressure_inlet 0.055622321
pressure_outlet 303975	pressure_outlet 0.071758971	pressure_outlet 405300	pressure_outlet 0.07788296	pressure_outlet 506625	pressure_outlet 0.25536099	pressure_outlet 50662.992	pressure_outlet 0.072860569
throat_inlet 202362.95	throat_inlet 14.884058	throat_inlet 304187.5	throat_inlet 14.884058	throat_inlet 453625.12	throat_inlet 14.887444	throat_inlet -50886.262	throat_inlet 14.88408
throat_outlet 199721.66	throat_outlet 14.887597	throat_outlet 301738.22	throat_outlet 14.887341	throat_outlet 408485.38	throat_outlet 14.88835	throat_outlet -53512.863	throat_outlet 14.887588
Net 304052.25	Net 0.094427392	Net 405385.34	Net 0.1011554	Net 508843.44	Net 0.2776117	Net 50744.168	Net 0.095599517

Throat Length 1		Throat Length 1.5		Throat Length 2		Throat Length 2.5	
Pressure	Velocity	Pressure	Velocity	Pressure	Velocity	Pressure	Velocity
				flow_inlet 268762.16	flow_inlet 1.1477411	flow_inlet 319433.81	flow_inlet 1.1477411
flow_inlet 167451.88	flow_inlet 1.1477411	flow_inlet 218105.58	flow_inlet 1.1477411				
				inlet 268721.38	inlet 1.17828	inlet 319393.03	inlet 1.1782794
inlet 167411.12	inlet 1.1782794	inlet 218064.84	inlet 1.1782792				
				outlet 202700.91	outlet 1.1783142	outlet 253363.97	outlet 1.1783148
outlet 101375.77	outlet 1.1783116	outlet 152038.83	outlet 1.1783088				
				pressure_inlet 202648.58	pressure_inlet 0.053003278	pressure_inlet 253311.55	pressure_inlet 0.053593852
pressure_inlet 101323.59	pressure_inlet 0.052603688	pressure_inlet 151986.56	pressure_inlet 0.053211484				
				pressure_outlet 202650	pressure_outlet 0.070641778	pressure_outlet 253312.98	pressure_outlet 0.071112379
pressure_outlet 101324.99	pressure_outlet 0.070194021	pressure_outlet 151987.98	pressure_outlet 0.070887409				
				throat_inlet -192371.91	throat_inlet 29.450436	throat_inlet -141708.28	throat_inlet 29.450439
throat_inlet -293687.56	throat_inlet 29.450439	throat_inlet -243022.02	throat_inlet 29.450432				
				throat_outlet -206167.83	throat_outlet 29.474524	throat_outlet -155502.06	throat_outlet 29.474527
throat_outlet -307476.94	throat_outlet 29.474527	throat_outlet -256807.5	throat_outlet 29.47452				
				Net 203203.09	Net 0.09328194	Net 253866.17	Net 0.093803145
Net 101878.27	Net 0.09286534	Net 152541.16	Net 0.093505047				

Throat Length 3		Throat Length 4		Throat Length 5		Throat Diameter 17% throat	
Pressure	Velocity	Pressure	Velocity	Pressure	Velocity	Pressure	Velocity
				low_inlet	flow_inlet	flow_inlet	flow_inlet
				572774.38	1.1477411	633593.44	1.1477411
flow_inlet	flow_inlet	flow_inlet	flow_inlet				
370077.34	1.1477411	471423.75	1.1477411	inlet	inlet	inlet	inlet
				572733.56	1.1782801	633552.69	1.1782804
inlet	inlet	inlet	inlet				
370036.56	1.1782782	471382.94	1.1782789	outlet	outlet	outlet	outlet
				506675.69	1.17831	506674.88	1.1783141
outlet	outlet	outlet	outlet				
304026.06	1.1783164	405350.94	1.1783117	pressure_inl	pressure_inle	pressure_inle	pressure_inle
				et	t	t	t
pressure_inlet	pressure_inlet	pressure_inlet	pressure_inlet	506623.38	0.056539316	506623.34	0.056897864
303973.53	0.053573612	405298.47	0.054956254				
				pressure_ou	pressure_outl	pressure_outl	pressure_outl
pressure_outlet	pressure_outlet	pressure_outlet	pressure_outlet	tlet	et	et	et
303975	0.071403503	405300	0.071951792	506625	0.074175783	506625	0.074048512
throat_inlet	throat_inlet	throat_inlet	throat_inlet	throat_inlet	throat_inlet	throat_inlet	throat_inlet
-91049.172	29.450428	10295.534	29.450438	111630.3	29.450439	-249554.7	40.734043
throat_outlet	throat_outlet	throat_outlet	throat_outlet	throat_outlet	throat_outlet	throat_outlet	throat_outlet
-104841.38	29.47452	-3494.262	29.474527	97839.367	29.474527	-276653.16	40.741272
Net	Net	Net	Net	Net	Net	Net	Net
304527.97	0.093937136	405853.19	0.094883814	507178.41	0.096756659	507783.62	0.096862718

Throat Diameter 15% throat		Throat Length 2 cm	Throat Diameter 20%	Throat Length 3 cm	Throat Diameter 20%
Pressure	Velocity	Pressure	Velocity	Pressure	Velocity
flow_inlet 718102.62	flow_inlet 1.1477411	flow_inlet 495556.59	flow_inlet 1.1477411	flow_inlet 505233.72	flow_inlet 1.1477411
inlet 718061.81	inlet 1.1782789	inlet 495515.72	inlet 1.1782815	inlet 505192.94	inlet 1.1782811
outlet 506676.44	outlet 1.1782521	outlet 405350.59	outlet 1.1782962	outlet 405351.25	outlet 1.1782982
pressure_inlet 506623.22	pressure_inlet 0.059024129	pressure_inlet 405298.03	pressure_inlet 0.062040783	pressure_inlet 405298.38	pressure_inlet 0.056380596
pressure_outlet 506625	pressure_outlet 0.076314121	pressure_outlet 405300	pressure_outlet 0.077909611	pressure_outlet 405300	pressure_outlet 0.073243275
throat_inlet -735949	throat_inlet 52.277817	throat_inlet 34092.074	throat_inlet 29.456968	throat_inlet 43728.309	throat_inlet 29.457003
throat_outlet -783794.62	throat_outlet 52.289833	throat_outlet 9749.625	throat_outlet 29.41601	throat_outlet 11002.521	throat_outlet 29.469091
Net 508649.94	Net 0.099028923	Net 406128.59	Net 0.10126194	Net 406238.31	Net 0.096201234

VITA

Maxine Janette Jones received her Bachelor of Science degree in chemical engineering in May 2002 from Mississippi State University in Starkville, MS. She began pursuing her doctoral degree at Texas A&M University in the Artie McFerrin Chemical Engineering Department in the fall of 2002, studying under Dr. Mark T. Holtzapple. Maxine completed her PhD in August 2007. Her contact information is Texas A&M University, 200 Brown Building, Mail Stop 3122, College Station, TX, 77843.